

**SEQUESTRATION AND CHARACTERIZATION OF
SOIL ORGANIC CARBON FOR SHELTERBELT
AGROFORESTRY SYSTEMS IN SASKATCHEWAN**

A Dissertation Submitted to the College of Graduate Studies and Research

in Partial Fulfillment of the Requirements

for the Degree of Doctor of Philosophy

in the Department of Soil Science

University of Saskatchewan

Saskatoon, SK, Canada

By

Gurbir Singh Dhillon

PERMISSION TO USE

In presenting this dissertation in partial fulfillment of the requirements for a Postgraduate degree from the University of Saskatchewan, I agree that the Libraries of this University may make it freely available for inspection. I further agree that permission for copying of this dissertation in any manner, in whole or in part, for scholarly purposes may be granted by the professor or professors who supervised my dissertation work or, in their absence, by the Head of the Department or the Dean of the College in which my dissertation work was done. It is understood that any copying or publication or use of this dissertation or parts thereof for financial gain shall not be allowed without my written permission. It is also understood that due recognition shall be given to me and to the University of Saskatchewan in any scholarly use which may be made of any material in my thesis. Requests for permission to copy or to make other uses of materials in this thesis in whole or part should be addressed to:

Head, Department of Soil Science

University of Saskatchewan

Saskatoon, Saskatchewan

Canada, S7N 5A8

DISCLAIMER

Reference in this dissertation to any specific commercial products, process, or service by trade name, trademark, manufacturer, or otherwise, does not constitute or imply its endorsement, recommendation, or favoring by the University of Saskatchewan. The views and opinions of the author expressed herein do not state or reflect those of the University of Saskatchewan, and shall not be used for advertising or product endorsement purposes.

ABSTRACT

The increase in atmospheric concentration of carbon dioxide (CO₂) is contributing to global climate change. Agroforestry systems, such as shelterbelts, can contribute to the mitigation of increasing CO₂ levels, through carbon (C) sequestration in plant biomass and soils. However, little information is available on the storage and dynamics of soil organic carbon (SOC) for shelterbelt systems. The objective of this research was to examine the effect of shelterbelt plantings on the storage, physical stabilization and chemical composition of SOC for major shelterbelt species across Saskatchewan compared to adjacent agricultural fields. Soil and litter samples were collected for six major shelterbelt species including green ash (*Fraxinus pennsylvanica*), hybrid poplar (*Populus* spp.), Manitoba maple (*Acer negundo*), white spruce (*Picea glauca*), Scots pine (*Pinus sylvestris*) and caragana (*Caragana arborescens*) and the adjacent agricultural fields at 59 sampling sites across the agricultural region of Saskatchewan. Measurement of SOC concentration for soil samples was preceded by fumigation with concentrated HCl (12N), which was determined to be the efficient method for SOC determination in carbonate-rich soils. Physical stabilization of SOC was characterized by using the density fraction technique to separate SOC into uncomplexed, plant-derived debris (i.e. light fraction) and mineral-associated organic matter (i.e. heavy fraction). Changes in SOC composition due to shelterbelt plantation were studied using attenuated total reflectance Fourier transform infrared (ATR-FTIR) spectroscopy and synchrotron based carbon K-edge X-ray absorption near edge structure (XANES) spectroscopy. Concentration of SOC for shelterbelts was significantly higher compared to agricultural fields throughout the soil profile (0-50 cm). Sequestration of SOC for shelterbelts varied from 6-38 Mg C ha⁻¹ under different shelterbelt species, along with 3-8 Mg C ha⁻¹ stored in the litter layer. Shelterbelts led to an increase in SOC

content for both the labile light fraction and the mineral-associated heavy fraction. The increase in the heavy fraction was higher in coniferous shelterbelt species including white spruce and Scots pine, while the increase in the light fraction C was higher in hybrid poplar, Manitoba maple, green ash and caragana. These trends were attributed to differences in quality and decomposition rate of litter among shelterbelt species. Maximum amount of SOC was sequestered at the 10-30 cm soil depth, and the majority (70%) of it was in the stable mineral-associated form. Light fraction C was predominant in the surface layer (0-10 cm), where it accounted for 92% of the total sequestered C. Younger shelterbelts tended to lose SOC in the early years of shelterbelt establishment, but eventually resulted in net addition of C after about 20 years of age. SOC sequestration potential of shelterbelts was positively related to shelterbelt characteristics including stand age, tree height, diameter and crown width and density of litter layer. These variables together explained 56-67% of the inter-site variability in the amount of SOC sequestered. Analysis of molecular composition of SOC revealed shelterbelts had higher abundance of processed forms of C such as aromatic and conjugated carboxyl groups for hybrid poplar and white spruce shelterbelts and aromatic and aliphatic C moieties for Manitoba maple shelterbelts. In contrast, agricultural field soils were enriched in easily degradable C forms such as polysaccharides. These results revealed a strong effect of initial litter quality and extent of decomposition on SOC composition. Together, these findings indicate that shelterbelt planting leads to sequestration of SOC, resulting in the decrease of atmospheric CO₂ concentration. Additionally, shelterbelts also influence organo-mineral association and molecular composition of SOC, which may affect stabilization and dynamics of sequestered SOC.

ACKNOWLEDGEMENTS

I would like to express my sincere appreciation and gratitude to my supervisor Dr. Ken Van Rees, for his guidance and encouragement throughout my Ph.D. program. I would also like to thank my advisory committee, Drs. Derek Peak, Mark Johnston, Steve Siciliano and Yuguang Bai for their helpful guidance and direction during this project.

I am also very thankful to Beyhan Amichev for his expertise and inputs to this project, especially with the selection of study sites. Special thanks to Adam Gillespie for his assistance with processing and analysis of XANES spectra. I would also like to thank Doug Jackson, Shannon Poppy, Brittany Letts and Lauren Reynolds for their help with the fieldwork and soil sampling. I am thankful to everyone who assisted with laboratory analysis and spectroscopic analysis of my samples.

Finally, I am thankful to my friends in the lab and the department for their friendship, support, and advice. I am especially grateful to my family for their support, and constant encouragement. Financial support provided by Agriculture and Agri-Food Canada through the Agricultural Greenhouse Gases Program is gratefully acknowledged.

TABLE OF CONTENTS

PERMISSION TO USE.....	i
DISCLAIMER.....	ii
ABSTRACT.....	iii
ACKNOWLEDGEMENTS.....	v
LIST OF TABLES.....	ix
LIST OF FIGURES.....	xi
1. INTRODUCTION.....	1
2. LITERATURE REVIEW.....	5
2.1 Soil carbon sequestration for mitigation of greenhouse gases.....	5
2.2 Shelterbelts in Canadian prairies.....	6
2.2.1 Ecological benefits of shelterbelts.....	8
2.2.2 Carbon sequestration potential of shelterbelts.....	9
2.3 Nature and dynamics of soil organic carbon.....	11
2.3.1 Effect of shelterbelts on SOC dynamics.....	14
2.4 Methods to determine SOC quality.....	15
2.4.1 Density fractionation technique.....	16
2.4.2 Fourier transform infrared (FTIR) spectroscopy.....	17
2.4.3 X-ray absorption near edge structure (XANES) spectroscopy.....	19
3. ACCURATE AND PRECISE MEASUREMENT OF ORGANIC CARBON CONTENT IN CARBONATE-RICH SOILS.....	22
3.1 Preface.....	22
3.2 Abstract.....	23
3.3 Introduction.....	23
3.4 Material and Methods.....	26
3.4.1 Soil samples.....	26
3.4.2 SOC analyses methods.....	28
3.4.3 Data analysis.....	30
3.5 Results and Discussion.....	30
4. SOIL CARBON SEQUESTRATION FOR SHELTERBELT AGROFORESTRY SYSTEMS IN SASKATCHEWAN.....	43
4.1 Preface.....	43
4.2 Abstract.....	44
4.3 Introduction.....	44

4.4 Materials and Methods	48
4.4.1 Selection of study sites	48
4.4.2 Sampling procedure.....	50
4.4.3 Laboratory analyses.....	51
4.4.4 Statistical analyses.....	52
4.5 Results.....	52
4.5.1 SOC distribution and pools under shelterbelts and fields	52
4.5.2 Shelterbelt characteristics and soil organic carbon	60
4.6 Discussion.....	65
4.6.1 SOC sequestration and distribution under the shelterbelts.....	65
4.6.2 Effect of shelterbelt characteristics on SOC sequestration.....	67
4.7 Conclusions.....	69
5. LIGHT AND HEAVY FRACTION DISTRIBUTION OF SOIL CARBON IN SASKATCHEWAN SHELTERBELTS	71
5.1 Preface	71
5.2 Abstract.....	72
5.3 Introduction.....	72
5.4 Materials and Methods	76
5.4.1 Site selection and sampling procedure	76
5.4.2 Laboratory analyses.....	76
5.4.3 Statistical analysis	77
5.5 Results.....	78
5.5.1 General distribution of density fractions in the bulk soil	78
5.5.2 Effect of shelterbelts on density fractions	79
5.5.3 Contribution of density fractions to increase in SOC stocks.....	88
5.6 Discussion.....	90
5.6.1 General characteristics of light and heavy fractions.....	90
5.6.2 Effect of shelterbelts on light and heavy fraction C	91
5.6.3 Distribution of light and heavy fraction C with soil depth and shelterbelt species.....	92
5.7 Conclusions.....	95
6. SPECTROSCOPIC INVESTIGATION OF SOIL ORGANIC CARBON COMPOSITION UNDER SHELTERBELT AGROFORESTRY SYSTEMS	96
6.1 Preface	96
6.2 Abstract.....	97
6.3 Introduction.....	98
6.4 Materials and Methods	100
6.4.1 Site selection and soil sampling	100
6.4.2 Analysis by attenuated total reflectance Fourier transform infrared (ATR- FTIR) spectroscopy.....	101
6.4.3 Analysis by Carbon K-edge X-ray absorption near edge structure (XANES) spectroscopy.....	103
6.4.4 Statistical analysis	105

6.5 Results.....	106
6.5.1 Deconvolution of ATR-FTIR spectra.....	106
6.5.2 Changes in SOC composition with depth and land use.....	108
6.5.3 SOC composition resolved by C K-edge XANES spectroscopy	118
6.6 Discussion.....	127
6.6.1 SOC composition resolved by ATR-FTIR spectroscopy	127
6.6.1.1 General composition and depth distribution	127
6.6.1.2 Effect of shelterbelts on SOC composition	127
6.6.1.3 Influence of shelterbelt species on SOC composition.....	129
6.6.2 SOC composition resolved by C K-edge XANES spectroscopy	130
6.6.3 Land use effects on SOC composition and dynamics	132
6.6.4 Application of ATR-FTIR spectroscopy to determine SOC composition	133
6.7 Conclusions.....	133
 7. SYNTHESIS AND CONCLUSIONS	 135
7.1 Summary of findings	136
7.2 Future research directions.....	140
 REFERENCES	 142
 APPENDICES	 167
Appendix A. Major stand characteristics of the sampling sites with hybrid poplar shelterbelt plantation	167
Appendix B. Major stand characteristics of the sampling sites with white spruce shelterbelt plantation	168
Appendix C. Major stand characteristics of the sampling sites with green ash shelterbelt plantation.....	169
Appendix D. Major stand characteristics of the sampling sites with Manitoba maple shelterbelt plantation	170
Appendix E. Major stand characteristics of the sampling sites with Scots pine shelterbelt plantation	171
Appendix F. Major stand characteristics of the sampling sites with caragana shelterbelt plantation.....	172
Appendix G. The script used for deconvolution of ATR-FTIR spectra of soil samples in the Fityk software package. Changes were made to this script depending upon the unique spectral features of the different soil samples.	173
Appendix H. The script used for deconvolution of C K-edge XANES spectra of soil samples in the Fityk software package. Minor changes were made to the script depending upon the unique spectral features of the different soil samples.....	175
Appendix I. Mean peak positions of the deconvoluted C K-edge XANES bands for shelterbelts and agricultural fields	177
Appendix J. Mean peak positions of the deconvoluted ATR-FTIR absorbance bands for shelterbelts and agricultural fields within the wavenumber range of 1800-900 cm ⁻¹	178

LIST OF TABLES

Table 3.1 Physical and chemical characteristics of the soil samples and standards used in the experiment.....	27
Table 3.2 Carbon contents (wt %) of soil samples and standard materials measured by different C analysis methods.....	34
Table 3.3 Organic C content of acid-treated samples (ranging from high to low organic carbon) dried at low and high temperature conditions (n=4).....	37
Table 4.1 Two-way mixed analysis of variance (ANOVA) of the effect of land cover type (i.e. shelterbelts and fields) within different soil clusters on the SOC concentration (g kg^{-1}) at 0-5, 5-10, 10-30 and 30-50 cm soil depths.....	53
Table 4.2 Mean SOC concentrations (g kg^{-1}) of shelterbelts and fields for different shelterbelt species at 0-5, 5-10, 10-30 and 30-50 cm soil depths.	54
Table 4.3 Mean SOC stock (Mg ha^{-1}) in the litter layer, 0-10, 10-30 and 30-50 cm soil layers under the shelterbelts and fields for different shelterbelt species.	58
Table 4.4 Mean stand characteristics for the six shelterbelt species.....	60
Table 4.5 Pearson correlations between the major shelterbelt characteristics.....	62
Table 4.6 Pearson correlations between the major shelterbelt characteristics and increase in SOC concentrations (g kg^{-1}) at 0-5, 5-10, 10-30 and 30-50 cm soil depth.	62
Table 4.7 Hierarchical multiple regression analysis predicting the change in SOC concentration of the shelterbelts due to shelterbelt species (model 1), shelterbelt age (model 2), Amount of litter (model 3), major tree characteristics (model 4), and major shelterbelt design characteristics (model 5).....	64
Table 5.1 Mean C content and % mass of density fractions of soil organic matter by soil depth for shelterbelts and adjacent agricultural fields averaged across all species.	79
Table 5.2 SOC concentration (g kg^{-1}) of light and heavy fractions at the 0-5, 5-10, 10-30 and 30-50 cm soil depths as affected by land cover and species of shelterbelt plantation.....	86
Table 5.3 Organic carbon stocks (Mg ha^{-1}) of the light fraction (a) and heavy fraction (b) at 0-10, 10-30 and 30-50 cm soil depths under the shelterbelts and agricultural fields for different shelterbelt species. Numbers in parenthesis represent standard error.	87
Table 5.4 Mean increase in organic carbon (OC) stocks (Mg ha^{-1}) of light and heavy fractions, and whole soil and estimated marginal means (EMM) of increase in light and heavy fraction C for different shelterbelt species, estimated for an equivalent increase in SOC stocks. Numbers in parenthesis represent standard error.....	90

Table 6.1 Two-way mixed analysis of variance (ANOVA) of the effect of land use (i.e. shelterbelts and fields) and interaction between land use and species on the relative intensity of absorbance of ATR-FTIR bands at 0-5, 5-10, 10-30 and 30-50 cm soil depths.	112
Table 6.2 Pearson correlations between the increase in relative intensity of absorbance of ATR-FTIR bands and increase in SOC concentrations (g kg^{-1}) at 0-5, 5-10, 10-30 and 30-50 cm soil depths.	118
Table 6.3 C K-edge XANES absorbance intensities (arbitrary units [a.u.]) of the various organic C functional groups identified by C K-edge XANES spectroscopy for shelterbelts and agricultural fields at 0-5, 10-30 and 30-50 cm soil depths.	123

LIST OF FIGURES

Fig. 3.1 Comparison of SOC measurements (N=5) in soil and standard materials of varying SOC and carbonate-C concentrations determined by the HCl-fumigation, HCl-addition, and Wang and Anderson methods. Height of boxes surrounding each plotted mean indicates the 95% confidence interval of the mean SOC (dark gray boxes) and Total C concentrations (gray boxes). For each sample, same upper (and lower) case letters indicate no significant difference between SOC (and total C) concentrations by the three methods.....	31
Fig. 3.2 Relationship between HCl-addition and HCl-fumigation methods for the measurement of organic C in the soil samples. The values on X- and Y-axes represent SOC values measured in percentage of dry sample weight.	32
Fig. 3.3 Effect of soil grinding on C measurement variability (N=5) at 840°C for 120 seconds. Height of boxes surrounding each plotted mean indicates the 95% confidence interval of the mean C concentration value. For each sample, same upper case letters indicate no significant difference between C concentrations of non-ground (<2 mm particle size) and ground soil samples (<250 µm particle size).	39
Fig. 3.4 Effect of soil grinding on total C measurement variability (N=5) at 1100°C. Height of boxes surrounding each plotted total C mean indicates the 95% confidence interval of the mean total C concentration value. For each sample, same upper case letters indicate no significant difference between total C concentrations of non-ground (<2 mm particle size) and ground soil samples (<250 µm particle size).	40
Fig. 3.5 Effect of combustion temperature on total C measurement (N=5) of ground soil and standard material samples (<250 µm particle size). Height of boxes surrounding each plotted mean indicates the 95% confidence interval of the mean total C concentration value. For each sample same upper case letters indicate no significant difference between C concentrations measured at 950 and 1100 °C combustion temperature.	41
Fig. 4.1 Distribution of sampling sites for six shelterbelt species (hybrid poplar, white spruce, green ash, Manitoba maple, caragana, Scots pine) within Saskatchewan, Canada.....	49
Fig. 4.2 Mean SOC concentration (a) and soil bulk density (b) of shelterbelts and fields at 0-5, 5-10, 10-30, and 30-50 cm soil depths. Bars represent standard error. Bars with the same letter within a soil depth are not significantly different at $p < 0.1$	55
Fig. 4.3 Difference in SOC concentration (g kg^{-1}) of different shelterbelt species (HP- Hybrid poplar; WS – White spruce; GA – Green ash; MM – Manitoba maple; CR- Caragana; SP – Scots pine) compared to adjacent fields at the 0-5, 5-10, 10-30, and 30-50 cm soil depths. Species with same letter are not significantly different at $p < 0.1$	56

Fig. 4.4 Relationship between the difference in SOC stocks (Mg ha^{-1}) of shelterbelts compared to adjacent fields and shelterbelt age.	59
Fig. 5.1 Mean SOC concentrations (g kg^{-1}) in the light- and heavy fractions of soil under shelterbelts and agricultural fields at the 0-5, 5-10, 10-30, and 30-50 cm soil depths. Bars with the same letter within a soil depth are not significantly different at $p < 0.1$	81
Fig. 5.2 Distribution of SOC in the light- and heavy fractions (bottom axis) and proportion of light fraction C in the total SOC (top axis) under shelterbelt species (HP- Hybrid poplar; WS – White spruce; GA – Green ash; MM – Manitoba maple; CR- Caragana; SP – Scots pine). SOC concentration (g kg^{-1}) represents the weighted average of SOC concentrations at 0-5, 5-10, 10-30 and 30-50 cm soil depths. Error bars indicate standard error. Bars with the same letter within a fraction are not significantly different at $p < 0.1$	82
Fig. 5.3 Difference in SOC concentration (g kg^{-1}) of the light fraction of different shelterbelt species (HP- Hybrid poplar; WS – White spruce; GA – Green ash; MM – Manitoba maple; CR- Caragana; SP – Scots pine) compared to adjacent agricultural fields at 0-5, 5-10, 10-30, and 30-50 cm soil depths. Species with same letter are not significantly different at $p < 0.1$	84
Fig. 5.4 Difference in SOC concentration (g kg^{-1}) of the heavy fraction of different shelterbelt species (HP- Hybrid poplar; WS – White spruce; GA – Green ash; MM – Manitoba maple; CR- Caragana; SP – Scots pine) compared to adjacent agricultural fields at 0-5, 5-10, 10-30, and 30-50 cm soil depths. Species with same letter are not significantly different at $p < 0.1$	85
Fig. 5.5 Contribution of the light and heavy fractions to increase in SOC stocks (Mg ha^{-1}) at the 0-10, 10-30, and 30-50 cm soil depths across all shelterbelt species. Error bars indicate standard error. Bars with the same letter for a given soil depth are not significantly different at $p < 0.1$	89
Fig. 6.1 A representative ATR-FTIR spectra of whole soil showing the fitted Gaussian peaks representing major C functional groups within the wavenumber range of 1800-900 cm^{-1} . Peaks are identified as follows: 1-917 cm^{-1} ; 2-986 cm^{-1} ; 3 – 1037 cm^{-1} ; 4-1103 cm^{-1} ; 5-1162 cm^{-1} ; 6-1370 cm^{-1} ; 7-1434 cm^{-1} ; 8-1509 cm^{-1} ; 9-1584 cm^{-1} ; 10-1644 cm^{-1}	103
Fig. 6.2 A typical deconvoluted C K-edge XANES spectra of whole soil showing the main ($1s-\pi^*$) peaks (1-7), transition peaks and the arctangent function. Peaks are identified as the following; 1-284.1 eV (unsaturated C); 2- 285.1 eV (Aromatic-C); 3 – 286.2 eV (Ketones); 4 – 287.3 eV (Aliphatic-C); 5 – 288.4 eV (Carboxylic-C); 6 – 289.4 eV (Polysaccharides); 7 – 290.6 eV (Carbonates).	105
Fig. 6.3 Mean relative absorbance intensities of different ATR-FTIR bands at 0-5, 10-30 and 30-50 cm soil depths for (A) shelterbelts and (B) agricultural fields.	108

Fig. 6.4 Change in the relative absorbance intensities of ATR-FTIR bands at 1034, 1103 and 1162 cm^{-1} for shelterbelts compared to agricultural fields at 0-5, 5-10, 10-30 and 30-50 cm soil depths. ‘s’ on the top of the bar indicates statistically significant effect of land use and ‘i’ indicates significant interaction between land use and species at $p < 0.1$	109
Fig. 6.5 Change in the relative absorbance intensities of the ATR-FTIR bands at 1034, 1103 and 1162 cm^{-1} for different shelterbelt species (HP- Hybrid poplar; WS – White spruce; GA – Green ash; MM – Manitoba maple; CR- Caragana; SP – Scots pine) compared to agricultural fields at 0-5, 5-10, 10-30 and 30-50 cm soil depths. ‘s’ on the top of the bar indicates statistical significance at $p < 0.1$	111
Fig. 6.6 Change in the relative absorbance intensities of ATR-FTIR bands at 1370, 1434 and 1509 cm^{-1} for shelterbelts compared to agricultural fields at 0-5, 5-10, 10-30 and 30-50 cm soil depths. ‘s’ on the top of the bar indicates statistically significant effect of land use and ‘i’ indicates significant interaction between land use and species at $p < 0.1$	113
Fig. 6.7 Change in the relative absorbance intensities of the ATR-FTIR bands at 1370, 1434 and 1509 cm^{-1} for different shelterbelt species (HP- Hybrid poplar; WS – White spruce; GA – Green ash; MM – Manitoba maple; CR- Caragana; SP – Scots pine) compared to agricultural fields at 0-5, 5-10, 10-30 and 30-50 cm soil depths. ‘s’ on the top of the bar indicates statistical significance at $p < 0.1$	114
Fig. 6.8 Change in the relative absorbance intensities of ATR-FTIR bands at 1584 and 1644 cm^{-1} for shelterbelts compared to agricultural fields at 0-5, 5-10, 10-30 and 30-50 cm soil depths. ‘s’ on the top of the bar indicates statistically significant effect of land use and ‘i’ indicates significant interaction between land use and species at $p < 0.1$	116
Fig. 6.9 Change in the relative absorbance intensities of the ATR-FTIR bands at 1584 and 1684 cm^{-1} for different shelterbelt species (HP- Hybrid poplar; WS – White spruce; GA – Green ash; MM – Manitoba maple; CR- Caragana; SP – Scots pine) compared to agricultural fields at 0-5, 5-10, 10-30 and 30-50 cm soil depths. ‘s’ on the top of the bar indicates statistical significance at $p < 0.1$	117
Fig. 6.10a Carbon K-edge XANES spectra of the whole soil samples of hybrid poplar shelterbelt and adjacent agricultural field at 0-5, 10-30 and 30-50 cm soil depths.	120
Fig. 6.10b Carbon K-edge XANES spectra of the whole soil samples of Scots pine shelterbelt and adjacent agricultural field at 0-5, 10-30 and 30-50 cm soil depths.	121
Fig. 6.10c Carbon K-edge XANES spectra of the whole soil samples of caragana shelterbelt and adjacent agricultural field at 0-5, 10-30 and 30-50 cm soil depths.....	122
Fig. 6.11 Mean C K-edge XANES absorbance intensities (arbitrary units [a.u.]) of different C functional groups at 0-5, 10-30 and 30-50 cm soil depths for (A) shelterbelts and (B) agricultural fields. Different letters above bars for each functional group indicate significant difference at $p < 0.1$	124

Fig. 6.12 Mean C K-edge XANES absorbance intensities (arbitrary units [a.u.]) of different C functional groups under shelterbelts and agricultural fields at 0-5, 10-30 and 30-50 cm soil depths, respectively. Different letters above bars for each functional group indicate significant difference at $p < 0.1$126

1. INTRODUCTION

Elevated atmospheric concentration of greenhouse gases (GHG) such as carbon dioxide (CO₂; 31% increase since 1750) has increased concerns about climate change and identification of strategies for its mitigation (Lal, 2004a). Soils are the largest terrestrial reservoir of actively cycling carbon (C), containing approx. 1500 Pg in the top 1 m of the profile (Batjes, 1996). As such, changes in soil organic carbon (SOC) levels may result in great variations in C balance at regional and global scales (Schlesinger and Andrews, 2000; Smith, 2004). Global soil C sequestration potential through sustainable management practices is estimated to range from 0.3 to 0.8 Mg ha⁻¹ yr⁻¹ (Follett and Kimble, 2000; Smith et al., 2000; Lal, 2004a; Smith, 2004). However, cultivation of soils has historically led to the loss of soil C stocks (Dumanski et al., 1998), thus making the agricultural sector a major source of GHG emissions (Lokupitiya and Paustian, 2006). Agroforestry practices, which involve deliberate integration of trees with agricultural crops for sustainable land use, can serve as an option for increasing the C storage potential of conventional cropping systems (Schoeneberger, 2009). Shelterbelts are one of the widely practiced agroforestry systems in the Canadian Prairies, covering more than 60,000 km in agricultural region of Saskatchewan (Amichev et al., 2015). Besides numerous agronomic, environmental and social benefits associated with shelterbelts, they also have the capacity to enhance terrestrial C storage in tree biomass as well as in soils (Nair et al., 2010; Lorenz and Lal, 2014).

Shelterbelt planting is associated with higher biomass production and litter input to soil compared to agricultural crops (Brandle et al., 1992; Kort and Turnock, 1998). There are also modifications to root depth (Jackson et al., 1996; Lorenz and Lal, 2005), fine root productivity (Schroth, 1998), and differences in aboveground and belowground biomass allocation (Bolinder et al., 1997; Mokany et al., 2006) compared to agricultural crops. All of these factors may influence the storage of SOC in surface and deeper soil horizons under the shelterbelts. While a number of studies acknowledge the potential of agroforestry systems for soil C sequestration (Nair et al., 2009a), field studies on mechanisms and processes associated with soil C storage for such systems are scanty. Moreover, the available studies on the effects of other tree-based systems (such as afforestation and tree plantations) on soil C pools are also not consistent, and have reported accumulation (Garten, 2002; Niu and Duiker, 2006; Grünzweig et al., 2007), losses (López-Ulloa et al., 2005; Richards et al., 2007) and no net change (Richter et al., 1999; Coleman et al., 2004; Sartori et al., 2007) in SOC pools associated with the establishment of trees. Clearly, there is a need for better understanding and estimation of C storage in soils for the agroforestry systems such as shelterbelts.

Soil C sequestration efforts involve not only the enhancement of the C pool but also its persistence and residence time in soil (Lorenz and Lal, 2014). Persistence of SOC is influenced by its chemical composition and interactions with the soil matrix (Six et al., 2002; Sollins et al., 1996). Organo-mineral complexes involving interaction of SOC with mineral surfaces and metal ions are one of the major factors controlling the stabilization of C in soils (Mikutta et al., 2006). Similarly, stabilization and functioning of SOC is also regulated by the inherent structural stability of organic molecules to microbial degradation (Krull et al., 2003). Shelterbelts may influence the dynamics and stabilization of SOC, through changes in quality ('quality' refers to

structural and chemical properties, that determine decomposition rate) of litter (Lorenz and Lal, 2005). Shelterbelts may also influence the activity and abundance of microorganisms (McCulley et al., 2004; Mitchell et al., 2010), and modify the microclimatic conditions including soil temperature and moisture regimes (McNaughton, 1988 Brandle et al., 2004), which may affect the stabilization mechanisms and decomposition rates of SOC. Determination of the changes in the short- and long-term stabilization processes of SOC under shelterbelts is critical for the comprehensive determination of soil C sequestration and dynamics.

The overall goal of this Ph.D. dissertation project was to study the sequestration and dynamics of SOC for major shelterbelt species, including green ash (*Fraxinus pennsylvanica*), hybrid poplar (*Populus* spp.), Manitoba maple (*Acer negundo*), white spruce (*Picea glauca*), Scots pine (*Pinus sylvestris*) and caragana (*Caragana arborescens*) and the adjacent agricultural fields across Saskatchewan. Sequestration potential of SOC for the shelterbelts was determined by measuring SOC pools for shelterbelts and comparing them to adjacent agricultural fields, using the paired-site design. Further, organo-mineral stabilization of SOC of shelterbelts and agricultural fields was compared using the density fractionation technique. Molecular chemistry of SOC under shelterbelts and agricultural fields was determined using attenuated total reflectance Fourier transform infrared (ATR-FTIR) spectroscopy and synchrotron-based C K-edge X-ray absorption near edge structure (XANES) spectroscopy.

This dissertation is structured in seven chapters. Following an introduction (Chapter 1) and review of literature (Chapter 2), there are four chapters written as stand-alone research studies, with a preface linking the objectives of each study to the overarching goal of this dissertation. Chapter 3 compares the accuracy of three major SOC measurement methods in order to determine the most appropriate method for measurement of SOC in carbonate-rich soils

of Saskatchewan. Chapter 4 determines the soil carbon sequestration potential of major shelterbelt species in Saskatchewan and relates the differences in SOC sequestration potential to shelterbelt characteristics including tree species, and stand design and structure. Chapter 5 compares the organo-mineral stabilization of the SOC between shelterbelts and agricultural fields, by measuring the SOC pools associated with uncomplexed, partly-decomposed organic matter and mineral-associated organic matter. Chapter 6 determines the changes in molecular composition of SOC under shelterbelts compared to adjacent fields by the application of spectroscopic techniques including ATR-FTIR and C K-edge XANES. Chapter 7 synthesizes the key findings from individual research studies (Chapters 3-6) and concludes with recommendations for future research work, and is followed by a list of references.

2. LITERATURE REVIEW

2.1 Soil carbon sequestration for mitigation of greenhouse gases

Global warming refers to the increase in the overall temperature of the earth's atmosphere, generally attributed to the increase in concentration of greenhouse gases (GHG), mainly carbon dioxide (CO₂), methane (CH₄) and nitrous oxide (N₂O). Global mean temperatures have increased by about 0.5°C in the last century (Folland et al., 1990) and are expected to increase by 1-3.5°C by the next century (IPCC, 1995). Carbon sequestration is one of the major strategies recommended by Intergovernmental Panel on Climate Change (IPCC) to offset GHG emissions in the atmosphere (IPCC, 2001). Carbon sequestration has been defined as the process of transfer and long-term storage of atmospheric CO₂ in the terrestrial biosphere, underground, or oceans, so that the buildup of CO₂ concentration in the atmosphere is reduced (Lal, 2008).

Soils are significant reservoirs of carbon (C) within the global carbon cycle, containing about 2370-2450 Pg of C up to a depth of 2 m (Baldock, 2007). Some agricultural soils have lost one-third to three-fourths of their original organic C content (approx. 30-40 Mg C ha⁻¹) due to cultivation and other disturbances, with a cumulative estimated loss of around 40-90 Pg C globally (Lal, 2004a; Smith, 2004). Carbon sequestration in soils can be achieved by increasing soil C stocks, especially, of agricultural and degraded soils that have been depleted in C (Smith, 2004). Lal (2004a) estimated the global soil C sequestration potential of 0.9±0.3 Pg yr⁻¹ by following sustainable soil management practices, which may offset one-fourth to one-third of the

annual increase in atmospheric CO₂ (3.3±0.2 Pg C yr⁻¹). Consequently, substantial attention is being paid to the adoption of sustainable agroecosystem management practices that encourage long-term sequestration of C in soils.

Agroforestry practices are considered one of the major climate-change mitigation tools capable of enhancing C sequestration on agricultural landscapes (Udawatta and Jose, 2011). Agroforestry practices consist of deliberate association of trees or perennial shrubs with agricultural crops on the same land unit to create integrated and sustainable land use systems (Schoeneberger, 2009). Agroforestry practices can sequester large amounts of C in the above- and below-ground biomass (Nair et al., 2010), and in soils (Lorenz and Lal, 2014), while providing numerous other benefits to the landowner and society (Brandle et al., 1992; Schroeder, 1994; Montagnini and Nair, 2004; Mize et al., 2008). Agroforestry practices in North America are generally divided into five broad categories – including riparian buffers, shelterbelts, alley cropping, silvopasture and forest farming, while other special applications, such as home gardens or horticultural trees on farms and rangelands, also exist (Schoeneberger, 2009; Nair et al., 2010). The focus of this dissertation is on shelterbelt agroforestry systems, which have been described in detail in the next section.

2.2 Shelterbelts in Canadian prairies

Canadian prairies are located in the semi-arid climate zone, with a frequent occurrence of droughts and dust storms (Wheaton, 1992; Bonsal et al., 2011). Study by Prairie Farm Rehabilitation Administration (PFRA) in 1983 estimated average annual soil loss of about 160 million tonnes in the Prairies due to wind erosion (PFRA, 1983). Shelterbelts have been widely adopted in the Canadian Prairies as an agroforestry practice in order to protect the crops, livestock and farmyard infrastructure from wind erosion (Kulshreshtha and Rempel, 2014).

Shelterbelts, also known as windbreaks, consist of one or more rows of linear plantations of trees around crop fields or homesteads in order to reduce wind speed and enhance the microclimate of the region (Schoeneberger, 2009). Establishment of shelterbelts in the Prairie Provinces has been actively encouraged through legislations such as the Prairie Farm Rehabilitation Act, which was enacted in 1930, and encouraged the establishment of field shelterbelts, including high-density field shelterbelt networks (Thevathasan et al., 2012). Tree and shrub seedlings for planting of shelterbelts have been provided through the federal tree nursery at Indian head, Saskatchewan, and through farm assistance programs such as Prairie Shelterbelt Program (PSP) of Agriculture and Agri-Food Canada, that has distributed over 600 million shelterbelt tree and shrub seedlings across the Prairies since 1903 (Wiseman et al., 2009). Dunlop (2000) reported more than 59 million trees distributed through PFRA to producers in the province of Saskatchewan from 1949-98, composed primarily of species such as caragana (*Caragana arborescens*), green ash (*Fraxinus pennsylvanica*), Siberian elm (*Ulmus pumila*), willow (*Salix* spp.), Manitoba maple (*Acer negundo*), American elm (*Ulmus americana*), chokecherry (*Prunus virginiana*), poplar (*Populus* spp.), lilac (*Syringa* spp.) and coniferous species including white spruce (*Picea glauca*), Colorado spruce (*Picea pungens*), Scots pine (*Pinus sylvestris*). Caragana, green ash and Siberian elm were predominant fields shelterbelt species in Saskatchewan, accounting for 42, 25 and 11% of total planted miles and 78, 8 and 5% of all trees distributed within 1949-98, respectively (Dunlop, 2000). Amichev et al. (2015) estimated 60,633 km of planted shelterbelts across five soil zones in agricultural Saskatchewan, with the majority of shelterbelts planted in the Dark Brown (75%) and Brown soil zones (17%).

2.2.1 Ecological benefits of shelterbelts

Shelterbelts provide a multitude of agronomic, environmental and economic benefits to the producer as well as the society as a whole. Properly spaced shelterbelts reduce wind speed below the soil entrainment threshold, thereby preventing soil erosion (Brandle et al., 2004; Mize et al., 2008). Reduction of weed speed by 30-40% is considered adequate on the Canadian Prairies (Ferguson et al., 1977). Reduction of wind speed leads to preservation of soil nutrients due to reduced soil erosion, and lessens wind-induced crop damage due to phenomena such as sandblasting, which is abrasion of plant tissue caused by sand particles suspended in the air, and lodging, which is flattening of crops from their upright positions (Brandle et al., 2004). In addition, shelterbelts help in the uniform distribution of snow in the crop fields through management of snowdrift, and conservation of soil moisture due to snow entrapment and retention (Scholten, 1988). Kort and Cherneski (1989) reported a 30% increase in snow retention of sheltered fields compared to the unsheltered ones. This process is especially important in the Canadian Prairies, where snow may account for 25-40% of the annual precipitation (Nicholaichuk and Norum, 1975; Kort et al., 2012). Shelterbelts alter the field microclimate by increasing the average daily temperature and humidity due to reduced wind speed, thus limiting atmospheric circulation in the vicinity of shelterbelts (McNaughton, 1988; Brandle et al., 2000, 2004). These microclimate modifications lead to reduced plant transpiration and soil evaporation (McNaughton, 1988), thereby increasing plant moisture availability and crop yield, especially in the rain-limited years (Frank and Willis, 1978; Davis and Norman, 1988). Increase in temperature helps in the rapid emergence, growth, development and maturity of sheltered crops (Drew, 1982; Ogbuehi and Brandle, 1982). All of these factors lead to higher vegetative growth and agronomic production of field and forage crops including winter wheat, barley, rye, millet,

alfalfa and hay in the sheltered areas (Kort, 1988). Brandle et al. (1984) reported a 15% increase in yield of winter wheat, while Pelton (1967) reported 24-43% increase in yield of spring wheat as influenced by field shelterbelts. Shelterbelts are also associated with a variety of other benefits including improvement of livestock health and productivity (Dronen, 1988; Quam et al., 1994), increase in biodiversity and wildlife habitat (Johnson and Beck, 1988), entrapment of snow to protect adjacent roads and highways (Shaw, 1988), barriers to dust, odors and pesticide drift (Schoeneberger et al., 2001; Balazy, 2002), improved water quality and soil conservation (Correll, 1997; Young, 1997), and enhancement of agricultural landscapes (Cook and Cable, 1995; Cable, 1999).

2.2.2 Carbon sequestration potential of shelterbelts

In addition to the abovementioned ecological benefits associated with shelterbelts, they also have high potential for sequestration of atmospheric CO₂ in the tree biomass (Schoeneberger, 2009). The carbon sequestration potential of tree-based agroforestry systems, including shelterbelts, in the above-ground biomass has been estimated by a number of studies (Brandle et al., 1992; Kort and Turnock, 1998; Thevathasan and Gordon, 2004; Peichl et al., 2006; Wotherspoon et al., 2014). Schroeder (1994) estimated the aboveground C sequestration potential of agroforestry systems in the semi-arid, sub-humid, humid and temperate ecozones to be 9, 21, 50 and 63 Mg C ha⁻¹ respectively. More specifically, shelterbelts were estimated to have an overall C sequestration potential of 4-8.79 Tg C yr⁻¹ in the USA (Nair et al., 2010; Udawatta and Jose, 2011). Similarly, Kort and Turnock (1998) estimated the mean aboveground C sequestration for shelterbelts in Saskatchewan to be 104 Mg C km⁻¹ for hybrid poplar, 31-40 Mg C km⁻¹ for other deciduous species, 24-41 Mg C km⁻¹ for coniferous shelterbelts, and 11-26 Mg C km⁻¹ for shrub shelterbelts. Biomass and C accumulation varied with the shelterbelt species,

with the fast-growing hybrid poplar trees sequestering the maximum amount of C. Similarly, Brandle et al. (1992) estimated aboveground C sequestration in the 20-year-old single-row conifer, hardwood and shrub shelterbelts in Nebraska to be 9.14, 5.41 and 0.68 Mg C km⁻¹ respectively.

Carbon is sequestered in agroforestry systems not only in the above and below ground biomass of trees but also by the increase in C content of soils through the decomposition of tree litter inputs (Nair et al., 2009a). Tree-based agroforestry systems are associated with higher biomass production and increased litter inputs compared to the tree-less systems such as croplands and pastures, thus leading to an increase in SOC storage (Lorenz and Lal, 2014). There are also modifications in root depth and distribution, which may affect SOC stocks in deeper horizons (Kell, 2012). Incorporation of trees may also enhance nutrient cycling and soil fertility (Nair et al., 1999; Oelbermann et al., 2006), improve field microclimate (McNaughton, 1988; Rao et al., 1998), soil microbial activity (McCulley et al., 2004; Mitchell et al., 2010) and reduce pests and weeds (Sileshi et al., 2007), thus increasing primary productivity and litter input to soils. However, there may also be negative interactions of trees with crops such as competition for resources (water, nutrients and light; Rao et al., 1998; Zhang et al., 2013), and secretion of harmful allelochemicals (Rizvi et al., 1999), which may reduce yield and biomass.

Despite the perceived benefits of tree-based systems on soil properties and C storage (Young, 1997; Nair et al., 2009a), only a few studies have monitored the change in SOC under such systems, especially shelterbelts (Sauer et al., 2007; Baah-Acheamfour et al., 2014). Sauer et al. (2007) estimated SOC sequestration under a 2-row shelterbelt composed of *Juniperus virginiana* and *Pinus sylvestris* trees and found that there was an overall increase of 371 g m⁻² of SOC under the shelterbelt compared to the adjacent cultivated field during the 35 year period,

representing an annual SOC sequestration rate of 10.6 g m^{-2} due to the shelterbelts. However, Baah-Acheamfour et al. (2014) found less SOC under the shelterbelts (47.7 g kg^{-1}) compared to other agroforestry practices, including hedgerow (65.2 g kg^{-1}) and silvopasture (81.3 g kg^{-1}), as well as agricultural fields (53.1 g kg^{-1}). They attributed this decrease to a lack of understory vegetation under the shelterbelts, as well as slow decomposition of coniferous litter of shelterbelts compared to the broad-leaved litter of hedgerow and silvopasture systems (Baah-Acheamfour et al., 2014). Similar disparities are found in the estimates of C sequestration potential of other tree-based systems, where some studies indicate high soil C sequestration (Jenkinson, 1970; Garten, 2002), while other studies report no increase in C storage (Richter 1999; Coleman et al., 2004; Sartori et al., 2007). These disparities may be attributed to differences in the net primary productivity of agroforestry systems, which may vary with tree species, age, growing conditions including soil and climatic conditions and management practices (Albrecht and Kandji, 2003). These observations indicate that there are knowledge gaps in our understanding of C sequestration and dynamics under agroforestry systems including shelterbelts, and more research needs to be done in this regard.

2.3 Nature and dynamics of soil organic carbon

Soil organic matter (SOM; including SOC) is a heterogeneous mixture of naturally occurring organic molecules ranging in size and complexity from simple monomers to mixtures of biopolymers, as well as with different inherent composition and stabilities (Sutton and Sposito, 2005; Kelleher and Simpson, 2006). Compartment-based models of SOM cycling, such as Rothamsted model (Jenkinson, 1991) and Century model (Parton et al., 1987), divide SOM into pools with different intrinsic decomposition rates including an active, labile pool with a mean residence time (MRT) of the order of a few years to decades and a passive, recalcitrant

pool with MRT in the order of decades to centuries (Schimel et al., 1994; Torn et al., 2009).

Major processes of organic matter (OM) stabilization include inherent biochemical resistance of OM to decomposition and physico-chemical protection of OM through association with the soil matrix (Six et al., 2002; Sollins et al., 1996). Biochemical resistance of OM to decomposition is attained through inherent chemical and structural stability of organic biomolecules to enzymatic degradation by soil microorganisms (Gleixner et al., 2001; Krull et al., 2003). Particulate OM debris incorporated initially into the soil is enriched in fresh plant tissues. With continued decomposition, easily decomposable plant tissues such as cellulose and hemicellulose are decomposed, while stable components, such as lignin and lipids, are enriched due to selective preservation (Kögel-Knabner et al., 1988). Beside the primary inherently stable components, chemical recalcitrance may also be attained through microbially synthesized cross-linked aliphatic polymers (Kögel-Knabner et al., 1992) and polyphenols (Hättenschwiler and Vitousek, 2000; Huang, 1990). At later stages of decomposition, stable primary sources and secondary chemical derivatives may also be degraded in the availability of suitable decomposer organisms (e.g. lignin-degrading fungi; Berg and McClaugherty, 2008; Grandy and Neff, 2008).

In the absence of soil minerals, such as in forest litter layers, biological stability and turnover rate of OM is entirely controlled by chemical recalcitrance of OM due to its molecular structure. However, in the presence of the soil matrix, turnover times of OM components may be partially regulated by physical and chemical protection mechanisms associated with the mineral soil (Baldock and Skjemstad, 2000). Physical stabilization mechanisms include encapsulation of OM within the soil micro and macro-aggregates, which serves to protect the OM from degradation by placing a spatial barrier between the OM and decomposer microorganisms as well as their extracellular enzymes (Amelung and Zech, 1996; Sollins et al., 1996). Studies such

as Bartlett and Doner (1988) and Priesack and Kisser-Priesack (1993) observed higher microbial activity and utilization of substrates including amino acid and glucose at the aggregate surface, which decreased with distance into the aggregate interior. Pore-size distribution of soils also affects the decomposition rate of SOM by regulating its accessibility to decomposer organisms (Ladd et al., 1993). Besides limited accessibility, the amount of available oxygen is restricted in the water-filled micro pores (Thomsen et al., 1999) as well as in the interior sections of micro-aggregates (Sexstone et al., 1985), which may limit biological oxidation of organic cores within aggregates. SOM may also be stabilized through adsorption and complexation of OM with clay particles and metal oxides (Kögel-Knabner et al., 2008). Relationships between SOM preservation and type of clay minerals (e.g. kaolinite, smectite; Feller and Beare, 1997), content of clay minerals (Ladd et al., 1985; Feller et al., 1991) and mineral oxides (Oades, 1988), and specific surface area of minerals (Saggar et al., 1996; Kaiser and Guggenberger, 2003) has already been established. The chemical nature of surface functional groups of SOM also influences the organomineral interactions. Jones and Singh (2014) observed discrete OM composition of different mineralogical groups, with Fe oxides and phyllosilicate minerals enriched in oxidized C species (C-O, C=O, O=C-O) and quartz and feldspar enriched in aliphatic C and protonated amide groups. While the organo-mineral associations are considered to be of major significance in regulating SOM stabilization (Mikutta et al., 2006; von Lützow et al., 2006), the relative importance of the physical and chemical stabilization mechanisms may depend on the type of soil (Spielvogel et al., 2008). Proper understanding of these short- and long-term stabilization processes (including compound chemistry, reactive mineral surfaces and inaccessibility to potential degraders) as well as the conceptual OM pools associated with them is critical for the comprehensive determination of soil C storage and dynamics.

2.3.1 Effect of shelterbelts on SOC dynamics

Plant litter represents the primary source for SOM formation (Kögel-Knabner, 2002) and the amount and composition of plant litter are major factors in controlling the formation and humification of SOM (Swift et al., 1979; Kögel-Knabner, 2002). Litter inputs derived from trees and arable crops are chemically distinct (Fründ and Lüdemann, 1989; Lorenz and Lal, 2005). Woody tree litter is high in lignin, while herbaceous crop litter is high in polysaccharides derived from cellulose and hemicellulose (Lorenz and Lal, 2005). Initial differences in litter may also persist into the later stages of decomposition, when plant litter is converted into SOM (Fierer et al., 2009). For example, Filley et al. (2008) observed an increase in cutin and suberin-derived aliphatic functional forms in particulate OM, accompanied with woody plant encroachment in grasslands. Litter chemistry may also influence microbial biomass (Ladd et al., 1994) and decomposer community structure (Aneja et al., 2006; Baumann et al., 2009). Yannikos et al. (2014) found higher fungal biomass under *Populus* trees compared to alfalfa (*medicago sativa*), leading to changes in SOM composition. Similarly, Mungai and Motavalli (2006) observed differences in microbial diversity and functionality under trees and intercropped components in the temperate alley cropping systems. Changes in SOM molecular composition and microbial activity, due to differences in litter chemistry, are expected to influence SOM function and inherent recalcitrance, since these are intrinsically linked to each other (Krull et al., 2003). Additionally, stereo-chemical arrangement of functional groups of SOM and their properties (e.g. affinity to water) also control their interaction with mineral surfaces (Gu et al., 1995; Kleber et al., 2007) and hence, may influence its physical stabilization processes.

Land use changes also affect the placement of litter inputs in soil. In permanently vegetated tree systems, plant litter inputs are left on the surface while in the agricultural soils,

aboveground inputs and roots are mechanically mixed in the surface soil layers (Guggenberger et al., 1994; Post and Kwon, 2000). Gale and Cambardella (2000) suggested that SOC accrual benefits in the no-till systems are primarily due to the increased retention of root-derived C in the soil. The placement of organic inputs affects SOC stability through changes in exposure to soil organisms and degree of contact with mineral soil. Incorporation of trees is also known to affect the structure and aggregation of soil (Blanco-Canqui et al., 2007; Udawatta and Jose, 2011), which may lead to increased stabilization of SOC. Microclimate differences due to the presence of trees may cause variations in soil temperature and moisture content (Brandle et al., 2004; Scholten, 1988), which may lead to differences in the decomposition rate of SOC (Davidson and Janssens, 2006).

2.4 Methods to determine SOC quality

While SOM is composed of a continuum of compounds with varying turnover times, it has to be divided into discrete functional pools with specific turnover rates, in order for it to be functionally characterized. Numerous fractionation schemes have been developed to separate SOM into discrete fractions. These include physical separation techniques based on soil aggregation, particle size, and density fractions; and chemical techniques that fractionate SOM according to solubility, hydrolysability, and resistance to oxidation or by destruction of the mineral phase (von Lutzow et al., 2007). Physical fractionation techniques are based on the premise that the spatial arrangement and associations of SOM affect its bioaccessibility and thus, play a key role in determining its decomposition rate (Balesdent et al., 1998; Gregorich et al., 2006). Thus, the physically defined fractions represent a diverse array of organic compounds with similar structural and spatial properties (Christensen, 1996).

2.4.1 Density fractionation technique

SOM associations with minerals play a key role in soil dynamics (Mikutta et al., 2006) and a better understanding of organo-mineral interactions relies on the identification of SOM fractions that show strong interactions with the mineral phase of soil. Density fractionation of SOM is based on the role of association of soil minerals with organic matter in SOC turnover, and isolates SOM that is not firmly associated with soil minerals (called light fraction) from organo-mineral complexes (called heavy fraction; Cambardella and Elliott, 1992; Christensen, 1992). Mineral-associated heavy fraction is composed of fine organic particles that are rendered less bio-accessible due to complex formation with the mineral surfaces (Eusterhues et al., 2005). It represents the recalcitrant fraction of SOM and is characterized by a density greater than 1.6 to 2 g cm⁻³ (von Lutzow et al., 2007). The light fraction consists of large organic fragments such as plant residues that have undergone little chemical transformation (Christensen, 1992). This fraction, operationally defined to be of density less than 1.6-2 g cm⁻³, is highly decomposable and responds faster to changes in soil management practices (Boone, 1994; Hassink, 1995). A review of SOM fractionation methods by von Lutzow et al. (2007) concluded that the active pool of SOM, with turnover periods of less than 10 years, is best represented by the light fraction of SOM separated by the density fractionation technique.

Density fractionation separates light and heavy fractions of SOM based on the difference in density between minerals and organic material. This is achieved by using organic liquids such as tetrabromoethane (2.96 g cm⁻³), bromoform (2.88 g cm⁻³), tetrachloromethane (1.59 g cm⁻³) and inorganic solutions such as sodium iodide (NaI) and sodium polytungstate (SPT) at any desired density (1 to 3.1 g cm⁻³; Six et al., 1999; von Lutzow et al., 2007). Optimum liquid density is a critical parameter in the separation of light and heavy fractions in the density fractionation

technique (Cerli et al., 2012). However, numerous density cut-off values have been used in the application of this technique (Golchin et al., 1994; Sohi et al., 2001; Swanston et al., 2002; Crow et al., 2007). A recent study by Cerli et al. (2012) demonstrated that density of 1.6 g cm^{-3} is the most appropriate liquid density for most soils since it resulted in the most accurate separation of the pure organic fraction from the organo-mineral fraction.

2.4.2 Fourier transform infrared (FTIR) spectroscopy

Physical and chemical fractionation methods, including density fractionation, provide only a rough differentiation of active and passive pools of SOM (von Lutzow et al., 2007). While the light fraction is a good representative of the active SOM pool, the heavy fraction is too heterogeneous and contributes to the intermediate and passive pools (Torn et al., 2009). The light fraction may also lead to overestimation of the active pool of SOM if appreciable quantities of charcoal are present in the soil (Skjemstad et al., 1990). Due to the heterogeneous nature of SOM, combined application of physical fractionation techniques, with spectroscopic techniques to determine molecular composition of SOC, may be desired in order to obtain comprehensive structural and functional information about SOM.

Fourier transform infrared (FTIR) spectroscopy is a powerful analytical tool to obtain molecular-scale information on mineralogy and organic matter composition of soils and sediments (Parikh et al., 2014). It is rapid, non-destructive and capable of simultaneous determination of several plant and soil constituents and properties (Janik et al., 1995, 1998). It is a vibrational spectroscopic technique that measures the absorption of infrared (IR) energy of specific molecular bonds due to stretching (symmetric and asymmetric), bending, rocking, and wagging vibrations, in the presence of dipole moments (Griffiths and De Haseth, 2007). Relative absorbance of the molecular bands at specific frequencies (i.e. wavenumbers) may be used to

determine their abundance. Various methods of spectral collection include transmission, attenuated total reflectance (ATR) and diffuse reflectance optical sampling. ATR-FTIR technique requires lesser amount and preparation of sample, avoids water interference and has strong potential for use in *in-situ* studies (Aslan-Sungur et al., 2013; Parikh et al., 2014).

Various organic functionalities, including aromatic (C=C), aliphatic (C-H), phenolic (C-OH), and polysaccharide (C-O), absorb in the mid-infrared region (4000-400 cm^{-1}) of the electromagnetic spectrum, thus making it possible to study the chemistry of OM using FTIR spectroscopy (Calderón et al., 2013). Overlap of functional C groups bands due to the heterogeneous nature of SOM, and interference due to the soil mineral phase remain as major challenges to FTIR spectral interpretation (Stenberg et al., 2010; Calderón et al., 2013).

However, despite the mineral interference, FTIR spectroscopy has been used to gain valuable chemical insights about SOM of whole soils, given similar mineralogy of the soils (Ellerbrock and Gerke, 2004; Šimon, 2007; Demyan et al., 2012; Matějková and Šimon, 2012).

Spectroscopic characterization of SOM extracts such as humic acid has also been performed, in order to reduce mineral interference, and gain information about recalcitrant SOM pool.

Molecular changes in humic acid extracts in response to organic amendments (Brunetti et al., 2012), manure and fertilizers (Watanabe et al., 2007) have been studied, in order to determine their influence on SOM. However, the functional relevance of these alkaline extracts to SOM has been questioned in recent studies (Kleber and Johnson, 2010; Schmidt et al., 2011). Other studies have used multivariate data analysis techniques such as principal component analysis (PCA; Chang et al., 2001) and partial least squares regression (PLSR; McCarty et al., 2002) in order to relate spectral information with soil properties of interest (Randhawa, 2008; Guler et al., 2011; Yang and Mouazen, 2012; Aslan-Sungur et al., 2013).

2.4.3 X-ray absorption near edge structure (XANES) spectroscopy

The advent of dedicated synchrotron facilities, capable of producing high energy and readily tunable synchrotron radiation, has led to the development of spectromicroscopic methods with high spectral and spatial resolution of 30 to 300 nm. Synchrotron-based techniques such as X-ray absorption near edge structure (XANES) spectroscopy are powerful and noninvasive, and can be used to carry out the *in situ* analyses of diluted samples at the sub-micron scale (Lehmann et al., 2009). XANES is a type of X-ray absorption spectroscopy (XAS), which uses incoming X-ray energy to assess the bonding environment of a specific element (Stöhr, 1992). It involves the excitation of core level electrons of the target atom causing their transition to unoccupied or partially occupied molecular orbitals, and the resulting phenomenon such as absorption of energy, fluorescence, or emission of photons are studied to gain information about the bonding environment of the target atom (Hitchcock et al., 2008; Lehmann et al., 2009). XANES absorption spectrum correspond to bound state transitions of the electrons, achieved by increasing incident photon energy throughout the absorption K-edge of the element of interest and beyond its ionization threshold (Lombi and Susini, 2009; Stöhr, 1992). Absorption K-edge is the energy level at which core electrons in the K-shell are promoted to higher orbitals or completely removed (above the ionization threshold) by the photons (Jacobsen et al., 2000) and it is unique for each element (284 eV for C). The excited phase of the inner-core (1s) electrons along the K-edge region is characteristic of the structure of the C functional group chemistry, and provides information about specific C forms. (Lehmann and Solomon, 2010). XANES is also known as near edge X-ray absorption fine structure (NEXAFS) spectroscopy, term generally applied when photon energy of incoming X rays is less than 2000 eV, as in the case of C (Lehmann et al., 2009).

C K-edge XANES absorption spectra show multiple energy positions of the main $1s-\pi^*$ transitions in the fine structure region (284-290 eV; Solomon et al., 2005). The shape of the carbon absorption spectrum is compared to the spectral features of well-characterized reference compounds in order to determine the molecular-level speciation of SOC (Stöhr, 1992; Lehmann et al., 2009). XANES spectroscopy is described as being element-specific, since the X-ray absorption edge energies of different elements are unique (Stöhr, 1992). Thus, there is no mineral or water interference in the determination of C, which is a major drawback for other spectroscopic techniques such as FTIR and nuclear magnetic resonance (NMR). However, the interpretation of soil C XANES spectra may sometimes be challenging due to the complexity of SOM and overlapping energy regions of the different C bonds (Cody et al., 1998; Schäfer et al., 2003).

Semi-quantitative determination of speciation of SOM has been performed, using approaches such as principal component analysis, spectral deconvolution, or least-squares linear combination fitting (Hutchison et al., 2001; Scheinost et al., 2001; Beauchemin et al., 2003; Jokic et al., 2003; Solomon et al., 2005, 2007). Spectral deconvolution uses a series of Gaussian or Lorentzian functions to describe pre-edge peaks and arctangent function to describe the edge (Lehmann and Solomon, 2010). C K-edge XANES spectroscopy has been successfully applied in the study of soils (Schumacher et al., 2005; Wan et al., 2007; Gillespie et al., 2011), humic extracts (Rothe et al., 2000; Scheinost et al., 2001; Solomon et al., 2005), biopolymers (Kikuma and Tonner, 1996), plant fossils (Boyce et al., 2002) and coal (Cody et al., 1996). The knowledge of structural characteristics of C and its speciation can be used to determine the role of structural moieties to the inherent recalcitrance of organic matter (Lehmann et al., 2005; Solomon et al., 2005; Lombi and Susini, 2009), impact of management on the composition and

biogeochemical cycling of organic C at the molecular level in terrestrial ecosystems (Jokic et al., 2003; Kinyangi et al., 2006; Scheinost et al., 2001; Solomon et al., 2005; Lehmann et al., 2007), distribution of carbon within soil microaggregates (Wan et al., 2007) as well as the microbial alteration of substrates (Kleber et al., 2010).

3. ACCURATE AND PRECISE MEASUREMENT OF ORGANIC CARBON CONTENT IN CARBONATE-RICH SOILS¹

3.1 Preface

In order to make accurate measurement of organic carbon in soils, it is essential to determine proper methodology to prevent interference of soil carbonates. This chapter compares the commonly used methods of SOC measurement, in order to determine their efficiency for organic carbon determination of carbonate-rich soils. The appropriate method of SOC measurement, as determined in this chapter, will be used for the measurement of OC content of whole soils, and density fractions of soil in Chapters 4 and 5, respectively.

¹ This chapter was published as Dhillon, G.S., B.Y. Amichev, R. de Freitas and K. Van Rees. 2015. Accurate and precise measurement of organic carbon content in carbonate-rich soils. *Commun. Soil Sci. Plant Anal.* 46: 2707-2720. Minor modifications have been made in order to maintain consistency in formatting. Dr. de Freitas contributed

3.2 Abstract

Accurate measurement of soil organic carbon (SOC) is dependent on precise and fast methods for the separation of organic and inorganic carbon. The widely used methods involving thermal decomposition of soil samples at a specific temperature in an automated C analyzer are susceptible to interference by carbonates and over-estimation of organic carbon, thus removal of carbonates by acid-pretreatment of samples is recommended. Two carbonate-removal pretreatments including HCl-addition and HCl-fumigation are compared using CaCO₃ standard and soil samples of varying SOC contents. Both pretreatment methods provided similar measurements of organic C indicating that both methods are efficient in removal of carbonates present in the soil. However, the HCl-fumigation method exhibited higher accuracy and precision compared to the HCl-addition method. Hence, SOC measurement procedure involving HCl-fumigation as a pre-treatment for the removal of carbonates is recommended for carbonate-rich soils.

3.3 Introduction

In a future global carbon (C) market, verifiable C credits (carbon offsets) from afforestation and reforestation projects, such as ecosystem C stocks (vegetation biomass and soil organic carbon (SOC)), would be the currency (Tietenberg et al., 1999). Carbon credits would be traded between firms (e.g. C credits sold by a forest land owner to a coal-burning facility owner) within a country, or between countries, with a goal of maintaining overall C emissions below set standards (Clarke, 1995; Tietenberg et al., 1999). Therefore, it is critically important that inexpensive and accurate methods are available to researchers, policy-makers, and landowners to measure and report C credits, particularly the amount of SOC sequestered in forest and agricultural soils.

Hitherto, a widely accepted wet oxidation procedure (Walkley and Black, 1934) has been used for soil organic matter (SOM) and SOC analyses in various soils around the world. One of the advantages of this method was that soil carbonates did not interfere with the final SOC estimate. However, Nelson and Sommers (1982) reported that the presence of significant amounts of Fe^{2+} or Cl^- in the soils leads to overestimation of SOC. Additionally, the presence of MnO_2 may lead to an underestimation of SOC, in case of rapid dichromate methods such as the Walkley and Black procedure (Nelson and Sommers, 1982). Due to the uncertainties associated with SOC estimation by the Walkley-Black procedure, this method could only provide a qualitative measure of SOC, and is not recommended for quantitative SOC analysis in soils (Nelson and Sommers, 1982; Skjemstad and Taylor, 1999).

A promising new group of C measurement techniques was based on the principle of combusting a soil sample in oxygen or air (thermal oxidation) in order to convert all soil C forms to carbon dioxide (CO_2), which was then trapped and measured by different techniques, including the commonly used infrared wavelength absorption. The C measurements from such thermal oxidation techniques were fast, reliable, accurate, and repeatable (i.e. precise), all of which were desired characteristics of any practical SOC measurement technique in a future global C market (Amichev, 2007). Wang and Anderson (1998) proposed a method, based on a thermal oxidation technique, in order to directly measure the organic carbon in soils. Their method involved the combustion of samples at a temperature of 840°C for 120 seconds, where organic C is completely oxidized while the decomposition of carbonates has not started (Wang and Anderson, 1998). The major disadvantage associated with this method is the high probability of interference from soil carbonates which, similar to SOM, could decompose to CO_2 at the

oxidation temperature (Froelich, 1980; Weliky et al., 1983), thus invalidating the final SOC estimate.

An alternative method to measure organic C involved the acid-treatment of samples to eliminate carbonates followed by total C analysis via automated C analyzers (Nieuwenhuize et al., 1994; Yamamuro and Kayanne, 1995; Amichev, 2007). Several acid-pretreatment methods have been developed to eliminate excess carbonate in the samples (Hedges and Stern, 1984; Verardo et al., 1990; Cutter and Radford-Knoery, 1991). The acid leaching method involves the addition of acid to the soil samples, followed by washing with deionized water, in order to remove carbonates and the residual sample is analyzed for total C (Gehman, 1962; Byers et al., 1978). However, this method may lead to an underestimation of SOC due to the leaching of acid-soluble components of SOM such as carbohydrate and carboxyl groups, and some aliphatic and lignin groups (Roberts et al., 1973; Froelich, 1980; Schulten, 1996). Roberts et al. (1973) found that the loss of acid-soluble SOC from natural carbonate sediments might be as high as 9 to 44%. Treatment of samples with hydrochloric (HCl) acid may also lead to an increase in weight of the acidified samples due to water absorption by the chloride salts, which also resulted in underestimation of SOC content (Van Iperen and Helder, 1985). The in-situ acidification method involves acidification of samples with liquid acid, followed by drying of samples, in order to avoid the loss of acid-soluble components (Waples and Sloan, 1980; Verardo et al., 1990). Another in-situ acidification method involves fumigation of samples using the HCl-acid vapors contained inside a closed vessel (Hedges and Stern, 1984; Harris et al., 2001). The in-situ acidification methods not only avoid the loss of acid-soluble SOM but also eliminate the error due to hydration of chloride salts since the reweighing of acid-treated samples is not required (Verardo et al., 1990).

The objective of this study was to determine the most appropriate method for SOC measurement in soils of Saskatchewan. For this purpose, this study compared the accuracy and precision of the following methods - 1) SOC measurement procedure based on in-situ HCl-acid (12 N) fumigation (Harris et al., 2001) as the carbonate-removal pre-treatment; 2) SOC measurement procedure based on in-situ HCl-addition, as recommended by LECO Corporation – St Joseph, Michigan, USA (LECO representative Liliane Eichenbaum, 2007, personal communication); 3) Thermal decomposition-based method by Wang and Anderson (1998), which has been frequently used in the carbon determination studies of soils in Saskatchewan (Landi et al., 2003; Mensah et al., 2003; Wu et al., 2004; Schnitzer et al., 2006).

3.4 Material and Methods

3.4.1 Soil samples

Five soils with varying SOC and carbonate content, and a CaCO₃ (12% C) calibration standard recommended for LECO carbon analyzer instruments (LECO Corporation, St. Joseph, MI, USA), were used in this study (Table 3.1). Three of the soils, CSSC 7, CSSC 10, and CSSC 12 were reference soil samples approved by the Canadian Soil Survey Committee (CSSC) for use in analytical laboratories across Canada (MacKeague et al., 1979). The remaining soils including PA_1 and Est_1 were collected from subsurface horizons in the research areas located in central Saskatchewan and in southern Saskatchewan, respectively. The PA_1 soil was collected at 30-60 cm soil depth of an Orthic Eutric Brunisol near Prince Albert, SK (53°21'18"N, 105°46'25"W, elevation 469 m) and Est_1 was collected at 10-20 cm soil depth of an Orthic Regosol near Estevan, SK (49°4'38"N, 102°52'37"W, elevation 537 m).

Table 3.1 Physical and chemical characteristics of the soil samples and standards used in the experiment

Soil I.D.	Location	Depth (cm)	Horizon	Clay (%)	pH
CSSC 7	Youngstown AB (51°28'N 110°15'W)	0-10	Ah	14 ^a	4.5 ^a
CSSC 10	Saskatchewan (52°10'N 106°27'W)	0-10	Ah	15 ^a	7.3 ^a
CSSC 12	Saskatchewan (52°10'N 106°27'W)	33-51	Ck	12 ^a	7.9 ^a
PA_1	Prince Albert, SK (53°21'18"N, 105°46'25"W)	30-60	Cca	1.9 ^b	6.8 ^b
Est_1	Estevan, SK (49°4'38"N, 102°52'37"W)	10-20	C	23 ^b	8.2 ^b

^aData from MacKeague et al. (1979).

^bData from Hangs et al. (2014)

3.4.2 SOC analyses methods

Three procedures were tested for the determination of organic C in the soils. The thermal oxidation based method proposed by Wang and Anderson (1998), henceforth referred to as the Wang and Anderson method in this paper, was used for the direct measurement of organic C in an automated carbon auto-analyzer (LECO C632). This method does not involve a pretreatment step for the removal of carbonates. In this method, samples <2 mm in particle size were combusted at the furnace combustion temperature of 840°C and 1100°C for 120 seconds to estimate organic and total C in the samples, respectively.

In the other two methods, carbonate-removal HCl-acid pretreatments were done prior to C analysis. The procedure of Harris et al. (2001) was followed for the acid-fumigation of the soil samples. Briefly, the collected soil samples were ground to <250 µm particle size. About 0.25 g of the soil sample was placed in a silver boat liner and the moisture content and dry weight of the sample was recorded. The samples were moistened by adding approx. 1 ml of distilled water in order to increase the efficiency of carbonate removal by the HCl fumes. These samples were placed in a vacuum desiccator along with a 150-ml beaker with 100 ml of concentrated HCl (12 M) for 24 hours to remove soil carbonates. After this period, the samples were removed from the desiccator and heated in a ventilated drying oven at 60°C for 4 hours to remove the residual moisture and excess HCl. These carbonate-free samples were analyzed for total C content (i.e., only SOC) by using an automated C632 LECO analyzer with a preset combustion temperature of 950°C and maximum combustion time of 10 minutes. In order to estimate total C (i.e., SOC plus carbonates-C), a separate set of samples without the HCl-pretreatment were directly combusted at 950°C for a maximum of 10 minutes.

For the in-situ addition of HCl, the procedure recommended by LECO Inc. was followed (LECO Corporation, St. Joseph, MI, USA). Approximately 0.25 g of soil samples, <250 μm in particle size, were placed in nickel boat liners and the weight and moisture content was recorded. An HCl:H₂O solution (1:1) was added to completely moisten the samples. The samples were heated in a drying oven at 60°C for one hour. These steps were repeated until no effervescence due to dissolution of carbonates was observed. The carbonate-free samples were analyzed in the C632 LECO carbon analyzer at a combustion temperature of 1100°C for a maximum of 10 minutes. In order to calculate total C, another set of samples was processed without HCl-addition and analyzed at the same temperature.

It is to be noticed that the Wang and Anderson method differed from the other methods that included acid-pretreatment, in terms of soil particle size. In order to study the effect of soil grinding on the measurement of C by this method, two sample sets were ground to particle sizes <2 mm and <250 μm , respectively. Samples were analyzed for organic and total C in the C632 LECO carbon analyzer using the furnace combustion temperatures of 840°C and 1100°C for 120 seconds, respectively. Similarly, the HCl-fumigation method and the HCl-addition method differed with respect to the combustion temperature (950°C and 1100°C respectively). In order to account for the effect of temperature on the measurement of C, two sample sets were combusted at 950°C and 1100°C, without any HCl-pretreatment.

All the results were reported as percent of C by sample weight (wt %). All C values were corrected for their moisture content, so that the final C result was based on an oven-dried soil weight (105°C for 24 hours). In case of methods involving carbonate-removal pretreatments, the original total sample weight was entered into the carbon analyzer rather than the sample weight measured after carbonate removal, to get the correct estimate of SOC concentration (wt %) of the

sample. The maximum analysis time of 10 min was sufficient to oxidize all organic-C matter (at 950 and 1100°C) in all samples in this study. Sample weights ranged from 0.2300 to 0.3000 g for the soils, and from 0.1400 to 0.2000 g for the CaCO₃ calibration standard.

3.4.3 Data analysis

One-way analysis of variance followed by Tukey's HSD were used to test for the difference in the concentration of organic C and total C in the samples for different analysis methods.

3.5 Results and Discussion

Results of SOC and the corresponding total C (SOC plus carbonate-C) concentrations measured by Wang and Anderson method (Wang and Anderson, 1998), HCl-fumigation method (Harris et al., 2001) and HCl-addition method for all soil samples and CaCO₃ standard are presented in Table 3.2. The Wang and Anderson method estimated 0.34 % of organic C in the CaCO₃ standard while the methods involving HCl pretreatment estimated organic C correctly in the expected error range of zero (± 0.1 %; Fig. 3.1). Additionally, the Wang and Anderson method also estimated significantly higher organic C content for the CSSC 12 soil standard, compared to the acid-treated samples (Fig. 3.1). This may be due to the relatively higher quantity of carbonates present in this soil, which would interfere with the estimation of SOC. The results for the CSSC 12 soil indicated that the Wang and Anderson method might be unsuitable for carbonaceous soils with low SOC content where separation of the organic and inorganic forms of carbon could be hindered. The Wang and Anderson method is based on the assumption that all SOC can be completely decomposed at the temperature of 840°C for 120 seconds, while the carbonates are not decomposed. However, the thermal degradation temperatures of organic and inorganic components of carbon may overlap resulting in over-estimation of organic C (Froelich,

1980). While the thermal decomposition of calcite begins at temperatures above 850°C, various other carbonate minerals including dolomite, magnesite and siderite begin decomposing to CO₂ at temperatures well-below 840°C (Dolomite 750-985°C; Magnesite 470-685°C; Siderite 500-605°C; Beck, 1950). Since Saskatchewan soils are rich in calcite and dolomite in the subsoil horizons (Landi et al., 2003), the Wang and Anderson method is not recommended for the accurate estimation of SOC in these soils.

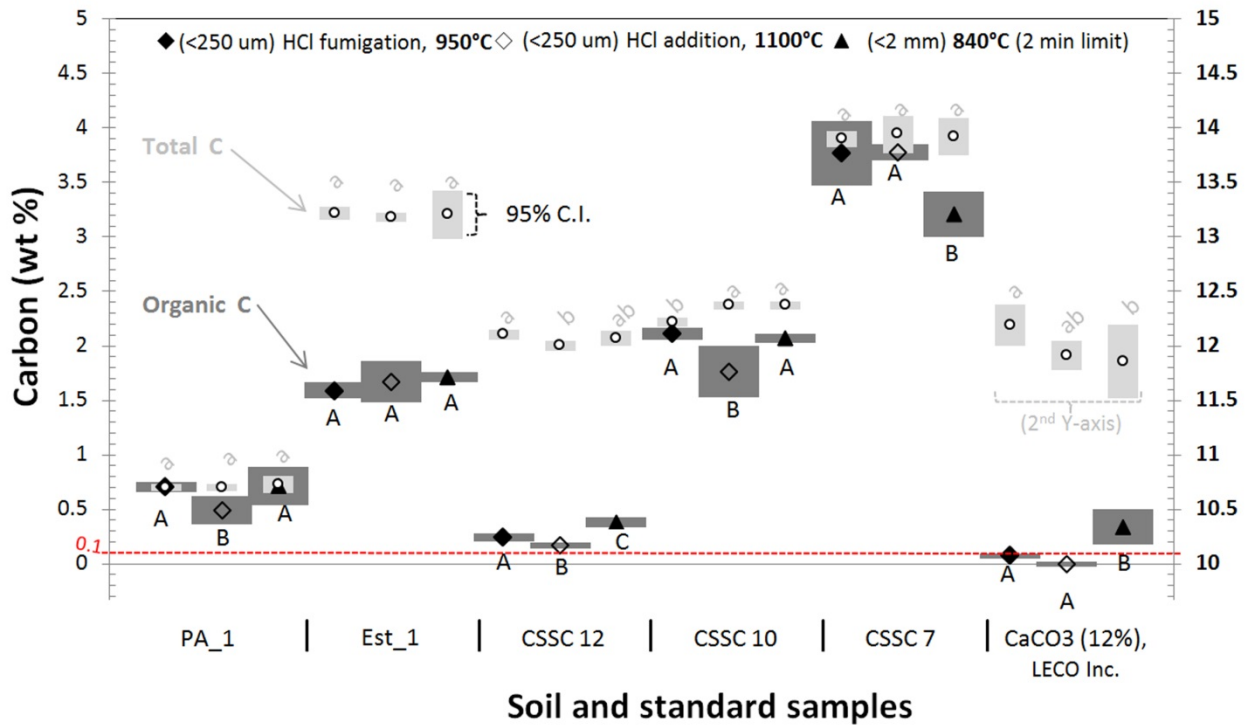


Fig. 3.1 Comparison of SOC measurements (N=5) in soil and standard materials of varying SOC and carbonate-C concentrations determined by the HCl-fumigation, HCl-addition, and Wang and Anderson methods. Height of boxes surrounding each plotted mean indicates the 95% confidence interval of the mean SOC (dark gray boxes) and Total C concentrations (gray boxes). For each sample, same upper (and lower) case letters indicate no significant difference between SOC (and total C) concentrations by the three methods.

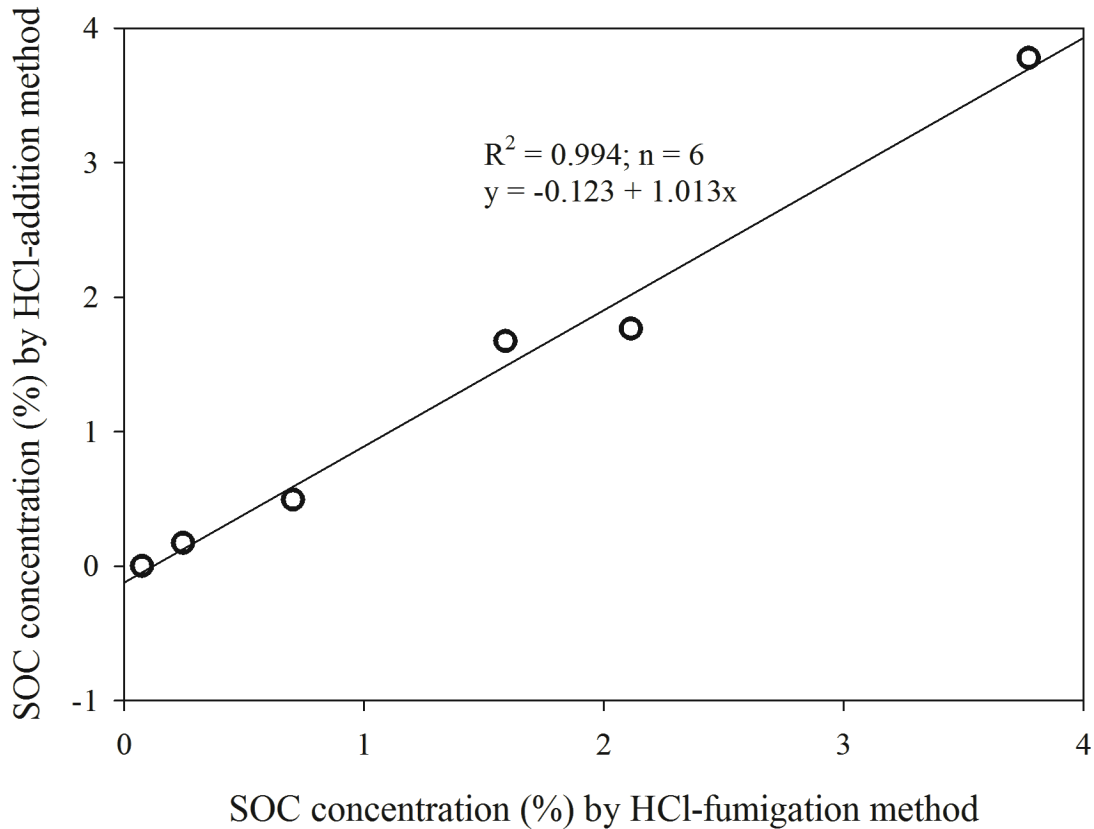


Fig. 3.2 Relationship between HCl-addition and HCl-fumigation methods for the measurement of organic C in the soil samples. The values on X- and Y-axes represent SOC values measured in percentage of dry sample weight.

In order to eliminate the effect of carbonates during sample combustion, pretreatment of soil samples to remove all carbonates is recommended (Harris et al., 2001; Kuhlbusch, 1995).

Fig. 3.2 represents the relationship between the SOC values determined after the samples were pretreated with HCl fumigation and HCl addition methods, respectively. The slope of the regression line is 1.013 ± 0.055 , which is not significantly different from unity. This indicates that both acid pretreatment methods provide similar results, and are efficient in the removal of carbonates. The SOC content of CSSC 10 and CSSC 12 soil standards as well as PA_1 soil sample is lower with HCl addition compared to acid fumigation and Wang and Anderson

methods (Fig. 3.1; Table 3.2). This indicates that the addition of HCl, instead of HCl fumigation, and subsequent heating may be resulting in the loss of volatile components of organic matter (Pocklington and Hagell, 1975). In contrast, acid fumigation with HCl of these soil samples did not lower their organic C content compared to the Wang and Anderson method, with the exception of CSSC 12 soil standard, which has high inorganic C content compared to SOC and thus susceptible to over-estimation by the Wang and Anderson method (Fig. 3.1). The HCl fumigation method was also found to be more precise compared to the HCl addition method for the majority of the samples, as indicated by the lower standard deviation of the acid-fumigated samples (Table 3.2). This is in agreement with Chang et al. (1991) who also found the HCl vapor pre-treatment method to be more precise compared to the HCl liquid acid (0.5 N) addition method although both methods produced similar SOC measurement values. Hedges and Stern (1984) had recommended that the HCl fumigation method should not be used in case of highly calcareous soils (>50% wt. CaCO_3). However, the addition of a small amount of distilled water as recommended by Harris et al. (2001), hastened the decomposition of carbonates and ensured complete removal of all carbonates from all our samples (including the pure CaCO_3 standard material) upon HCl fumigation. Thus the HCl fumigation method, as described by Harris et al. (2001), is recommended as an efficient technique to completely remove all inorganic C present in the carbonaceous Saskatchewan soils, thus yielding accurate and precise SOC measurements.

Table 3.2 Carbon contents (wt %) of soil samples and standard materials measured by different C analysis methods.

Method	Targeted C form	Soil sample	N	Carbon (wt %)					
				Min	Max	Mean	Std. Deviation	Std. Error	
HCl-fumigation method	Organic C ¹	PA_1	5	0.66	0.76	0.70	0.039	0.017	
		Est_1	5	1.52	1.67	1.59	0.061	0.027	
		CSSC 12	5	0.21	0.29	0.25	0.030	0.014	
		CSSC 10	5	2.07	2.19	2.11	0.046	0.021	
		CSSC 7	5	3.43	4.01	3.77	0.238	0.107	
		CaCO ₃	4	0.05	0.10	0.07	0.020	0.010	
		Total C ²	PA_1	5	0.66	0.73	0.70	0.025	0.011
	Est_1		5	3.16	3.28	3.21	0.049	0.022	
	CSSC 12		5	2.06	2.14	2.10	0.036	0.016	
	CSSC 10		5	2.18	2.26	2.22	0.035	0.016	
	CSSC 7		5	3.80	3.94	3.90	0.058	0.026	
	CaCO ₃		5	12.03	12.39	12.19	0.152	0.068	
	HCl-addition method		Organic C ³	PA_1	5	0.35	0.60	0.49	0.104
		Est_1		5	1.45	1.79	1.67	0.151	0.068
CSSC 12		5		0.14	0.20	0.17	0.023	0.010	
CSSC 10		5		1.59	1.99	1.76	0.187	0.084	
CSSC 7		5		3.72	3.86	3.78	0.062	0.028	
CaCO ₃		5		0.00	0.03	0.00	0.019	0.009	
Total C ⁴		PA_1		5	0.67	0.74	0.70	0.026	0.011
		Est_1	5	3.13	3.22	3.18	0.033	0.015	
		CSSC 12	5	1.95	2.04	2.00	0.038	0.017	
		CSSC 10	5	2.33	2.41	2.37	0.031	0.014	
		CSSC 7	5	3.79	4.15	3.94	0.138	0.062	
		CaCO ₃	5	11.79	12.00	11.91	0.108	0.048	

Table 3.2 (continued) C contents (wt %) of all soil and standard materials under different C analysis methods

Method	Targeted C form	Soil sample	N	Carbon (wt %)				
				Min	Max	Mean	Std. Deviation	Std. Error
Wang and Anderson method	Organic C ⁵	PA_1	5	0.60	0.95	0.71	0.144	0.064
		Est_1	5	1.66	1.76	1.71	0.040	0.018
		CSSC 12	5	0.34	0.42	0.38	0.035	0.016
		CSSC 10	5	2.03	2.11	2.07	0.035	0.016
		CSSC 7	10	2.41	3.43	3.21	0.293	0.093
		CaCO ₃	5	0.16	0.52	0.34	0.131	0.059
		PA_1	5	0.65	0.80	0.73	0.064	0.028
	Total C ⁶	Est_1	5	3.05	3.44	3.20	0.177	0.079
		CSSC 12	5	1.99	2.12	2.07	0.056	0.025
		CSSC 10	5	2.33	2.40	2.37	0.028	0.013
		CSSC 7	5	3.69	4.05	3.92	0.138	0.062
		CaCO ₃	5	11.58	12.28	11.86	0.273	0.122
		PA_1	5	0.67	0.70	0.69	0.015	0.007
	Wang and Anderson method (with samples <250 µm)	Organic C ⁷	Est_1	5	1.70	1.75	1.72	0.020
CSSC 12			5	0.31	0.34	0.33	0.015	0.007
CSSC 10			4	2.00	2.03	2.02	0.014	0.007
CSSC 7			5	2.22	3.29	3.04	0.459	0.205
CaCO ₃			5	0.20	0.39	0.27	0.069	0.031

¹ SOC determination method including an HCl-acid (12 N) fumigation sample pre-treatment to remove soil carbonates; C analysis of ground soil samples (< 250 µm particle size) at 950°C without a time constraint (Amichev 2007; Harris et al. 2001)

² Total soil C (SOC plus carbonate-C) determination method of ground soil samples (<250 µm) at 950°C without a time constraint

³ SOC determination method including sample pre-treatment of multiple HCl-acid (6N) liquid additions (followed by drying) to remove soil carbonates; C analysis of ground soil samples (<250 µm) at 1100°C without a time constraint (LECO Inc. representative Liliane Eichenbaum, 2007, personal communication)

⁴ Total soil C determination method of ground soil samples (<250 μm) at 1100°C without a time constraint

⁵ Method to determine SOC; C analysis of the fine soil fraction (no grinding used, < 2mm particle size) at 840°C for 2 min (Wang and Anderson 1998)

⁶ Method to determine total soil C; C analysis of the fine soil fraction at 1100°C without a time constraint

⁷ Method to determine SOC; C analysis of ground soil samples (<250 μm) at 840 °C for 2 min.

A cautionary note about repeated analysis of HCl acid-pretreated soil samples is the potential of corrosion of internal components of the LECO C632 analyzer due to the evaporation of acid-derived chlorine compounds from the samples and their subsequent accumulation into the combustion tube of the analyzer. Despite using chlorine absorbent in the scrubber tube of the LECO C632 analyzer for chlorine removal, we noticed acid corrosion damage to the analyzer components. Kristensen and Andersen (1987) also reported corrosion inside the combustion system of their CHN analyzer from repeated analyses of acid-treated samples, although Amichev (2007) did not experience such corrosion damage to any components of the analyzer. Such damage may lead to leakage and malfunctioning of the instrument, which could be costly to repair.

In order to prevent acid corrosion damage to LECO analyzer components, the residual HCl concentration in the acid-treated samples has to be minimized. The excess acid may be removed by washing the samples after acidification. However, washing of the acid-treated samples leads to loss of acid-soluble organic matter resulting in the under-estimation of SOC content (Roberts et al., 1973). Increasing the temperature at which HCl-treated samples are dried after the pre-treatment, from 60°C to 105°C can decrease the residual HCl in the samples. At

105°C the capillary water inside the soil samples is evaporated, which may otherwise contain traces of dissolved HCl. While soil sample drying at high temperatures such as 105°C may alter some of the SOC fractions, we found no significant C loss from the HCl-fumigated samples (to which distilled water was added as part of the procedure). There were no significant differences between SOC measurements by the HCl-fumigation method with regular drying temperature (i.e. 60°C for 4 hours) and with increased temperature (105°C for 16 hours), respectively (Table 3.3). Previous studies have also used higher temperature in the estimation of SOC. Nieuwenhuize et al. (1994) dried the samples at 120°C for 1 hour to get rid of excess HCl without any loss of volatile organic matter. Similarly, Mills and Quinn (1979) did not find any loss of volatile organic carbon from drying the samples at 110°C for 4 hours. Hence, drying of acid-pretreated samples at 105°C for 16 hours, instead of 60°C for 4 hours is recommended to get rid of excess HCl in acid-treated samples. The residual HCl amount in the samples is also expected to be lower with HCl-fumigation method, compared to HCl-addition method.

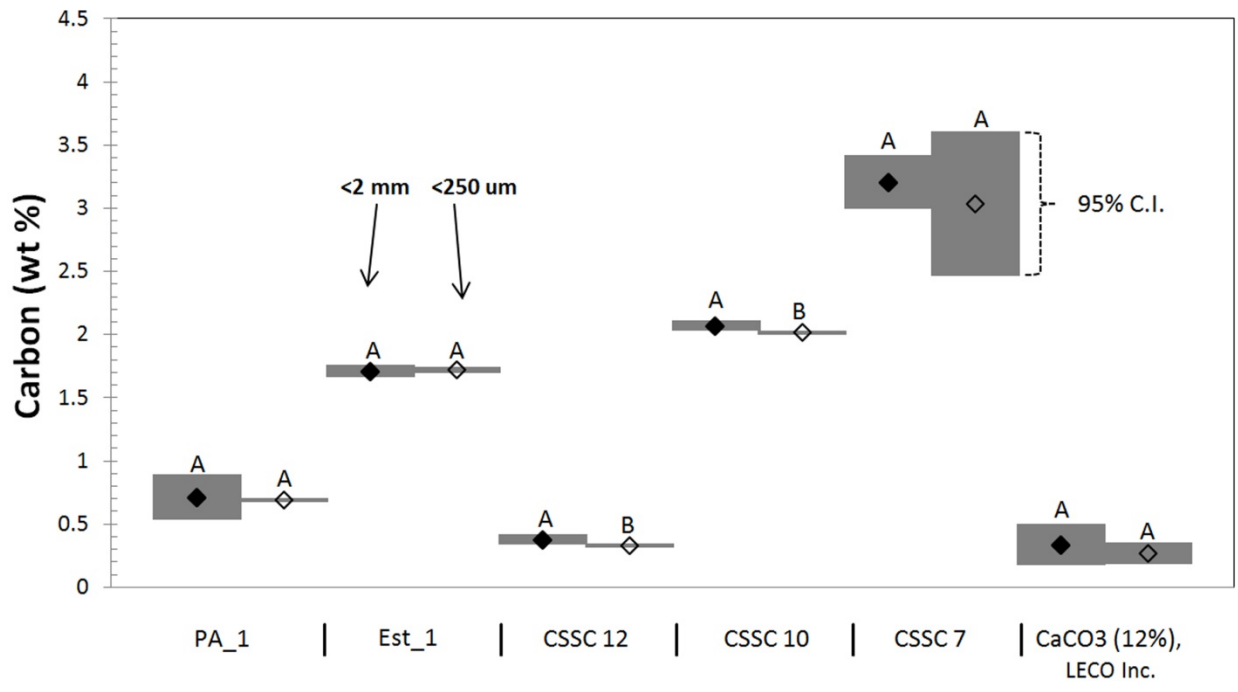
Table 3.3 Organic C content of acid-treated samples (ranging from high to low organic carbon) dried at low and high temperature conditions (n=4)

Sample no.	OC % (60°C for 4 hours)	OC % (105°C for 16 hours)	RMSE %	Bias %
1	5.85a†	5.65a	4.7	3.3
2	5.13a	4.82a	10.5	5.5
3	1.95a	1.89a	6.5	3.2
4	2.51a	2.58a	4.2	-2.9
5	0.72a	0.68a	8.5	4.7
6	0.81a	0.79a	18.3	1.7

†Values followed by same letter in a row are not significantly different at $p < 0.05$. RMSE is the root mean square error.

The effects of soil grinding (from <2 mm down to <250 µm particle size) and combustion temperature on the measurement of SOC were also studied. Soil grinding did not affect the

accuracy of measurement of organic C at 840°C and total C at 1100°C (Figs. 3.3 and 3.4). However, the measurement precision was higher in case of the ground samples as indicated by the lower standard deviation in case of <250 µm ground soils (Figs. 3.3 and 3.4). Similarly, different combustion temperatures (950°C vs. 1100°C) performed equally well for total C measurements, which were with similar accuracy and precision (Fig. 3.5). While the total C measurements for CSSC 10 and CSSC 12 soil standards as well as the CaCO₃ standard were significantly different at the temperatures of 950 and 1100°C, the lack of a consistent trend among these three samples indicates that these differences may be due to an experimental error in the subsampling and handling of samples (Fig. 3.5). Since soil grinding and combustion temperature have no significant effect on the accuracy of C measurement, it is reasonable to attribute any observed SOC differences to the methods used for the separation of organic and inorganic carbon in the carbonaceous soils of Saskatchewan.



Soil and standard samples

Fig. 3.3 Effect of soil grinding on C measurement variability (N=5) at 840°C for 120 seconds. Height of boxes surrounding each plotted mean indicates the 95% confidence interval of the mean C concentration value. For each sample, same upper case letters indicate no significant difference between C concentrations of non-ground (<2 mm particle size) and ground soil samples (<250 μm particle size).

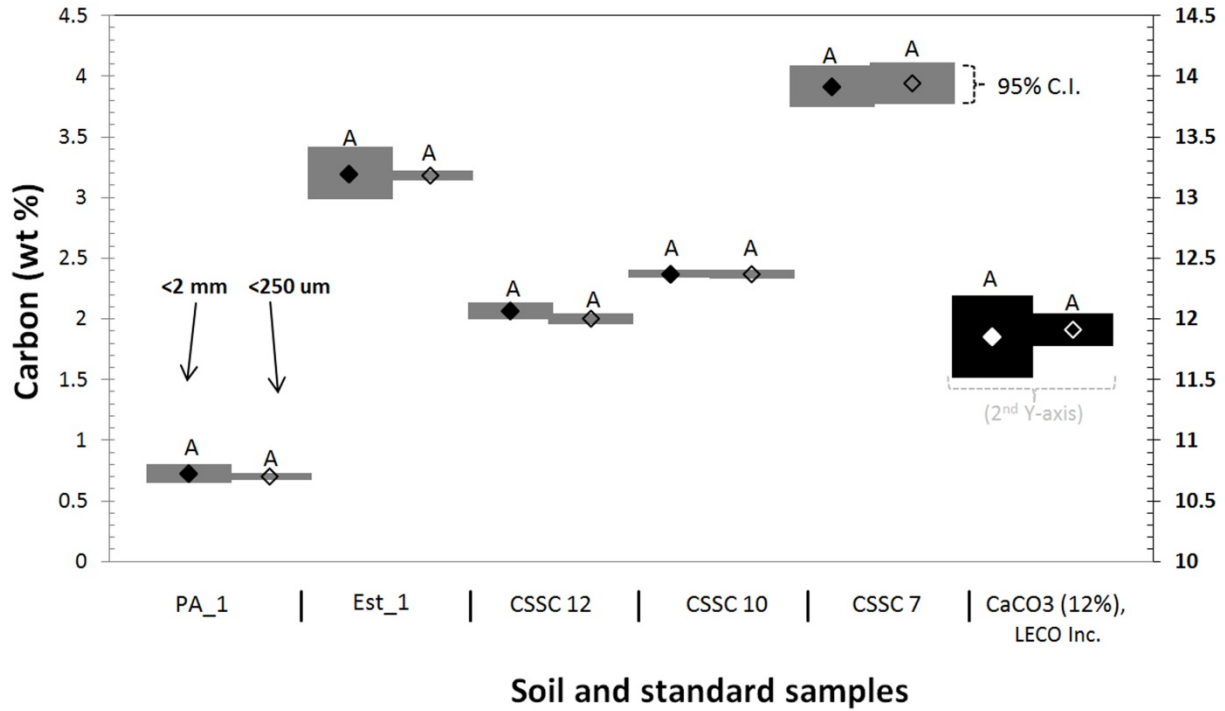


Fig. 3.4 Effect of soil grinding on total C measurement variability (N=5) at 1100°C. Height of boxes surrounding each plotted total C mean indicates the 95% confidence interval of the mean total C concentration value. For each sample, same upper case letters indicate no significant difference between total C concentrations of non-ground (<2 mm particle size) and ground soil samples (<250 μm particle size).

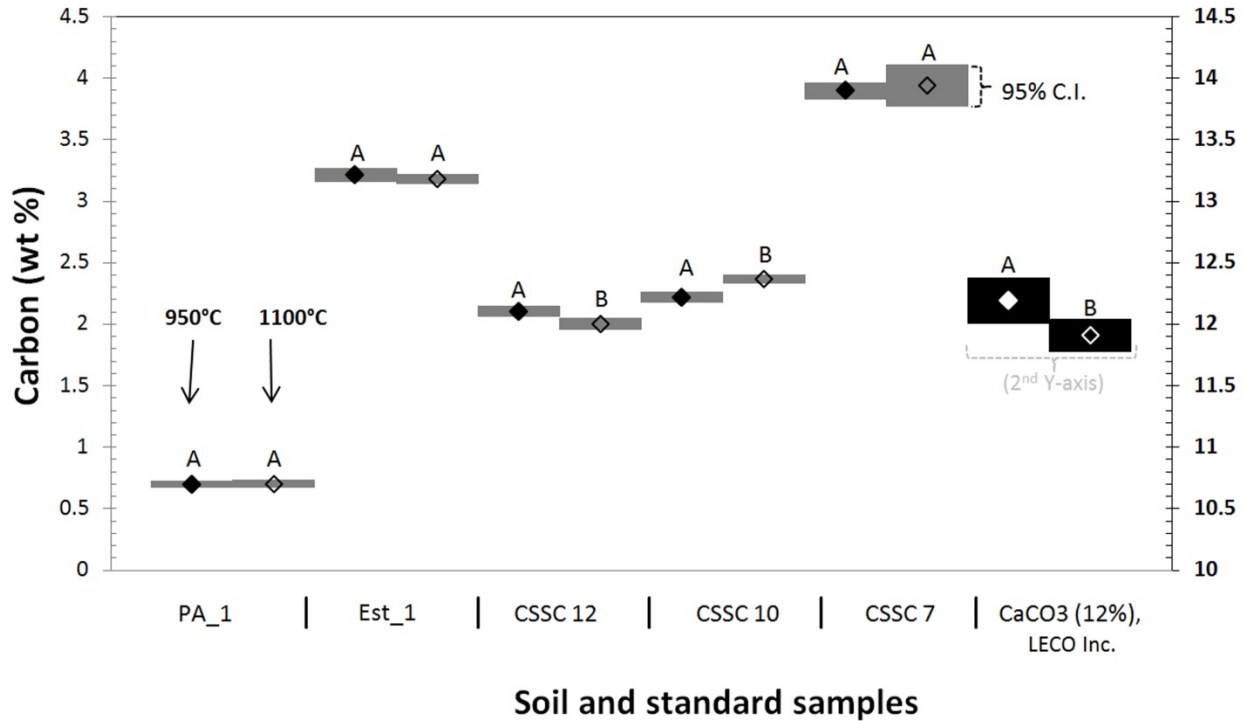


Fig. 3.5 Effect of combustion temperature on total C measurement (N=5) of ground soil and standard material samples (<250 μm particle size). Height of boxes surrounding each plotted mean indicates the 95% confidence interval of the mean total C concentration value. For each sample same upper case letters indicate no significant difference between C concentrations measured at 950 and 1100 $^{\circ}\text{C}$ combustion temperature.

3.6 Conclusions

Among the methods used to determine the SOC concentration in carbonaceous soils, we recommend the SOC measurement procedure based on HCl-acid (12 N) fumigation (Harris et al., 2001) as carbonate-removal pretreatment followed by elemental C analysis via automated C analyzer. With these modifications, the method is less susceptible to over-estimation of organic C due to interference by the carbonates compared to the Wang and Anderson method and is more precise compared to the method involving HCl acid addition as the pre-treatment. It is recommended that all HCl-fumigated samples be dried at higher temperatures (105 $^{\circ}\text{C}$ for 16

hours) prior to elemental C analysis in order to avoid any potential acid corrosion damage to any components of the C analyzer instrument.

4. SOIL CARBON SEQUESTRATION FOR SHELTERBELT AGROFORESTRY SYSTEMS IN SASKATCHEWAN²

4.1 Preface

Shelterbelts have been widely planted around the agricultural fields in Canadian Prairie provinces, including Saskatchewan, mainly to prevent damage by wind erosion. In addition to their ecological advantages, they may also provide the additional benefit of sequestering C, thus helping to offset the atmospheric CO₂ levels and combat climate change. However, few studies have examined the potential of shelterbelts to sequester CO₂, especially in the form of soil organic carbon (SOC). This chapter seeks to estimate the SOC sequestration potential of major shelterbelt species in Saskatchewan, compared to their adjacent agricultural fields. It also examines the influence of shelterbelt characteristics such as tree species, stand age, stand structure and design, on their ability to sequester C in soils.

² This chapter, co-authored with Dr. Ken Van Rees, has been submitted for publication to Canadian Journal of Soil Science. The laboratory and data analyses, and initial writing of the manuscript were completed by the lead author (Gurbir Singh Dhillon), and editing and review of manuscript was done by the co-authors.

4.2 Abstract

Carbon (C) sequestration through the implementation of agroforestry practices is identified as one of the major strategies in the reduction of greenhouse gas (GHG) emissions from the agricultural sector. The objective of this study was to examine the soil C sequestration potential of major hardwood and conifer shelterbelts across the five soil zones of Saskatchewan compared to agricultural fields. Soil samples were collected for six major shelterbelt species including green ash (*Fraxinus pennsylvanica*), hybrid poplar (*Populus* spp.), Manitoba maple (*Acer negundo*), white spruce (*Picea glauca*), Scots pine (*Pinus sylvestris*) and caragana (*Caragana arborescens*) and the adjacent agricultural fields and measured for soil organic carbon (SOC). Shelterbelts had a significantly higher amount of SOC compared to adjacent agricultural fields with an average increase of 6-38 Mg C ha⁻¹ depending on shelterbelt species. An additional 3-8 Mg C ha⁻¹ was contained in the tree litter layer. Younger shelterbelts tended to lose SOC in the early years of shelterbelt establishment; however, the SOC accrual was positively related to shelterbelt stand age. Besides stand age, other shelterbelt stand characteristics, including tree height and diameter, crown width and density of litter layer were also positively correlated with the increase in SOC concentration, and all variables together explained 56-67% of the variability in the amount of SOC sequestered within the shelterbelt sites. Highest amount of SOC accumulated in the 10-30 cm soil depth and was attributed to root-C inputs. The findings of this study support the hypothesis that shelterbelts as an agroforestry system can lead to a significant amount of soil C sequestration for agroecosystems.

4.3 Introduction

The increase in temperature of the earth's near-surface air and oceans in recent decades, known as global warming, is among the most serious of the contemporary environmental issues

(Nair et al., 2010). The global mean temperature is further expected to increase by 1.0-3.5°C over the next century due to the increase in atmospheric greenhouse gas (GHG) concentrations, especially carbon dioxide (CO₂) (IPCC, 1995; Wu et al., 2011). Soils are the largest terrestrial pool of organic carbon (C) and have a significant potential of storing carbon by acting as carbon sinks, thereby removing CO₂ from the atmosphere (Canadell et al., 2007; Powlson et al., 2011). A 5-15% increase in the amount of soil organic carbon (SOC) stored in the soils up to a 2 m depth could decrease atmospheric CO₂ concentration by 16–30% (Baldock, 2007; Kell, 2011). Currently, agricultural activities are a major source of anthropogenic GHG emissions and contribute to about 20% of global GHG emissions (Lokupitiya and Paustian, 2006). Cultivated Canadian soils are reported to have lost about 15-35% of the organic carbon compared to the pre-settlement levels, thus contributing to the build-up of GHG levels (Dumanski et al., 1998). However, implementation of proper agricultural management practices has the potential to increase C stocks in agricultural soils globally by about 400 to 800 Mt C yr⁻¹ (Cole et al., 1996; Paustian et al., 2000). Thus, there is a need to adopt sustainable agroecosystem management practices to encourage the long-term sequestration of C in soils in order to reduce the terrestrial GHG emissions to the atmosphere.

Agroforestry systems, consisting of the deliberate association of trees with crops on the same land-unit, have been recommended by the Intergovernmental Panel on Climate Change (IPCC) as a sustainable alternative to single-crop systems in order to mitigate GHG emissions (Schoeneberger, 2009). Such systems have the ability to sustain or enhance agricultural productivity (Kang et al., 1985; Kort, 1988; Thevathasan and Gordon, 1995), while also helping in soil conservation (Montagnini and Nair, 2004), maintenance of soil fertility (Thevathasan and Gordon, 2004), restoration of degraded ecosystems (Montagnini, 2001) and nutrient and organic

matter cycling and retention in soils (Fassbender et al., 1987; Beer, 1988). Shelterbelts or windbreaks is an agroforestry practice that consists of linear rows of trees around agricultural fields, primarily for the purpose of controlling wind speed and erosion in order to protect soils, crops and farmyards (Brandle et al., 2004; Mize et al., 2008). Shelterbelts have been historically planted extensively on the Canadian prairies and Great Plains of the USA since the early nineteenth century (Watters, 2002; Udawatta and Jose, 2011) and are associated with a variety of social, monetary and ecological benefits including snow entrapment and moisture retention (Scholten, 1988), increase in crop and livestock productivity (Kort, 1988) and enhancement of agricultural landscapes (Cook and Cable, 1995; Cable, 1999). Along with these ecological benefits, shelterbelts also offer great potential for C sequestration (Brandle et al., 1992; Kort and Turnock, 1998). Kort and Turnock (1998) estimated the aboveground C sequestration potential in the shelterbelts of Canadian prairies to range from 11-105 Mg C km⁻¹ depending upon the tree species. However, these C stock estimates did not include belowground biomass and soil C stocks. In order to gain complete and accurate assessment of the C sequestration potential of the shelterbelts, C stock estimates should also include soil C and tree litter estimates along with the biomass (Nair and Nair, 2003).

There are a number of studies that advocate the strong potential benefits of incorporation of trees into the agricultural fields for the sequestration of C in soils (Nair et al., 2009a). Trees can be significant sinks of atmospheric C compared to agricultural crops primarily due to high C inputs associated with aboveground litter and decomposition of fine roots of trees (Young, 1997; Oelbermann et al., 2004). However, only a few studies have determined C storage in the soils under agroforestry systems (Peichl et al., 2006; Sauer et al., 2007; Baah-Acheamfour et al., 2015), and our understanding of C sequestration and dynamics under agroforestry systems is

inadequate (Nair et al., 2009b). While the studies on afforestation (Paul et al., 2002; Laganier et al., 2010a; Vesterdal et al., 2013) may provide insight on the effect of agroforestry trees on SOC storage, the C sequestration potential of agroforestry systems is expected to be different from afforested tree plantations or conventional forests due to differences in tree configurations and growth patterns (Udawatta and Jose, 2011). Moreover, the findings about SOC sequestration potential of afforested and tree plantation systems are also not consistent. While some studies indicate high soil C sequestration potential (Jenkinson, 1970; Garten, 2002), other studies have demonstrated limited to no increase in the soil C stocks (Richter et al., 1999). Agroforestry systems may also differ amongst themselves in terms of C sequestration potential, since the productivity of agroforestry systems varies greatly depending upon biophysical characteristics of the systems such as age, stand structure as well as management practices (Albrecht and Kandji, 2003). Thus, there is a need to determine the soil C storage under different agroforestry systems under varying ecological conditions in order to obtain a better understanding of soil carbon sequestration potential of these systems.

The objectives, therefore, of this study, were to (i) determine the role of six shelterbelt species in facilitating long-term C storage in the mineral soil (0–50 cm) and litter layer compared to adjacent agricultural fields, and (ii) identify the influence of various biophysical characteristics associated with the shelterbelts, including stand age and structure, tree species and shelterbelt design characteristics, on the SOC sequestration potential of shelterbelts. This study is based on the hypothesis that soil C storage under the shelterbelts will be greater compared to adjacent agricultural fields.

4.4 Materials and Methods

4.4.1 Selection of study sites

Six shelterbelt species - green ash (*Fraxinus pennsylvanica*), hybrid poplar (*Populus* spp.), Manitoba maple (*Acer negundo*), white spruce (*Picea glauca*), Scots pine (*Pinus sylvestris*) and caragana (*Caragana arborescens*) were sampled for this study. The shelterbelt sites for sampling were identified by a site-selection approach that has been described in detail by Amichev et al. (2016). Briefly, 106 ecodistricts within Saskatchewan, as defined by the National Ecological Framework for Canada, were grouped into 31 soil zone clusters based on the similarity of 32 climatic, site and soil variables obtained from the national ecological framework for Canada dataset and 10 additional variables taken from the data of the Soil Landscapes of Canada (SLC v3.2). In this way, the agricultural land area of Saskatchewan within the five soil zones was divided into a manageable number of clusters for further analysis. The cluster with the highest number of trees shipped for shelterbelt planting of a particular species, according to the Prairie Farm Rehabilitation Administration (PFRA) tree orders database, was chosen for sampling of that species. Green ash, hybrid poplar, and Scots pine had the highest tree numbers in the Black soil zone, caragana in the Brown soil zone, Manitoba maple in the Dark Brown soil zone and white spruce in the Dark Gray soil zone. The randomized branch sampling (RBS) procedure was applied within each of the chosen soil clusters in order to randomly select the specific sampling sites for each of the shelterbelt species. A total of 59 sites were selected on the arable portions of Saskatchewan across the Boreal Plain and Prairie ecozones (Fig. 4.1). The selected sites consisted of 10 sites each for hybrid poplar, Manitoba maple and caragana, 11 sites for Scots pine and nine sites for green ash and white spruce shelterbelts.

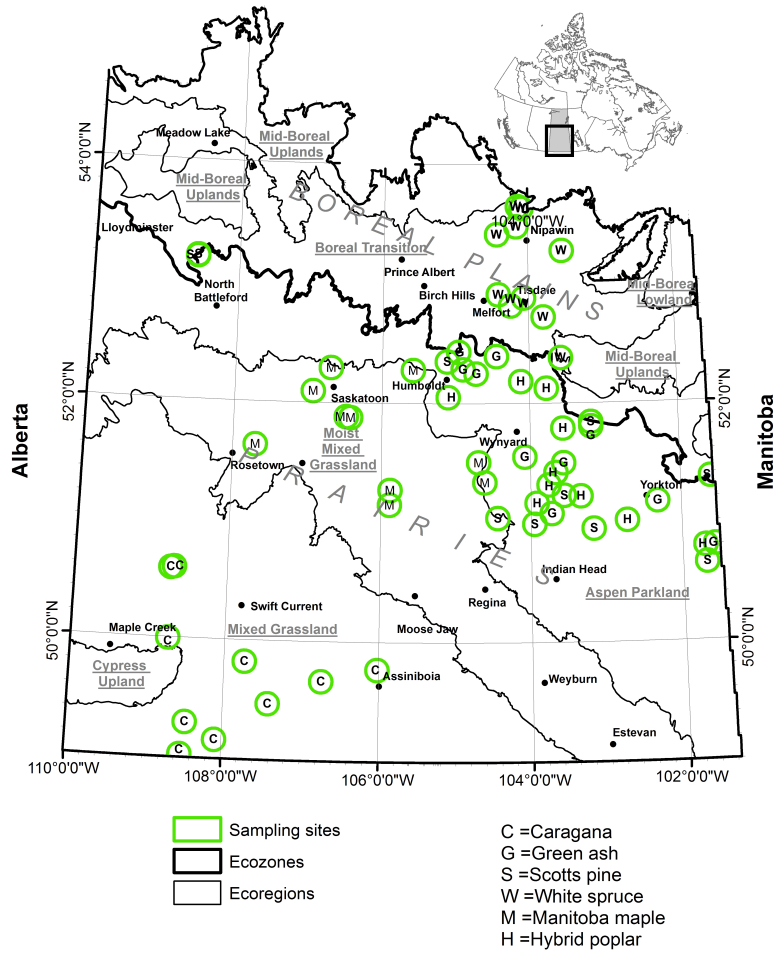


Fig. 4.1 Distribution of sampling sites for six shelterbelt species (hybrid poplar, white spruce, green ash, Manitoba maple, caragana, Scots pine) within Saskatchewan, Canada.

4.4.2 Sampling procedure

At each sampling site, three replicate locations (20 m apart) were chosen for soil sampling along a transect in the middle of the shelterbelt row. Similarly, three replicate locations were chosen in the adjacent agricultural field at a fixed distance perpendicular to the shelterbelt. The distance of the field transect from the shelterbelt was more than twice the height of the shelterbelt trees to avoid the influence of the shelterbelts and ranged from 50 to 100 m. At each replicate location, soil samples were collected at 0-5, 5-10, 10-30 and 30-50 cm depths using a hand auger (6.58 cm dia.). Prior to soil sampling, aboveground tree litter was also collected at each site from a 0.5 m x 0.5 m area centered on sampling points within the shelterbelt row. Soil bulk density was measured for both the shelterbelt and field sites at 0-10 cm, 10-30 cm and 30-50 cm by using a core sampler (5.4 cm dia. x 3 cm length). Soil and litter samples were collected in plastic bags and air-dried at room temperature prior to processing and storage for laboratory analysis. At each sampling site, tree diameter at breast height (DBH), and tree height measurements were taken for hardwood and coniferous trees. For caragana shelterbelts, diameter was obtained at 30 cm height from the ground. Additionally, crown width of trees was measured by taking the average of four measurements, including two measurements diagonally through the tree canopy to make an 'x', one measurement straight through the canopy perpendicular to the shelterbelt row and one measurement parallel to the shelterbelt row on the outside of the tree canopy. Tree age was determined by using an increment borer to obtain tree cores, which were later analyzed in the lab.

4.4.3 Laboratory analyses

Soil and litter samples were ground and sieved to a size of $< 250 \mu\text{m}$. Soil pretreatment consisting of an acid fumigation procedure with concentrated hydrochloric acid (12N HCl) to remove soil carbonates was performed on the soil samples for accurate estimation of SOC (Dhillon et al., 2015; Harris et al., 2001). Approximately 0.25 g of the powdered soil sample was placed in a silver boat liner, weighed, and 1 ml of distilled water was added to the soil samples in order to moisten them, which increased the efficiency of carbonate removal by the HCl fumes (Harris et al., 2001). The moistened samples were exposed to the HCl-fumes by placing them in a vacuum desiccator along with a 150-ml beaker with 100 ml of concentrated HCl (12 M) for 24 hours to remove soil carbonates. Finally, the carbonate-free samples were heated in a ventilated area with a drying oven at 105°C for 16 hours to remove the residual moisture and excess HCl. These samples were analyzed for SOC content by using an automated C632 LECO analyzer (LECO Corporation, St. Joseph, MI, USA) at a combustion temperature of 1100°C and a maximum combustion time of 10 minutes. Soil bulk density was determined by oven-drying the soil samples at 105°C for 24 hours and dividing the oven-dried mass of the sample with the core volume. Pools of SOC (Mg ha^{-1}) under the shelterbelts and fields were determined using the measured bulk density values (g cm^{-3}) and the SOC content (%) of the samples. Carbon stocks in the litter were determined using the measured C content of litter samples (%), litter mass (g) and sampling area (0.25 m^2). A weighted average of SOC concentration for the whole soil profile (0-50 cm soil depth) was calculated based on the SOC concentration of the individual soil layers (0-5, 5-10, 10-30 and 30-50 cm).

4.4.4 Statistical analyses

Data were analyzed using a two-way mixed analysis of variance (ANOVA) procedure, with the land cover (i.e. shelterbelts vs. fields) analyzed as the within-subjects factor. In the presence of a significant interaction, simple main effects were considered. Residuals were checked for normality using Q-Q plots. Assumption of sphericity and homogeneity of covariance were checked using Mauchly's test of sphericity and Box's test of equality of co-variance matrices, respectively. One-way analysis of variance (ANOVA), followed by post-hoc analysis by Fisher's LSD, was performed to examine the differences among shelterbelt species. In addition, hierarchical multiple regression analysis was performed in order to estimate the effect of stand characteristics as explanatory variables on the increase in SOC concentration under the shelterbelts. Pearson correlation analysis was performed in order to determine the relationship between stand characteristics and the increase in SOC concentration. For the statistical analysis, a p-value of 0.1 was used to assess the significance. This was done in order to reduce the risk of failing to detect the existing differences between land use types (type II error), since a substantial variation in the soil properties and vegetation composition was expected due to the geographic expansion of the study. Statistical analysis was performed with IBM SPSS Statistics version 23 (IBM Inc., Armonk, NY, USA).

4.5 Results

4.5.1 SOC distribution and pools under shelterbelts and fields

There was a significant increase in the concentration of SOC for shelterbelts compared to agricultural fields at all soil depths (Table 4.1; Fig. 4.2a). Mean SOC concentration across the soil profile was greater by 30% for shelterbelts compared to the agricultural fields. Similar to SOC concentration, SOC stocks, expressed as the areal mass (Mg ha^{-1}), were also greater for

shelterbelts. However, the increase in SOC stocks (19%) was less pronounced compared to the increase in SOC concentration (30%), which can be attributed to lower soil bulk density under the shelterbelts compared to the agricultural fields (Fig. 4.2b). Soil bulk density of shelterbelts was lower by 13% at 0-10 cm depth and 7% at 10-30 cm depth compared to agricultural fields. The magnitude of increase in SOC concentration of the shelterbelts was highest at 0-5 cm (11.5 g kg⁻¹) and declined with soil depth at 5-10 (6 g kg⁻¹), 10-30 (6.5 g kg⁻¹) and 30-50 cm (0.9 g kg⁻¹; Fig. 4.2a). In contrast, the percentage increase in SOC concentration for the shelterbelts was highest at 10-30 cm soil depth (43%), compared to 0-5 (37%), 5-10 (23%) and 30-50 cm (8%) soil depths. Similarly, maximum amount of SOC was sequestered at 10-30 cm depth, which showed a 34% increase in SOC stocks for shelterbelts with an average sequestration of 13 Mg C ha⁻¹. The surface layer (0-10 cm soil depth) sequestered around 4 Mg C ha⁻¹ of SOC that was equivalent to an increase of about 12% in SOC stocks, while the 30-50 cm soil layer sequestered around 1.4 Mg C ha⁻¹, equivalent to an increase of 5% in SOC stocks.

Table 4.1 Two-way mixed analysis of variance (ANOVA) of the effect of land cover type (i.e. shelterbelts and fields) within different soil clusters on the SOC concentration (g kg⁻¹) at 0-5, 5-10, 10-30 and 30-50 cm soil depths.

Depth (cm)	Land cover type			Soil Cluster			Interaction		
	df	F	P	df	F	P	df	F	P
0-5	1	30.32	<0.005	5	9.22	<0.005	5	2.57	0.04
5-10	1	18.38	<0.005	5	12.32	<0.005	5	1.62	0.17
10-30	1	49.51	<0.005	5	11.93	<0.005	5	2.16	0.07
30-50	1	6.48	0.01	5	0.68	0.64	5	0.32	0.12

Table 4.2 Mean SOC concentrations (g kg^{-1}) of shelterbelts and fields for different shelterbelt species at 0-5, 5-10, 10-30 and 30-50 cm soil depths.

Species	Land cover	Soil Depth (cm)			
		0-5	5-10	10-30	30-50
Hybrid Poplar	Shelterbelt	52.4 (6.2) a†	42.5 (3.4) a	27.3 (1.9) a	13.1 (1.5) a
	Field	31.8 (2.7) b	29.2 (2.9) b	16.1 (1.9) b	10.3 (1.2) b
White Spruce	Shelterbelt	57.9 (8.8) a	31.0 (4.6) a	19.1 (2.1) a	11.9 (1.8) a
	Field	37.1 (3.9) b	27.4 (3.4) a	11.5 (1.7) b	10.1 (1.8) b
Green Ash	Shelterbelt	46.8 (5.2) a	43.2 (4.6) a	30.4 (3.4) a	11.9 (0.8) a
	Field	46.0 (2.0) a	40.3 (1.7) a	23.5 (2.3) b	11.7 (0.6) a
Manitoba maple	Shelterbelt	34.8 (3.4) a	25.6 (2.4) a	17.5 (1.6) a	9.8 (0.5) a
	Field	29.6 (2.8) a	23.1 (2.3) a	14.1 (1.1) a	9.7 (0.6) a
Caragana	Shelterbelt	23.4 (4.0) a	17.0 (2.3) a	11.9 (1.1) a	9.8 (1.0) a
	Field	15.8 (1.7) b	12.6 (0.5) b	9.9 (0.6) a	9.7 (0.7) a
Scots Pine	Shelterbelt	44.3 (4.4) a	34.0 (4.6) a	23.5 (3.0) a	10.9 (1.1) a
	Field	30.4 (1.9) b	25.4 (1.9) b	15.8 (1.2) b	10.5 (1.2) a

† Values with the same letter within a column and shelterbelt species group are not significantly different at $p < 0.1$.

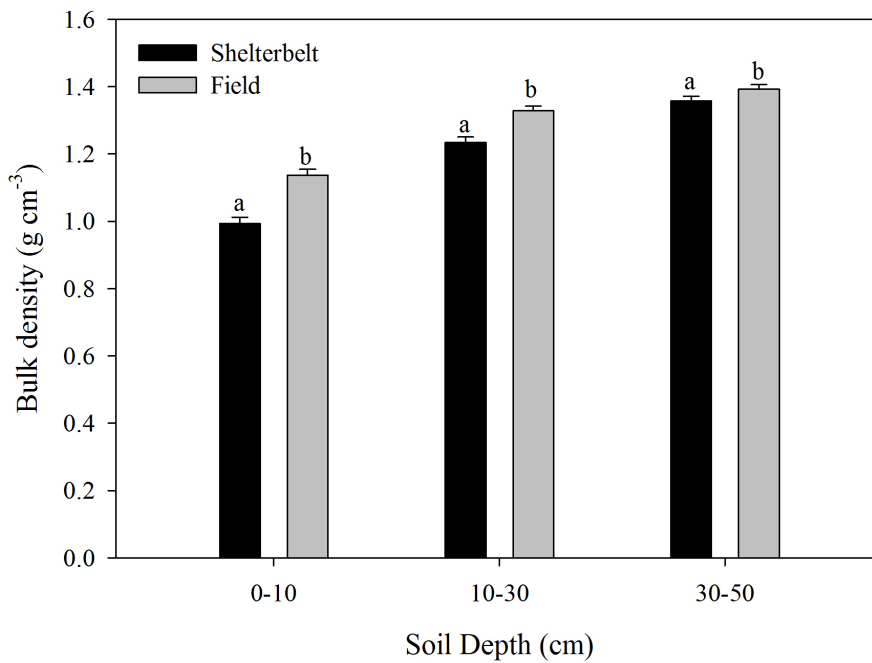
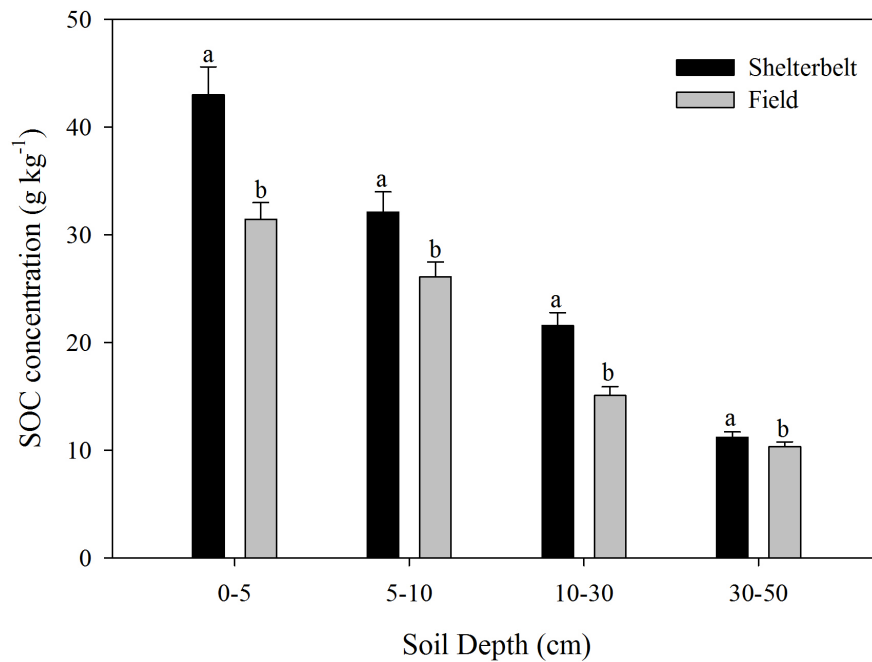


Fig. 4.2 Mean SOC concentration (a) and soil bulk density (b) of shelterbelts and fields at 0-5, 5-10, 10-30, and 30-50 cm soil depths. Bars represent standard error. Bars with the same letter within a soil depth are not significantly different at $p < 0.1$.

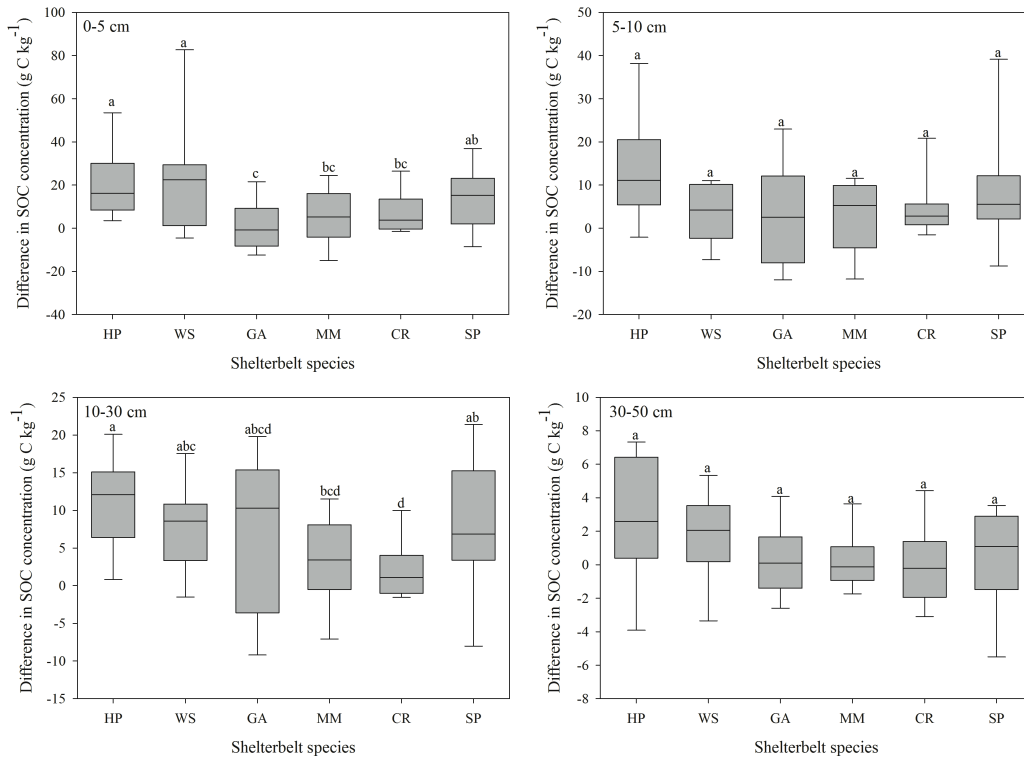


Fig. 4.3 Difference in SOC concentration (g C kg^{-1}) of different shelterbelt species (HP- Hybrid poplar; WS – White spruce; GA – Green ash; MM – Manitoba maple; CR- Caragana; SP – Scots pine) compared to adjacent fields at the 0-5, 5-10, 10-30, and 30-50 cm soil depths. Species with same letter are not significantly different at $p < 0.1$.

Differences in SOC concentration for shelterbelts varied with the species of shelterbelt plantation (Table 4.2; Fig. 4.3). At 0-5 cm soil depth, the maximum difference in the mean SOC concentration under shelterbelts compared to fields was observed for white spruce ($+20.8 \text{ g C kg}^{-1}$) and hybrid poplar shelterbelts ($+20.7 \text{ g C kg}^{-1}$), followed by Scots pine ($+13.9 \text{ g C kg}^{-1}$), caragana ($+7.6 \text{ g C kg}^{-1}$), Manitoba maple ($+5.1 \text{ g C kg}^{-1}$), and green ash ($+0.8 \text{ g C kg}^{-1}$). At 10-30 cm soil depth, the difference in SOC concentration for hybrid poplar shelterbelts ($+11.2 \text{ g C kg}^{-1}$) was higher compared to Manitoba maple ($+3.4 \text{ g C kg}^{-1}$) and caragana ($+2.1 \text{ g C kg}^{-1}$). The difference between species was not statistically significant at 5-10 and 30-50 cm soil depths (Fig. 4.3). Averaged across the entire soil profile (0-50 cm), the maximum difference in mean SOC concentration compared to adjacent agricultural fields was observed for hybrid poplar ($+54\%$)

shelterbelts, followed by white spruce (+41%), Scots pine (+34%), caragana (+19%), Manitoba maple (+15%) and green ash (+14%) shelterbelts. Similarly, the average differences in SOC stocks (0-50 cm depth) between shelterbelts and the adjacent agricultural fields were positive for all shelterbelt species, and decreased in the order of: hybrid poplar (+ 38 Mg C ha⁻¹), white spruce (21 Mg C ha⁻¹), Scots pine (+ 20 Mg C ha⁻¹), green ash (+15 Mg C ha⁻¹), Manitoba maple (+ 11 Mg C ha⁻¹) and caragana (+ 6 Mg C ha⁻¹) (Table 4.3).. Besides the SOC stored in the mineral soil profile, additional carbon was also stored in the litter layer under the shelterbelts. Mean carbon storage in the litter layer varied from 3.1 Mg ha⁻¹ to 8.3 Mg ha⁻¹ with the highest litter C found for Scots pine and white spruce shelterbelts (Table 4.3).

Table 4.3 Mean SOC stock (Mg ha⁻¹) in the litter layer, 0-10, 10-30 and 30-50 cm soil layers under the shelterbelts and fields for different shelterbelt species.

Species†	Litter	Soil Depth (cm)					
		0-10		10-30		30-50	
		Shelterbelt	Field	Shelterbelt	Field	Shelterbelt	Field
HP	5.0 (0.8)	43.2 (3.5) a‡	34.4 (2.9) b	64.9 (4.6) a	42.4 (4.7) b	35.3 (3.6) a	28.6 (3.2) b
WS	5.6 (0.9)	39.2 (4.2) a	34.5 (3.7) a	42.2 (5.3) a	29.0 (4.1) b	30.2 (4.2) a	27.0 (4.9) a
GA	3.1 (0.7)	43.4 (3.2) a	44.5 (2.1) a	75.3 (8.4) a	58.3 (5.9) a	30.6 (1.9) a	31.2 (1.9) a
MM	3.6 (0.8)	33.5 (3.0) a	29.8 (2.2) a	45.7 (5.0) a	38.3 (2.6) a	27.3 (1.2) a	26.9 (1.6) a
CR	3.2 (0.5)	20.4 (2.6) a	17.3 (1.3) a	31.1 (2.5) a	27.4 (1.4) a	28.0 (2.8) a	29.0 (2.4) a
SP	8.3 (1.3)	37.3 (3.7) a	33.0 (2.3) a	58.0 (6.9) a	42.4 (3.1) b	29.2 (2.8) a	29.2 (3.4) a

†Abbreviations: HP- Hybrid poplar; WS – White spruce; GA – Green ash; MM – Manitoba maple; CR- Caragana; SP – Scots pine

‡Values with different letters within a row at each soil depth are not significantly different at $p < 0.1$.

Soil organic carbon stored in the top 50 cm of soil for shelterbelts and adjacent agricultural fields averaged 119.1 Mg ha⁻¹ and 100.5 Mg ha⁻¹, respectively. Thus, there was an average increase of 18.6 Mg ha⁻¹ of SOC for shelterbelts in the mineral soil. The estimates of SOC sequestered under the shelterbelts varied from a loss of SOC of 49 Mg ha⁻¹ to a gain of 85 Mg ha⁻¹ of SOC for different shelterbelt sites. The younger shelterbelt plantations tended to show a loss in SOC compared to the agricultural fields (Fig. 4.4). Out of the 59 sites studied, 16 sites showed a loss of SOC for the shelterbelts. Of these 16 sites, 13 sites had a stand age of 20 years or less. While the younger shelterbelts showed negative SOC accrual, SOC accrual rates increased with an increase in shelterbelt age and tended to stabilize with shelterbelt maturity. The median SOC accrual rate was 0.7 Mg C ha⁻¹ year⁻¹ for shelterbelt plantations, ranging in age from 5 to 63 years.

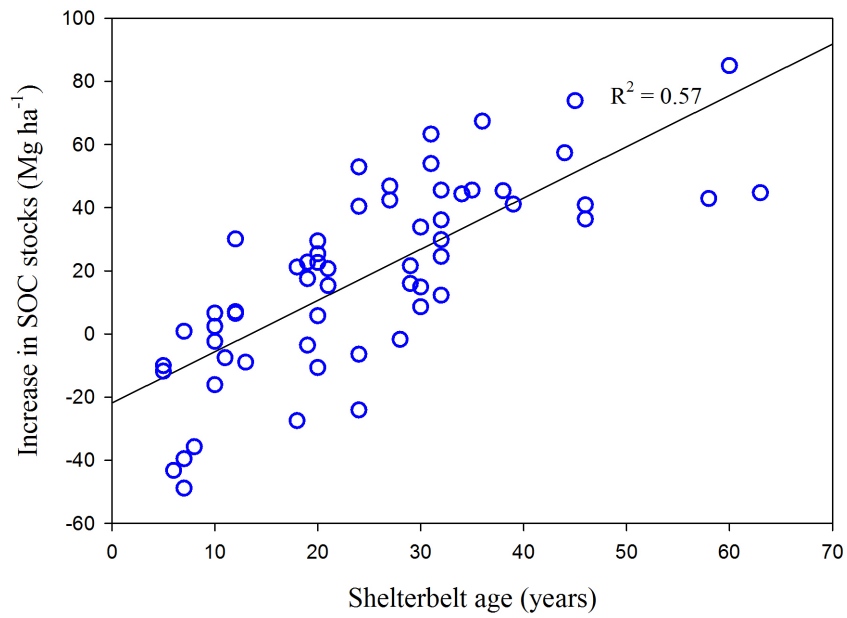


Fig. 4.4 Relationship between the difference in SOC stocks (Mg ha⁻¹) of shelterbelts compared to adjacent fields and shelterbelt age.

Table 4.4 Mean stand characteristics for the six shelterbelt species.

Stand characteristics	Hybrid poplar	White spruce	Green ash	Manitoba maple	Caragana	Scots pine
Tree Spacing - by length (m)	2.6a	2.7a	2.2a	2.6a	0.9b	2.7a
Tree Spacing - by width (m)	2.5b	2.5b	5.7a	2.5b	0.3c	2.9b
Shelterbelt length (m)	66.9b	82.7b	77.2b	62.9b	301.0a	36.8b
Shelterbelt area (m ²)	1021.1a	749.3a	1285.0a	1161.6a	1246.5a	401.5a
Avg. Crown Width (m)	8.7a	4.7b	4.5b	5.0b	4.8b	5.7b
Avg. Tree height (m)	14.6a	7.8b	6.8bc	4.4cd	3.0d	8.8b
Avg. Tree Diameter (cm)	26.1a	17.4bc	12.7cd	11.8d	n/a	19.5b
Stand age (yrs)	30.6a	27.4a	19.6a	21.7a	18.2a	31.3a
Mortality (%)	17.9a	22.8a	9.6a	17.3a	2.9a	13.1a
Trees per kilometer	396.6b	341.1b	486.9b	368.8b	1301.3a	380.1b
Amount of litter (g m ⁻²)	1170.8bc	1424.4ab	802.6c	1015.1bc	1006.9bc	1767.5a

† Values with the same letter within a row are not significantly different at $p < 0.1$.

*n/a – not available

4.5.2 Shelterbelt characteristics and soil organic carbon

Stand characteristics are considered to be important in regulating the SOC stocks; thus, they were compared as potential determinants of SOC accrual for shelterbelts. The stand characteristics that were considered included biotic factors such as tree height, tree diameter, crown width and abiotic factors such as shelterbelt design characteristics including tree density and spacing etc. While the SOC content is known to be strongly related to climatic factors such as precipitation and temperature, as well as soil properties such as texture (Paul et al., 2002), these factors were assumed to be uniform within the shelterbelt plantation and the agricultural field and hence not considered. This assumption is reasonable given the close proximity of each

shelterbelt to its reference field in the paired site design. The stand characteristics of all the shelterbelt species are summarized in Table 4.4 while the stand characteristics for the individual sites are summarized in Appendices A-F.

Hybrid poplar shelterbelts had significantly higher average crown width, tree height and tree diameter compared to the other shelterbelt species (Table 4.4). The coniferous species, white spruce and Scots pine, also had higher average tree height and tree diameter compared to green ash, Manitoba maple and caragana. Similarly, the density of the litter layer was also high in Scots pine compared to the hardwood species and caragana shelterbelts. Tree density was highest for caragana, but did not differ significantly for other shelterbelt species. Pearson correlation analysis indicated that the stand characteristics were strongly correlated with each other (Table 4.5). Stand age was positively correlated with average tree height (Pearson correlation coefficient (r) = 0.605, $p < 0.001$), average tree diameter ($r = 0.627$, $p < 0.001$), average crown width ($r = 0.411$, $p = 0.001$), and the amount of litter produced ($r = 0.719$, $p < 0.001$). Similarly, there was strong relationship between average tree height, average tree diameter, average crown width and amount of litter (Table 4.5). However, there was also a strong correlation between the stand characteristics and the increase in SOC concentration under the shelterbelts (Table 4.6). Across all depths, the increase in SOC content was positively related to the age of shelterbelt, average tree diameter and tree height, average crown width of the trees and the amount of litter produced. Tree density (trees per kilometer) had a weak negative relationship with the increase in SOC content; however, this relationship was not statistically significant.

Table 4.5 Pearson correlations between the major shelterbelt characteristics

Stand characteristics	Avg. tree diameter	Amount of litter	Trees per kilometer	Avg. crown width	Age	Mortality
Avg. tree height	0.872*	0.476*	-0.284*	0.519*	0.605*	0.042
Avg. tree diameter		0.536*	-0.027	0.688*	0.627*	-0.106
Amount of litter			-0.051	0.169	0.719*	0.003
Trees per kilometer				-0.259*	-0.251	-0.455*
Avg. crown width					0.411*	0.171
Age						0.264*

*Correlations significant at 0.05 level

Table 4.6 Pearson correlations between the major shelterbelt characteristics and increase in SOC concentrations (g kg^{-1}) at 0-5, 5-10, 10-30 and 30-50 cm soil depth.

Soil Depth (cm)	Avg. tree height	Avg. tree diameter	Amount of litter (g m^{-2})	Trees per kilometer	Avg. crown width	Age	Mortality
0-5	0.611*	0.607*	0.695*	-0.157	0.294*	0.745*	0.286*
5-10	0.499*	0.567*	0.588*	-0.104	0.539*	0.684*	0.083
10-30	0.653*	0.656*	0.597*	-0.158	0.463*	0.701*	-0.004
30-50	0.558*	0.572*	0.441*	0.021	0.282*	0.468*	-0.075

*Correlations significant at 0.05 level

While the correlation analysis indicated that the stand characteristics are strongly related to increase in SOC, a multiple regression analysis was performed in order to determine their relative importance in the determination of SOC sequestration within the shelterbelts. A hierarchical multiple regression analysis was performed in order to establish if the addition of age of shelterbelts (model 2), amount of litter (model 3), tree characteristics including average crown width and average tree height (model 4) and shelterbelt design characteristics including tree density, tree spacing and the number of tree rows (model 5) improved the determination of

SOC sequestration over and above the species (model 1) of shelterbelt plantation (Table 4.7). Stand age was the most important predictor for an increase in SOC and contributed highly to a statistically significant increase in the coefficient of determination (R^2) at all the soil depths. The amount of litter produced also contributed significantly to the model throughout the soil profile, although the change in R^2 associated with the addition of litter was less compared to age. Tree physiological characteristics including average crown width and average tree height contributed significantly at only the intermediate soil depths (5-10 and 10-30 cm). Shelterbelt design characteristics such as tree spacing, tree density and number of tree rows did not contribute significantly to the increase in SOC concentration at any soil depth. This trend implies that variability in stand design characteristics did not play a major role in the determination of SOC sequestration within the shelterbelts. The maximum adjusted R^2 of the models at the 0-30 cm depths varied from 0.560 to 0.665 indicating that around 56 to 67 % of the variability in determination of SOC sequestration in the top 30 cm could be explained by these models. At the 30-50 cm soil depth, the model could explain only about 33% of the variability in the increase of SOC.

Table 4.7 Hierarchical multiple regression analysis predicting the change in SOC concentration of the shelterbelts due to shelterbelt species (model 1), shelterbelt age (model 2), Amount of litter (model 3), major tree characteristics (model 4), and major shelterbelt design characteristics (model 5).

Model	Variables added†	0-5 cm soil depth				5-10 cm soil depth			
		R ²	Adj R ²	ΔR ²	p-value	R ²	Adj R ²	ΔR ²	p-value
1	Species	0.195	0.119	0.195	0.038	0.132	0.051	0.132	0.172
2	Age	0.627	0.584	0.432	<0.001	0.524	0.469	0.392	<0.001
3	Amount of litter	0.689	0.647	0.063	0.002	0.567	0.507	0.042	0.030
4	Avg. crown width, Avg. tree height	0.713	0.661	0.024	0.14	0.628	0.560	0.062	0.023
5	Tree spacing by length, Tree spacing by width, Number of rows, Trees per kilometer	0.74	0.665	0.027	0.343	0.633	0.527	0.005	0.959

Model	Variables added†	10-30 cm soil depth				30-50 cm soil depth			
		R ²	Adj R ²	ΔR ²	p-value	R ²	Adj R ²	ΔR ²	p-value
1	Species	0.169	0.091	0.169	0.072	0.147	0.066	0.147	0.124
2	Age	0.556	0.505	0.387	<0.001	0.311	0.232	0.164	0.001
3	Amount of litter	0.606	0.551	0.049	0.015	0.374	0.288	0.063	0.028
4	Avg. crown width, Avg. tree height	0.648	0.583	0.042	0.063	0.419	0.313	0.045	0.158
5	Tree spacing by length, Tree spacing by width, Number of rows, Trees per kilometer	0.671	0.575	0.023	0.544	0.477	0.326	0.058	0.306

† The new explanatory variables in each model are added to the variables from the previous model i.e. model 1 consists of species as the explanatory variable, model 2 consists of species and age, model 3 consists of species, age and amount of litter, model 4 consists of species, age, amount of litter, avg. crown width and avg. tree height, and model 5 consists of species, age, amount of litter, avg. crown width, avg. tree height, tree spacing by length and by width, number of rows and trees per kilometer as the explanatory variables, respectively.

4.6 Discussion

4.6.1 SOC sequestration and distribution under the shelterbelts

Shelterbelts generally had a higher SOC content compared to the agricultural fields indicating that the shelterbelts have added significant amounts of C to the soils (Table 4.2). Similar trends of higher SOC content have been observed in other agroforestry systems when the trees were incorporated into agricultural systems (Sauer et al., 2007; Bambrick et al., 2010; Baah-Acheamfour et al., 2015). Greater SOC accumulation under the shelterbelts is attributed to higher C inputs from the aboveground leaf litter as well as belowground root litter and rhizodeposition (Lorenz and Lal, 2014). Shelterbelts may also increase SOC by intercepting blowing wind leading to deposition of wind-blown organic detritus, as well as a reduction of surface soil C loss owing to wind erosion (Mize et al., 2008). Lower SOC content in the agricultural soils may also be due to higher decomposition rates of SOC due to practices such as cultivation and tillage, leading to the breakdown of soil aggregates (Dick et al., 1998; West and Post, 2002). In addition, the removal of crop biomass through harvested products such as grains or straw can also lead to a reduction in SOC inputs to the soil (Paustian et al., 2000).

Shelterbelts were observed to have lower soil bulk density compared to agricultural fields in our study (Fig. 4.2b), which has also been observed in other studies (Hansen, 1993; Messing et al., 1997). This trend is attributed to the increase in organic matter content of soils (Davidson et al., 1967), lack of soil compaction due to heavy machinery (Hamza and Anderson, 2005), and increased abundance of tree roots (Lorenz and Lal, 2014) and soil invertebrates such as earthworms (Price and Gordon, 1998) under the tree component of the agroforestry system.

While the SOC concentration was higher under the shelterbelts compared to agricultural fields throughout the soil profile (Fig. 4.2a), there was greater accumulation of SOC under the

trees at the intermediate soil depth of 10-30 cm (Table 4.3). The increase in SOC stocks with depth under trees is primarily due to the turnover of the deeper tree roots and rhizodeposition (Lorenz and Lal, 2005; 2014). The root-derived C inputs may equal or exceed the aboveground C inputs due to leaves from litterfall (Scheu and Schauer mann, 1994; Jackson et al., 1997). Upson and Burgess (2013) similarly reported a maximum increase in SOC concentration in the 20-40 cm soil depth, which also had the greatest quantity of coarse roots in a poplar-based temperate agroforestry system. Reduced C accumulation in the surface layers could be attributed to a greater loss of SOC due to mineralization compared to the subsurface layers, especially in the younger shelterbelts (Hansen, 1993). The root-derived C inputs to the subsurface layers are considered more stable compared to the shoot-derived C, due to the higher chemical recalcitrance of root-derived C (Lorenz and Lal, 2005) and increased the physico-chemical protection through the interaction with soil minerals (Rasse et al., 2005). Thus, C in sub-surface layers may play a prominent role in increasing the soil C stocks and their residence time and must be taken into account in determining the C sequestration potential of agroforestry systems.

Average SOC stored under the tree species varied from 80-149 Mg ha⁻¹ (Table 4.3), which is within the reported range of 30-300 Mg C ha⁻¹ for agroforestry systems (Nair et al., 2010). The average amount of C sequestered up to the depth of 50 cm under the shelterbelt species ranged from 6-38 Mg ha⁻¹, with a median SOC accrual rate of 0.7 Mg ha⁻¹yr⁻¹. These SOC sequestration values are comparable to the C sequestration potential of other agroforestry systems reported in the literature. Sauer et al. (2007) reported an average C sequestration of 3.7 Mg ha⁻¹ (0-15 cm depth) in a 35-year-old shelterbelt composed of *Juniperus virginiana* and *Pinus sylvestris* trees. Upson and Burgess (2013) reported an increase of 19 Mg C ha⁻¹ up to a 60 cm depth in a 19-year-old poplar intercropping system, although SOC decreased for lower soil

depths (60-150 cm). Similarly, Bambrick et al. (2010) reported an increase of 6.2 and 33.1 Mg C ha⁻¹ in 21-year-old and 8-year-old tree-based intercropping systems in Canada, respectively. Younger shelterbelts showed a loss in SOC compared to the reference agricultural plots (Fig. 4.4). Soil carbon loss can accompany tree stand establishment, followed by net gains as the stand matures (Grigal and Berguson, 1998; Wang et al., 2013). This temporary loss of soil C is due to the rapid mineralisation of SOC during plantation establishment and depends on the site preparation methods (Johnson, 1992; Hansen, 1993).

4.6.2 Effect of shelterbelt characteristics on SOC sequestration

While all the six studied shelterbelt systems showed higher C sequestration potential compared to conventional agricultural systems, hybrid poplar showed the highest sequestration of SOC followed by white spruce and Scots pine (Table 4.3; Fig. 4.3). The broadleaved species, green ash and Manitoba maple, as well as the shrub, caragana had lower amounts of C sequestered in the soil. These trends are similar to the other studies on agroforestry systems, which found higher SOC sequestration under hybrid poplar followed by the coniferous species (Peichl et al., 2006; Wotherspoon et al., 2014). The variation in SOC sequestration potential of the species may be attributed to the differences in overstory stand characteristics among the species (Table 4.4). Tree overstory characteristics such as crown width as well as tree height and diameter were highest in hybrid poplar followed by white spruce and Scots pine (Table 4.4). Similarly, the density of the litter layer was also highest for Scots pine and white spruce. These findings indicate that hybrid poplar and coniferous stands were composed of larger trees with a closed canopy structure and higher net primary production, while the other broadleaved and caragana shelterbelts consisted of smaller trees. The overstory characteristics of tree plantations

can influence SOC accumulation by affecting the litterfall input from overstory and understory vegetation, or indirectly by affecting the soil microclimatic conditions (Woldeselassie, 2009).

The effect of the stand overstory characteristics on SOC storage was further studied by using Pearson correlation and hierarchical multiple regression analyses. Soil organic carbon storage beneath the shelterbelts was most significantly related to stand age and amount of litter accumulated under the trees. Earlier studies on soil C sequestration have also found stand age (Hansen, 1993) and carbon inputs to the soil via litter production (Grogan and Matthews, 2002; Garten et al., 2011) to be important determinants of soil carbon storage. Higher quantity of surface litter not only increases the SOC accumulation in surface layers due to increased C inputs, but also leads to increased production of dissolved organic carbon (DOC) that may leach to deeper soil horizons and contribute to subsoil C storage (Vesterdal et al., 2013). Besides stand age and litterfall, the increase in SOC was significantly correlated to overstory structure characteristics including tree height and diameter, and crown width (Table 4.6). Since the overstory characteristics are also significantly related to the amount of litterfall (Table 4.5), their effect on SOC accumulation may be partially linked to their contribution to an increase in net primary production. However, hierarchical multiple regression analysis revealed that the overstory structure characteristics contributed to SOC sequestration over and above the addition of litterfall amounts at the intermediate depths (5-10 and 10-30 cm) (Table 4.7). This trend may be attributed to the influence of canopy structure on understory vegetation and soil microclimate, thus regulating SOC loss through decomposition (Woldeselassie, 2009). Shelterbelt design characteristics such as tree density and tree spacing, however, did not affect the amount of SOC sequestered. While tree density is generally considered to be an important predictor of SOC stocks due to its influence on biomass production and litter input (Saha et al., 2009; Kunhamu et

al., 2011), our results are in agreement with the recent studies that did not observe the effect of tree density on SOC stocks (Davis et al., 2007; Laganier et al., 2010a; Woldeslassie et al., 2012). The combination of stand age, structural and design characteristics could explain 56-67% of variability in SOC increase in the 0-30 cm soil depth. This finding is comparable to other studies where the site variables explained about 50-65% of the variability in SOC stock (Grigal and Ohmann, 1992; Hontoria et al., 1999). The unexplained variability is attributed to within-site SOC variability and measurement errors (Hontoria et al., 1999). In the 30-50 cm layer, only 33 % of the variability could be explained, perhaps due to the increased variability in SOC content of the deeper horizons (Kravchenko and Robertson, 2011).

4.7 Conclusions

Shelterbelts, as an agroforestry system, show significant potential for the sequestration of soil C compared to agricultural cropping systems. All six shelterbelt species showed net gains in SOC compared to agricultural fields; however, hybrid poplar showed the highest SOC sequestration potential. The shelterbelt stand characteristics such as tree height, diameter and crown width accounted for 56-67% of the within-site variability in SOC sequestration potential; however, there is still a need for further research into the effect of soil, climatic and management factors on the soil C sequestration potential of agroforestry systems in order to better exploit their potential for mitigating GHGs. A major portion of SOC was sequestered in the subsurface soil layers (10-30 cm), thus underscoring the importance of including deeper soil horizons in the determination of C sequestration potential of agroforestry systems. Younger shelterbelts tended to show a loss in soil C, indicating that major benefits of soil C sequestration under the shelterbelts may only be achieved at decadal time scales.

Quantification of SOC stocks under shelterbelt trees is necessary to complement the aboveground and belowground biomass C stock estimates in order to determine the full potential of shelterbelts as a strategy for carbon sequestration. This study indicates that soil and litter C stocks can significantly contribute to the overall C sequestration potential of shelterbelt systems, and can play an important role in offsetting the GHG emissions due to agricultural practices in Canada.

5. LIGHT AND HEAVY FRACTION DISTRIBUTION OF SOIL CARBON IN SASKATCHEWAN SHELTERBELTS³

5.1 Preface

In Chapter 4, the ability of shelterbelts to increase soil organic carbon (SOC) accumulation compared to adjacent agricultural fields was determined. However, tree-based agroforestry systems, such as shelterbelts, may affect not only the accumulation of SOC, but also its stabilization and dynamics, which are associated with long-term SOC sequestration potential. In this chapter, the effect of shelterbelts on long-term physical stabilization of SOC was studied by using the density fraction technique. The SOC pools associated with labile uncomplexed organic debris (called light fraction) and mineral-stabilized organic matter (called heavy fraction) were determined and compared for shelterbelts and adjacent agricultural fields.

³ This chapter, co-authored with Dr. Ken Van Rees, has been submitted for publication to Soil Science Society of America Journal. While the data analysis and manuscript writing were carried out by the lead author (Gurbir Singh Dhillon), editing and review of manuscript was completed by the co-authors.

5.2 Abstract

Agroforestry systems play an important role in sequestration of carbon (C), in order to reduce atmospheric carbon dioxide (CO₂) levels and combat climate change. However, the extent of long-term C sequestration will depend on physical stabilization of the sequestered C. The objective of this study was to characterize the effect of shelterbelts on soil organic carbon (SOC) distribution in the density fractions compared to agricultural fields. Soil samples were collected for six major shelterbelt species and adjacent agricultural fields, and separated into light- and heavy fractions using sodium iodide solution (NaI, density = 1.6 g cm⁻³) and were measured for organic C concentration. There was an increase in SOC content of the labile light fraction as well as the stable heavy fraction for shelterbelts compared to agricultural fields. The SOC concentration for shelterbelts increased by 71% for the light fraction and 22% for the heavy fraction. The majority of SOC added at the 0-10 cm soil depth was in the form of labile light fraction (92%), while the heavy fraction contributed to 70% of the increase in SOC stocks at the 10-30 cm soil depth. The increase in the light fraction C stocks was higher for coniferous species, white spruce and Scots pine, and accounted for about 50% of the increase in SOC stocks under these species. In contrast, hardwood species showed a higher increase in the mineral-associated heavy fraction, and only 28-31% of the total increase in SOC stocks was in the form of the light fraction for hardwood species. This trend was attributed to differences in the amount and quality of litter between coniferous and hardwood species. This study concluded that the presence of shelterbelts enhances SOC stocks of uncomplexed plant-derived debris as well as mineral-associated organic matter, thus improving storage and stabilization of soil C.

5.3 Introduction

Soils are the largest reservoir of organic carbon (C) in terrestrial ecosystems, and contain

about twice the amount of C present in the atmosphere (Post et al., 1982). As such, soil organic carbon (SOC) plays an important role in the global carbon cycling, representing an important strategy in the mitigation of atmospheric greenhouse gas (GHG) emissions (Lal, 2004b; Smith et al., 2008). Small fluctuations in the SOC pool can have a dramatic impact on atmospheric carbon dioxide (CO₂) concentration levels and global climate change (Baldock, 2007; Smith et al., 2008). Many recent studies have focused on sequestration of C in soils through land-use change and management practices (Dumanski et al., 1998; Post and Kwon, 2000; Follett, 2001). Improved land management practices are estimated to sequester up to 150 Pg CO₂-C over the next century (Baldock, 2007). However, there is considerable uncertainty in our understanding of key factors that regulate the cycling, dynamics and storage of C in soils, thus limiting our ability to predict long-term C sequestration potential of soils.

Organic C in soils occurs in the form of a diverse range of naturally occurring organic molecules, which may vary in size and complexity from simple monomers to mixtures of biopolymers (Piccolo, 2002; Sutton and Sposito, 2005). Strong heterogeneity in the physical and chemical form and functions of these organic compounds makes it challenging to estimate the turnover times and stabilization processes associated with soil organic matter (SOM). In order to overcome the problem posed by SOM heterogeneity, SOM is divided into distinct pools, which are linked to different structural or functional components of organic matter (OM) within the soil, and thereby, to different rates of biological turnover (Wander, 2004; von Lützow et al., 2007). These pools generally include an active, labile pool with a residence time of a few months to years and a passive, recalcitrant pool with a residence time in the order of decades (Schimel et al., 1994; Torn et al., 2009). Reliable estimation of C dynamics in soils requires the analytical determination of these conceptual OM pools and the stabilization processes associated with them

(von Lützow et al., 2007).

Major processes of OM stabilization include inherent biochemical recalcitrance of OM to microbial degradation, and physical stabilization of OM through association with silt and clay minerals and through encapsulation within the soil micro aggregates (Sollins et al., 1996; Six et al., 2002). Recent studies have indicated that SOM decomposition is primarily controlled by spatial disconnection of OM from decomposers and their degradative enzymes, while the molecular structure of the OM plays a secondary role in determining its turnover (Mikutta et al., 2006; von Lützow et al., 2006). Physical fractionation of soil emphasizes the role of spatial arrangement of SOM and its association with inorganic mineral particles in regulating the decomposition of OM by controlling its accessibility to microorganisms (Elliott and Cambardella, 1991; Christensen, 2001). Organo-mineral complexes involving the interaction of OM with mineral surfaces and metal ions are considered the most important mechanism for the stabilization of OM in soils (Mikutta et al., 2006; Lorenz and Lal, 2014). The density fractionation technique involves the physical separation of SOM into a low-density fraction composed of partly decomposed plant debris (called light fraction) and a heavy-density fraction composed of organic matter adsorbed on the mineral surfaces or entrapped within organo-mineral microaggregates (called heavy fraction) (Christensen, 1992). The light fraction (LF) decomposes rapidly compared to the heavy fraction (HF), primarily due to the lack of protection by inorganic colloids (Spycher et al., 1983; Boone, 1994). Dalal and Mayer (1986) observed 2 to 11 times greater loss of organic C from light- compared to heavy fraction under a continuously cultivated cereal cropping system. However, the light fraction plays an important role in the cycling of nutrients and maintenance of soil productivity (Janzen et al., 1992; Haynes, 2005). The heavy fraction, on the other hand, is stabilized by complexation with mineral-surfaces and

forms a major component of the old, recalcitrant OM pool in the soils (Gregorich et al., 1996).

Isolation and quantification of these C pools and their dynamics can help determine the effects of land management practices on soil C sequestration potential as well as its quality and fertility.

Agroforestry systems are suggested to have a high potential to accumulate C in soils due to increased input of litter associated with aboveground foliage and deep root systems (Nair et al., 2009b; Lorenz and Lal, 2014). Thus, agroforestry systems are considered as one of the major strategies for soil C sequestration and mitigation of greenhouse gases within agroecosystems (Nair et al., 2009a, 2010). Nevertheless, in order to determine their long-term soil C sequestration potential, the influence of agroforestry systems on the stabilization of SOC, along with its storage and accumulation, needs to be studied. Stability of SOC is affected by quantity and quality of litter inputs (Prescott et al., 2000; Lorenz and Lal, 2005) as well as diversity and abundance of soil microorganisms and macrofauna (González and Seastedt, 2001; Hättenschwiler et al., 2005; Hedde et al., 2007), which, in turn, are influenced by the incorporation of trees (DeBellis et al., 2006; Lamarche et al., 2007; Laganière et al., 2009). Planting trees also improves soil physical properties such as soil aggregation, which may enhance stabilization of SOC (Blanco-Canqui et al., 2007; Sarkhot, et al., 2008). Few studies have determined the effect of tree establishment on labile and stable C pools, and while some studies report a significant increase in only the labile C pools (Leite et al., 2014; Baah-Acheamfour et al., 2015); other studies have suggested an increase in the stable C pools (Garten, 2002; Teklay and Chang, 2008; Youkhana and Idol, 2011). Overall, the contribution of different physical and chemical processes for stabilization of C in soils under agroforestry systems is not well understood (Jastrow et al., 2006; Lorenz and Lal, 2014). The determination of the distribution of SOM in soil particle and density fractions can help us to improve our

understanding of the influence of agroforestry practices on the stabilization of SOM.

This study is based on the hypothesis that the plantation of shelterbelts will influence the stabilization of SOM through organo-mineral associations, because of the differences in quantity and quality of litter inputs for shelterbelts compared to the agricultural fields. The objective, therefore, of this study is to determine the effect of hardwood and coniferous shelterbelt species on the storage and stabilization of SOC pools through the quantification of C stored in light- and heavy density fractions of whole soil.

5.4 Materials and Methods

5.4.1 Site selection and sampling procedure

Soil sampling was performed for six major shelterbelt species - green ash (*Fraxinus pennsylvanica*), hybrid poplar (*Populus* spp.), Manitoba maple (*Acer negundo*), white spruce (*Picea glauca*), Scots pine (*Pinus sylvestris*) and caragana (*Caragana arborescens*). A total of 59 sites were sampled for the study including 10 sites for hybrid poplar, Manitoba maple and caragana, 11 sites for Scots pine and 9 sites for green ash and white spruce shelterbelts. Selection of sampling sites and procedure of soil sampling at each site have been described in Chapter 4.

5.4.2 Laboratory analyses

The density fractionation technique was used to separate the light- and heavy fractions from the whole soil, using the process described in Janzen et al. (1992). Briefly, 10 g of coarsely ground (< 2mm) soil was added to a centrifuge tube along with 40 ml of sodium iodide (NaI) solution. The specific density of NaI solution was 1.6 g cm⁻³, as recommended by Cerli et al. (2012). The tubes were shaken on a shaker for 30 minutes and then centrifuged at 3000 rpm for 10 minutes in order to accelerate the sedimentation of heavy particles. The light fraction, suspended on the surface of the solution, was aspirated together with the solution and filtered

using a fiberglass filter (Whatman GF/A, 47 mm dia.). This process was repeated until there was no more light fraction suspended in the solution, indicating that the light and heavy fractions had separated completely. The light and heavy fractions were washed with 50 ml of 0.01 M CaCl₂, followed by 50 ml of deionized water and dried at 60° C for 48 hours and, the dry weights of light and heavy fractions were taken. Heavy fraction samples were treated with HCl fumes to remove soil carbonates, according to the HCl-fumigation procedure (described in Dhillon et al., 2015). Following the removal of carbonates, heavy fraction samples were analyzed for organic C content using an automated C632 LECO analyzer (LECO Corporation, St. Joseph, MI, USA). The light fraction samples were also analyzed for organic C content using C632 LECO analyzer; however, the HCl-fumigation pretreatment was not applied to the light fraction samples, since their carbonate content is assumed to be negligible. Carbon content (g C kg⁻¹ of the fraction) of the fractions and their mass percentage (%) in the whole soil was used to determine SOC concentration (g C kg⁻¹ of soil) and SOC stocks (Mg C ha⁻¹) within the light- and heavy fractions. A weighted average of soil parameters (light and heavy fraction mass and C concentration) for the whole soil profile (0-50 cm soil depth) was calculated based on the C (or mass) content of the individual soil layers (0-5, 5-10, 10-30 and 30-50 cm).

5.4.3 Statistical analysis

Two-way mixed analysis of variance (ANOVA) procedure was used to determine the differences between shelterbelts and fields, with the land cover (i.e. shelterbelts vs. agricultural fields) analyzed as within-subject factor. In the presence of a significant interaction, simple main effects were considered. One-way analysis of covariance (ANCOVA) was used to determine the effect of shelterbelt species on increase in light and heavy fraction C stocks, with the increase in SOC mass taken as a covariate. Post-hoc analysis was performed by using Fisher's LSD. A p-

value of 0.1 was used to signify statistical significance. This was done in order to reduce the risk of type II error due to the presence of significant natural within-site variation. Statistical analysis was performed using IBM SPSS Statistics version 23 (IBM Inc., Armonk, NY, USA).

5.5 Results

5.5.1 General distribution of density fractions in the bulk soil

Characteristics of density fractions in the bulk soil associated with sampling depths are listed in Table 5.1. On average, the masses of light and heavy fractions accounted for 4.4% and 91.3% of the dry soil mass, respectively throughout the soil profile (0-50 cm). Averaged across both land covers (i.e. shelterbelts and agricultural fields), percentage mass of light fraction decreased with soil depth from 8.6% at 0-5 cm to 1.9% at 30-50 cm, while the percentage mass of heavy fraction increased from 86.9% at 0-5 cm to 93.8% at 30-50 cm. Similarly, the C content (g C kg⁻¹ of fraction) of both fractions decreased with soil depth (Table 5.1). However, C content of the light fraction was significantly higher than the heavy fraction at all depths ($p < 0.001$; Table 5.1). On average, the C content of the light fraction was 60 g C kg⁻¹, while the C content of heavy fraction was 16 g C kg⁻¹ across all land covers and soil depths. Average recovery of SOC in the density fractions was 94% across all soil depths and shelterbelt species. The majority of the OC in the soil was contained in the heavy fraction at all soil depths (Fig. 5.1). Light fraction C was higher in the surface soil layers compared to the deeper layers. Across both land covers, heavy fraction C accounted for 68% of the total SOC concentration at 0-5 cm depth, 74% at the 5-10 cm depth, 78% at 10-30 cm depth and 86% at 30-50 cm depth. Light fraction C accounted for 27%, 20%, 16% and 8% of the total SOC concentration at the 0-5, 5-10, 10-30 and 30-50 cm soil depths, respectively.

Table 5.1 Mean C content and % mass of density fractions of soil organic matter by soil depth for shelterbelts and adjacent agricultural fields averaged across all species.

Depth (cm)	Land cover	Light fraction		Heavy fraction	
		C content†	% Mass	C content†	% Mass
0-5	Shelterbelt	130.7 (8.8) a‡	9.5 (0.3) a	31.6 (1.6) a	86.2 (0.4) a
	Field	82.7 (4.6) b	7.7 (0.2) b	26.6 (1.3) b	87.6 (0.2) b
5-10	Shelterbelt	82.2 (5.2) a	8.5 (0.3) a	26.5 (1.5) a	87.4 (0.3) a
	Field	66.9 (3.5) b	7.1 (0.2) b	22.4 (1.2) b	88.8 (0.3) b
10-30	Shelterbelt	63.3 (5.9) a	5.8 (0.2) a	18.6 (1.1) a	89.9 (0.3) a
	Field	52.2 (2.7) b	4.3 (0.2) b	13.2 (0.7) b	91.5 (0.2) b
30-50	Shelterbelt	51.1 (4.2) a	2.0 (0.1) a	10.3 (0.5) a	93.6 (0.2) a
	Field	44.1 (3.2) b	1.8 (0.1) a	9.7 (0.4) b	94.0 (0.2) a

† C content was measured in g C kg⁻¹ of the density fraction

‡ Values with same letters within a column at each soil depth are not significantly different at p < 0.1.

5.5.2 Effect of shelterbelts on density fractions

Significant differences were observed among shelterbelts and agricultural fields with respect to mass distribution as well as C content (g C kg⁻¹ of fraction) of the light- and heavy fractions down the soil profile (Table 5.1). In terms of mass percentage of whole soil, shelterbelts had a higher amount of light fraction but lower amounts of heavy fraction compared to the agricultural fields down to a 30 cm soil depth (Table 5.1). However, there was a significant increase in the C content of both fractions (light and heavy) under the shelterbelts compared to agricultural fields down the soil profile. Mean C content increased by 26 and 24% for the light and heavy fractions, respectively under the shelterbelts compared to the agricultural fields.

The SOC concentration of both density fractions was higher for shelterbelts compared to agricultural fields at all depths (Fig. 5.1). Averaged across the whole profile, shelterbelts had 71% more C in the light fraction and 22% more C in the heavy fraction compared to the agricultural fields. The increase in the light fraction C was higher at the top of the soil profile compared to the deeper layers (Fig. 5.1). At 0-5 cm soil depth, SOC in the light fraction was

115% (7.3 g kg^{-1}) higher in the shelterbelts compared to the adjacent agricultural fields across all the sites. Moving down the soil profile, the increase in light fraction C was less pronounced at 5-10 (51%; 2.4 g kg^{-1}), 10-30 (61%; 1.3 g kg^{-1}) and 30-50 cm (30%; 0.2 g kg^{-1}) soil depths. Heavy fraction SOC increased under the shelterbelts compared to agricultural fields by 16% at 0-5 and 5-10 cm soil depths (3.7 and 3.2 g kg^{-1} , respectively), 39% at 10-30 cm depth (4.7 g kg^{-1}) and 7% at 30-50 cm soil depth (0.6 g kg^{-1} ; Fig. 5.1).

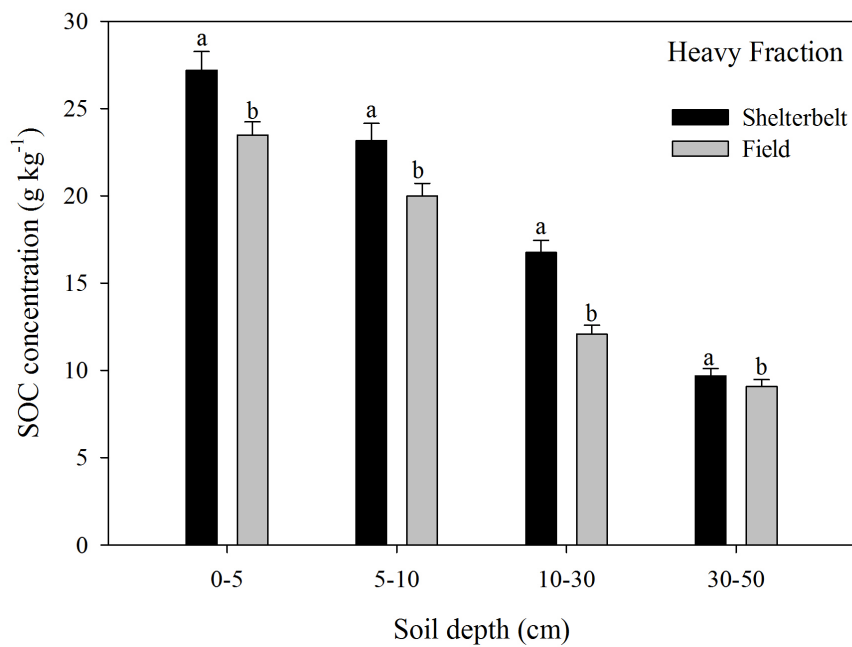
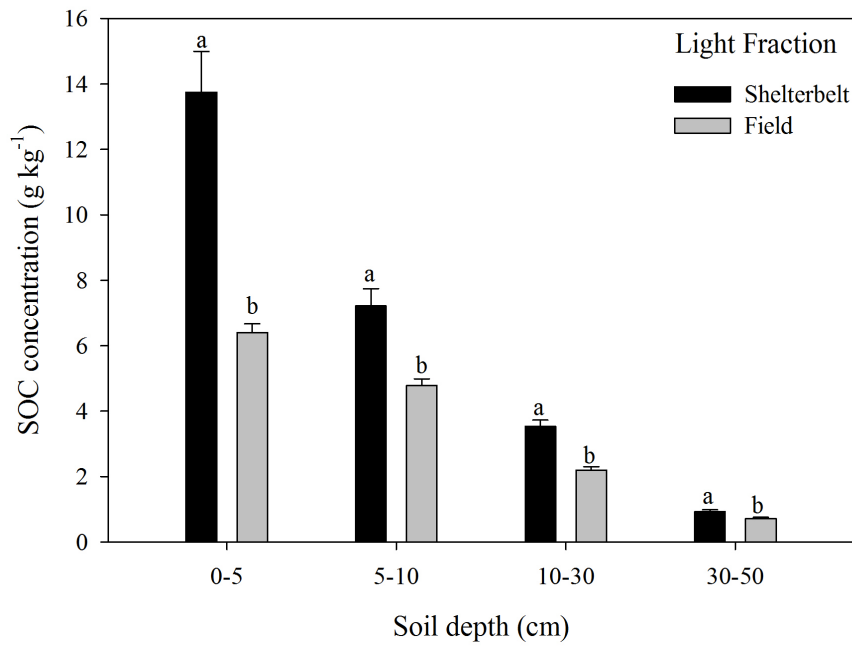


Fig. 5.1 Mean SOC concentrations (g kg^{-1}) in the light- and heavy fractions of soil under shelterbelts and agricultural fields at the 0-5, 5-10, 10-30, and 30-50 cm soil depths. Bars with the same letter within a soil depth are not significantly different at $p < 0.1$.

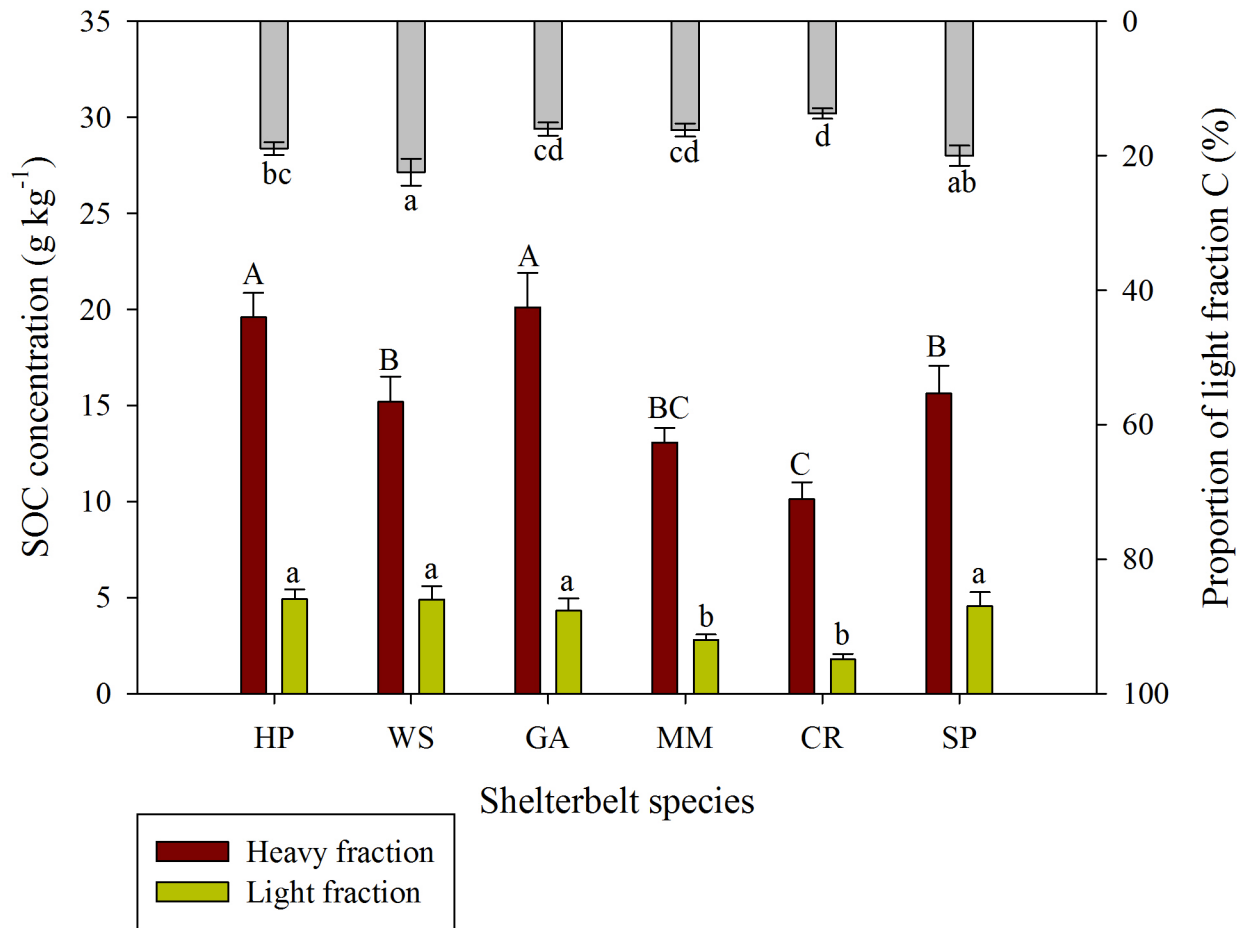


Fig. 5.2 Distribution of SOC in the light- and heavy fractions (bottom axis) and proportion of light fraction C in the total SOC (top axis) under shelterbelt species (HP- Hybrid poplar; WS – White spruce; GA – Green ash; MM – Manitoba maple; CR- Caragana; SP – Scots pine). SOC concentration (g kg⁻¹) represents the weighted average of SOC concentrations at 0-5, 5-10, 10-30 and 30-50 cm soil depths. Error bars indicate standard error. Bars with the same letter within a fraction are not significantly different at $p < 0.1$.

The amount of SOC stored in density fractions varied with the shelterbelt species (Fig. 5.2). Green ash and hybrid poplar had significantly higher SOC concentration compared to white spruce, Scots pine, Manitoba maple and caragana in the heavy fraction, while hybrid poplar, white spruce, green ash and Scots pine had significantly higher SOC concentration in the light fraction compared to Manitoba maple and caragana shelterbelts. Relative proportion of SOC stored in light fraction was higher for white spruce and Scots pine shelterbelts (22 and 20%, respectively), compared to hybrid poplar (19%), Manitoba maple (16%), green ash (16%) and caragana (14%) shelterbelts (Fig. 5.2). The increase in light- and heavy fraction C concentrations under the shelterbelts compared to agricultural fields also differed with shelterbelt species (Figs. 5.3 and 5.4; Table 5.2). The increase in light fraction SOC for shelterbelts compared to agricultural fields, was significantly higher for hybrid poplar, white spruce and Scots pine shelterbelts compared to the other species at the surface layer (0-5 cm; Fig. 5.3). In the subsurface layers, differences in increase of light fraction SOC between species were not statistically significant. Increase in heavy fraction SOC for shelterbelts, compared to adjacent agricultural fields, was significantly higher for hybrid poplar than green ash, Manitoba maple and caragana species at 0-5 and 10-30 cm soil depths (Fig. 5.4).

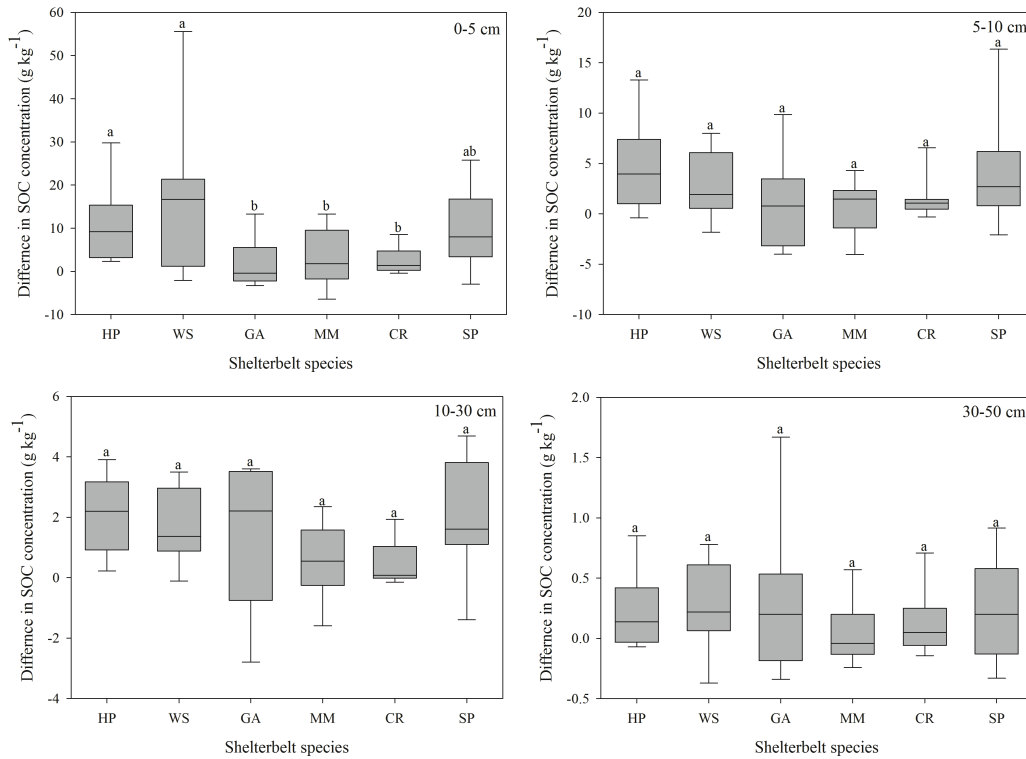


Fig. 5.3 Difference in SOC concentration (g kg^{-1}) of the light fraction of different shelterbelt species (HP- Hybrid poplar; WS – White spruce; GA – Green ash; MM – Manitoba maple; CR- Caragana; SP – Scots pine) compared to adjacent agricultural fields at 0-5, 5-10, 10-30, and 30-50 cm soil depths. Species with same letter are not significantly different at $p < 0.1$.

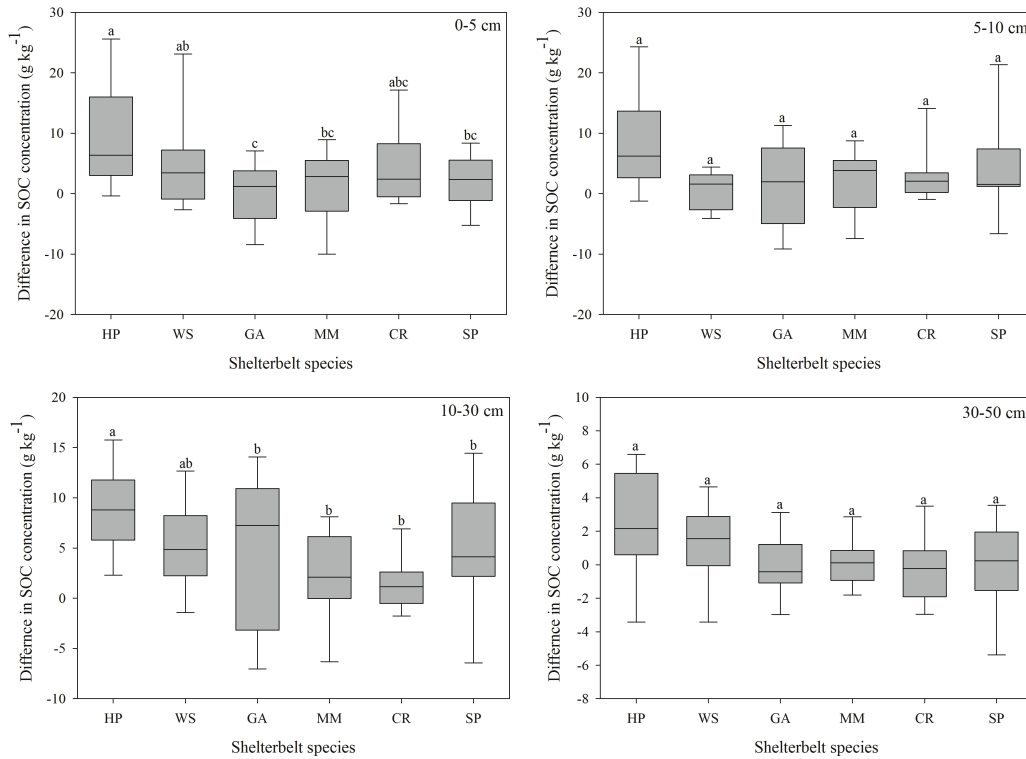


Fig. 5.4 Difference in SOC concentration (g kg^{-1}) of the heavy fraction of different shelterbelt species (HP- Hybrid poplar; WS – White spruce; GA – Green ash; MM – Manitoba maple; CR- Caragana; SP – Scots pine) compared to adjacent agricultural fields at 0-5, 5-10, 10-30, and 30-50 cm soil depths. Species with same letter are not significantly different at $p < 0.1$.

Table 5.2 SOC concentration (g kg^{-1}) of light and heavy fractions at the 0-5, 5-10, 10-30 and 30-50 cm soil depths as affected by land cover and species of shelterbelt plantation.

Species	Land cover	Soil Depth (cm)			
		0-5	5-10	10-30	30-50
— Light Fraction —					
Hybrid Poplar	Shelterbelt	17.4 (3.1) a†	10.2 (1.3) a	4.6 (0.4) a	0.9 (0.1) a
	Field	6.7 (0.7) b	5.5 (0.8) b	2.4 (0.3) b	0.6 (0.1) b
White Spruce	Shelterbelt	23.1 (5.8) a	7.7 (1.3) a	3.4 (0.4) a	1.1 (0.2) a
	Field	7.8 (0.9) b	4.9 (0.6) b	1.7 (0.3) b	0.8 (0.2) b
Green Ash	Shelterbelt	11.1 (2.1) a	8.3 (1.5) a	4.8 (0.6) a	1.1 (0.2) a
	Field	9.0 (0.4) a	7.3 (0.4) a	3.4 (0.4) a	0.8 (0.1) a
Manitoba maple	Shelterbelt	9.1 (1.7) a	4.7 (0.6) a	2.7 (0.3) a	0.9 (0.1) a
	Field	6.2 (0.9) a	4.1 (0.5) a	2.1 (0.2) a	0.8 (0.1) a
Caragana	Shelterbelt	5.6 (1.2) a	3.7 (0.7) a	1.6 (0.2) a	0.6 (0.1) a
	Field	2.9 (0.3) b	2.2 (0.1) b	1.2 (0.1) b	0.4 (0.04) a
Scots Pine	Shelterbelt	16.3 (2.8) a	8.7 (1.8) a	4.1 (0.6) a	1.0 (0.2) a
	Field	5.9 (0.4) b	4.7 (0.4) b	2.4 (0.2) b	0.7 (0.1) b
— Heavy Fraction —					
Hybrid Poplar	Shelterbelt	32.8 (3.3) a	30.2 (2.1) a	21.6 (1.5) a	11.6 (1.3) a
	Field	23.7 (1.9) b	22.1 (2.1) b	12.7 (1.5) b	9.1 (1.0) b
White Spruce	Shelterbelt	32.0 (3.2) a	21.5 (3.1) a	14.5 (1.5) a	10.1 (1.5) a
	Field	26.8 (2.8) b	20.9 (2.7) a	9.1 (1.4) b	8.8 (1.6) a
Green Ash	Shelterbelt	33.7 (3.0) a	32.0 (3.0) a	23.6 (2.6) a	10.2 (0.7) a
	Field	33.8 (1.7) a	30.6 (1.2) a	18.8 (2.0) b	10.3 (0.6) a
Manitoba maple	Shelterbelt	23.3 (1.7) a	19.4 (2.0) a	13.6 (1.2) a	8.4 (0.5) a
	Field	21.8 (1.6) a	17.6 (1.7) a	11.2 (0.9) a	8.3 (0.6) a
Caragana	Shelterbelt	16.4 (2.5) a	12.4 (1.6) a	9.5 (0.8) a	8.6 (0.9) a
	Field	12.0 (1.3) b	9.5 (0.4) b	8.0 (0.5) a	8.8 (0.7) a
Scots Pine	Shelterbelt	25.1 (1.6) a	23.5 (2.6) a	17.7 (2.1) a	9.2 (0.9) a
	Field	22.8 (1.5) b	19.3 (1.5) a	12.7 (0.9) b	9.2 (1.1) a

† Values with same letters within a column and shelterbelt species group are not significantly different at $p < 0.1$.

Table 5.3 Organic carbon stocks (Mg ha^{-1}) of the light fraction (a) and heavy fraction (b) at 0-10, 10-30 and 30-50 cm soil depths under the shelterbelts and agricultural fields for different shelterbelt species. Numbers in parenthesis represent standard error.

a) Light fraction

Species†	Soil Depth (cm)					
	0-10		10-30		30-50	
	Shelterbelt	Field	Shelterbelt	Field	Shelterbelt	Field
HP	12.3 (1.5) a‡	6.8 (0.7) b	10.8 (0.9) a	6.4 (0.8) b	6.1 (3.8) a	5.2 (3.5) b
WS	13.2 (2.2) a	6.8 (0.7) b	7.6 (1.1) a	4.2 (0.7) b	2.9 (0.4) a	2.2 (0.5) b
GA	9.2 (1.3) a	8.4 (0.5) a	11.9 (1.5) a	8.5 (1.0) a	2.8 (0.4) a	2.2 (0.2) a
MM	7.6 (1.1) a	5.8 (0.6) a	7.0 (0.9) a	5.7 (0.5) a	2.4 (0.2) a	2.3 (0.2) a
CR	4.6 (0.8) a	3.2 (0.2) b	4.2 (0.5) a	3.2 (0.3) b	1.6 (0.2) a	1.3 (0.1) a
SP	11.7 (2.0) a	6.2 (0.4) b	10.1 (1.5) a	6.3 (0.5) b	2.7 (0.4) a	2.0 (0.3) a

b) Heavy fraction

Species†	Soil Depth (cm)					
	0-10		10-30		30-50	
	Shelterbelt	Field	Shelterbelt	Field	Shelterbelt	Field
HP	28.8 (2.0) a‡	25.9 (2.1) a	51.3 (3.6) a	33.5 (3.7) b	31.7 (3.2) a	25.8 (2.9) b
WS	23.9 (2.6) a	25.5 (2.8) a	31.9 (3.8) a	23.0 (3.2) b	25.7 (3.6) a	23.4 (4.2) a
GA	31.9 (1.9) a	33.1 (1.4) a	58.5 (6.6) a	46.6 (4.9) a	26.5 (1.7) a	27.5 (1.8) a
MM	23.7 (2.1) a	22.4 (1.6) a	35.5 (3.7) a	30.6 (2.2) a	23.3 (1.2) a	22.9 (1.4) a
CR	14.6 (1.7) a	13.1 (1.0) a	24.7 (1.8) a	22.1 (1.1) a	24.7 (2.6) a	26.1 (2.1) a
SP	23.2 (1.6) a	24.8 (1.7) a	43.8 (4.9) a	34.0 (2.5) b	24.5 (2.2) a	25.4 (3.1) a

† Abbreviations: HP- Hybrid poplar; WS – White spruce; GA – Green ash; MM – Manitoba maple; CR- Caragana; SP – Scots pine

‡ Values with same letters within a row at each soil depth are not significantly different at $p < 0.1$.

5.5.3 Contribution of density fractions to increase in SOC stocks

On average, there was an increase of 18.6 Mg ha⁻¹ of SOC for the shelterbelts compared to agricultural fields, as described in Chapter 4. Light and heavy fractions accounted for 7 Mg ha⁻¹ (38%) and 10.4 Mg ha⁻¹ (56%) of the increase in SOC stocks under shelterbelts, respectively (Table 5.3). Light fraction C was especially important in the surface layer, where it accounted for 92% of the total increase in C stocks (Fig. 5.5). At the 10-30 cm soil depth, heavy fraction C increased more than the light fraction C, such that only 22% of the increase in C stocks was in the form of the light fraction and 70% of the increase in C stocks was in the form of the heavy fraction. At 30-50 cm soil depth, there was no significant difference in the increase of light and heavy fraction C stocks, and the light and heavy fractions contributed to 37 and 60% of the increase in SOC stocks, respectively.

The effect of shelterbelts species on the change in heavy and light fraction C stocks was determined using ANCOVA analysis, after controlling for the difference in SOC stock among species (Table 5.4). Results indicated a statistically significant difference between shelterbelt species for the change in light (F (5,52)=4.138, p=0.003) and heavy (F (5,52)=5.885, p <0.001) fraction C stocks. Estimated marginal means (EMM) suggested a higher increase in the light fraction C stocks for white spruce and Scots pine shelterbelts compared to other shelterbelt species, for equivalent increase in SOC stocks (Table 5.4). In contrast, the increase in heavy fraction C stocks was higher for hybrid poplar, green ash, Manitoba maple and caragana species, compared to white spruce and Scots pine, for equivalent increase in SOC stocks. These results were also supported by the relative proportion of C sequestered in light and heavy fractions under different shelterbelt species (Table 5.4). The light fraction accounted for 50, 49 and 48% of the total increase in SOC stocks for Scots pine, white spruce and caragana, respectively;

however, the light fraction to total SOC sequestered was lower for green ash (31%), hybrid poplar (29%) and Manitoba maple (29%).

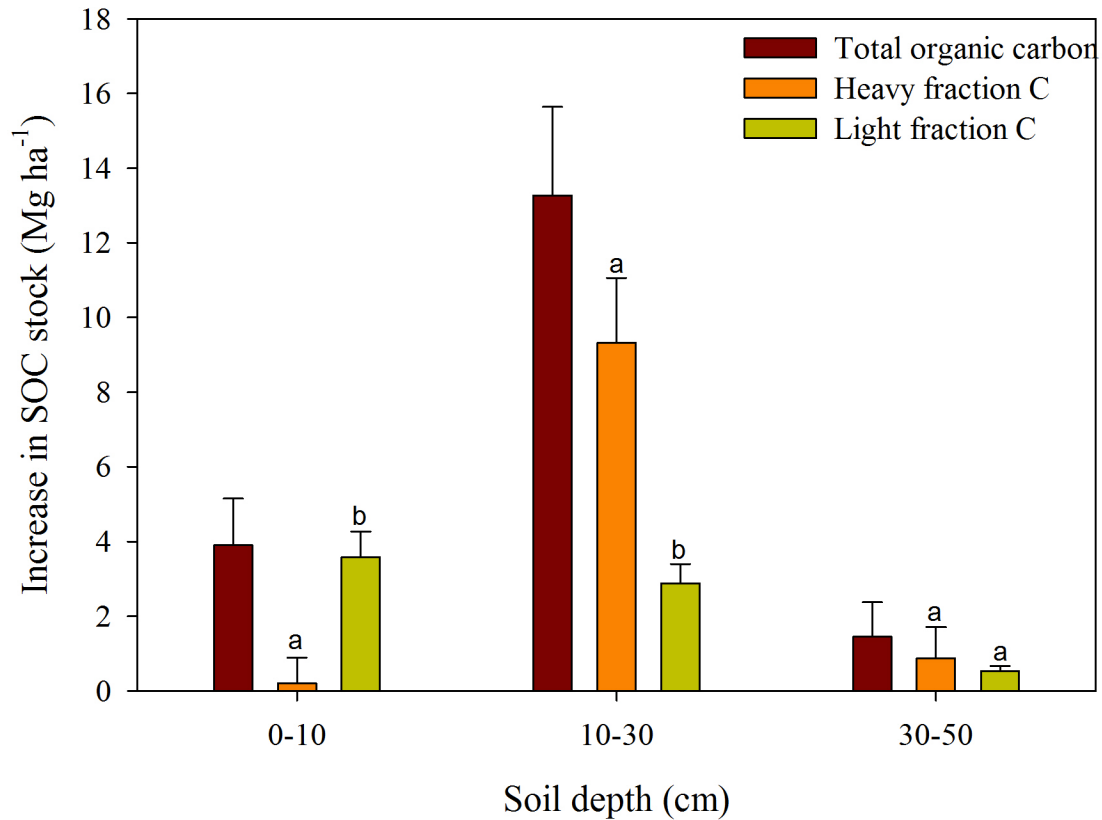


Fig. 5.5 Contribution of the light and heavy fractions to increase in SOC stocks (Mg ha⁻¹) at the 0-10, 10-30, and 30-50 cm soil depths across all shelterbelt species. Error bars indicate standard error. Bars with the same letter for a given soil depth are not significantly different at $p < 0.1$.

Table 5.4 Mean increase in organic carbon (OC) stocks (Mg ha^{-1}) of light and heavy fractions, and whole soil and estimated marginal means (EMM) of increase in light and heavy fraction C for different shelterbelt species, estimated for an equivalent increase in SOC stocks. Numbers in parenthesis represent standard error.

Species†	Light fraction		Heavy fraction		Whole soil	
	Mean	EMM	Mean	EMM	Mean	% LF
HP	10.8 (2.1)	5.6 (1.1) a‡	26.5 (5.7)	13.8 (1.2) a‡	37.9 (8.1)	28.5
WS	10.4 (2.8)	9.8 (1.1) b	9.5 (5.1)	7.8 (1.2) b	21.1 (7.6)	49.3
GA	4.8 (3.6)	5.7 (1.1) a	9.6 (9.2)	11.7 (1.2) a	15.4 (13.3)	31.0
MM	3.3 (2.3)	5.2 (1.0) a	6.7 (6.2)	11.5 (1.1) a	11.5 (8.5)	28.5
CR	2.8 (1.2)	6.3 (1.0) a	2.7 (4.0)	11.2 (1.1) a	5.8 (5.5)	48.2
SP	9.9 (3.5)	9.6 (1.0) b	7.4 (6.6)	6.5 (1.1) b	20.0 (10.9)	49.8

† Abbreviations: HP- Hybrid poplar; WS – White spruce; GA – Green ash; MM – Manitoba maple; CR- Caragana; SP – Scots pine

‡ Values of EMM with same letters within a column for light and heavy fractions are not significantly different at $p < 0.1$.

5.6 Discussion

5.6.1 General characteristics of light and heavy fractions

The light fraction accounted for 10-27% of the SOC content for the shelterbelts and 9-19% of the SOC content for the agricultural fields (Table 5.3). These results are within the range of values reported in the literature for soils under permanent vegetation (15-40%; Christensen, 2001) and for arable soils (9-24%; Bremer et al., 1994), respectively. Carbon content of the light fraction was higher compared to heavy fraction across all land use and depths. This observation is also consistent with previous studies (Spycher et al., 1983; Teklay and Chang, 2008) and reflects the higher proportion of C-depleted metabolic products of microbial decomposition in the heavy fraction (Baisden et al., 2002). Average recovery of the soil C during density fractionation was 94% across all treatments. Incomplete recovery of soil C during the fractionation procedure may be due to the loss of soluble organic compounds in the discarded filtrate during repeated washing (Cerli et al. 2012) and complex formation between organic

matter and the iodide (I-) anion of the NaI solution, which also may lead to loss of SOM (Conceição et al., 2007).

5.6.2 Effect of shelterbelts on light and heavy fraction C

Shelterbelts led to a greater accumulation of SOC in the light- as well as heavy fraction compared to agricultural fields (Tables 5.2 and 5.3). The increase in the light fraction C is due to higher litter input for shelterbelts (Lorenz and Lal, 2014), which is the source of uncomplexed plant debris constituting the light fraction. Other studies have reported a similar increase in the light fraction C following increased additions of organic material to the soil as a result of practices such as no-tillage, residue management and tree mulching (Paulis, 2007; Youkhana and Idol, 2011). Accumulation of light fraction C under shelterbelts may also be due to conditions favoring reduced decomposition of plant detritus such as lack of soil disturbance due to practices such as tillage (Dick et al., 1998; West and Post, 2002) and differences in litter quality and microclimate (Mungai and Motavalli, 2006) compared to agricultural fields. An increase in C stocks of the heavy fraction represents increased complexation of organic matter with the soil minerals under the shelterbelts compared to agricultural fields. These results are in agreement with the studies by Youkhana and Idol (2011) and Garten (2002), who reported an increase in mineral-associated C pools in response to planting of trees. Increases in mineral-associated organic matter can be attributed to diffusion of fine organic particles, formed during the enzymatic breakdown of plant material, into soil pores and their adsorption on mineral surfaces (Leifeld and Kögel-Knabner, 2005). Additionally, oxidative degradation and solubilization of plant litter produces dissolved organic matter (DOM), which passes through the soil profile and adsorbs onto the reactive mineral surfaces to form mineral-associated organic matter (Kaiser and Guggenberger, 2000).

The relative increase of light fraction C for the shelterbelts was greater compared to heavy fraction C, both in terms of C concentration (LF 71%, HF 22%; Table 5.2) and C stocks (LF 48%, HF 13%; Table 5.3). This is in agreement with other studies, which reported that the light fraction C is more responsive to land use and management changes, compared to the stable fraction or bulk soil (Janzen et al., 1992; Bremer et al., 1994; Gregorich, et al., 2006). However, organic C in the light fraction decomposes quickly and has a relatively short residence time compared to mineral-associated organic C in the heavy fraction (Christensen, 1996). The importance of reactive soil minerals phases such as aluminum (Al) and iron (Fe) oxyhydroxides for the stabilization of organic matter has been demonstrated through incubation experiments (Jones and Edwards, 1998; Miltner and Zech, 1998). Whalen et al. (2000) observed negligible mineralization of C from the mineral-associated component of cultivated and forest soils, indicating that the heavy fraction of soils could be a major sink for C storage in soils. Consequently, increases in C stocks of the heavy fraction under shelterbelts represent more stable, long-term sequestration of atmospheric C in soils (Table 5.3). In contrast, C sequestered in the light fraction C may be lost rapidly in response to future changes in climate (Garten Jr. et al., 1999) and land use or management practices (Bremer et al., 1994; Post and Kwon, 2000). Nevertheless, despite the dynamic nature and shorter turnover time of the labile C pool (months to a few years), it plays an important role in rapid accumulation of soil C especially in low-quality, coarse textured soils (Garten, 2002; Baah-Acheamfour et al., 2015) as well as in cycling of nutrients and as source of energy for soil organisms (Janzen et al., 1992; Haynes, 2005).

5.6.3 Distribution of light and heavy fraction C with soil depth and shelterbelt species

The light fraction accounted for a larger proportion of SOC in the surface layers compared to deeper layers under both land use systems (Fig. 5.1). Similar observations regarding

the distribution of light- and heavy fractions have been made by other studies such as Janzen et al. (1992) and Spycher et al. (1983) for agricultural and forest soils, respectively. This trend is attributed to the distribution of plant detrital inputs through the soil profile (Spycher et al., 1983). Similarly, SOC sequestered under shelterbelts was dominated by the contribution from the light fraction C in the surface layers, and the heavy fraction C in the deeper layers (Fig. 5.5), indicating different sources and mechanisms of SOC accrual in the surface and deeper layers. Tree litter is the primary C input at the surface layers, while the subsurface layers are dominated by C inputs through root-derived compounds and rhizodeposition (Rasse et al., 2005; Lorenz and Lal, 2014). Close association of root-derived products with the soil mineral matrix tends to enhance their physical interaction and stabilization (Oades, 1995). Root-derived organic acids are also readily sorbed onto soil mineral phase due to the negative charge associated with their functional groups (Jones, 1998). Subsurface horizons, with comparatively low organic matter content, have higher available specific surface area (SSA) of the minerals, which enhances effective adsorption of organic matter at mineral sites (Kaiser and Guggenberger, 2003). A combination of these factors may have resulted in a higher contribution of mineral-associated components to soil C accrual in the subsurface layers. Increased stability of SOC due to adsorption with mineral surfaces, along with maximum C accumulation (as described in Chapter 4) at the 10-30 cm soil depth, indicates that the subsurface layers may play an important role in long-term storage of C under shelterbelts.

Results of our study suggest that tree species affect the distribution of SOC into physical density fractions (Fig. 5.2). This observation is supported by other studies that observed the influence of tree species on physicochemical stabilization of C within the size and density fractions of soil (Blanco-Canqui et al., 2007; Woldeselassie et al., 2012). The coniferous species,

white spruce and Scots pine, led to a higher increase in SOC stocks of the labile light fraction, in contrast to hybrid poplar, Manitoba maple, green ash and caragana that led to a higher increase in the stable heavy fraction (Table 5.4). Variance in the relative abundance of light- and heavy fractions and their contribution to sequestered C under coniferous and hardwood shelterbelts may be explained by the differences in the amounts and quality of litterfall inputs within the shelterbelt species. The coniferous shelterbelts had a higher density of litter layer compared to the broadleaved species, as described in Chapter 4 (Table 4.4). Moreover, the coniferous litter, primarily composed of needles and cones, generally has a lower decomposition rate due to its acidic nature, complex molecular structure and higher lignin and polyphenol content compared to the broadleaf litter (Prescott et al., 2000). These factors may account for lower mineralization rates of the coniferous litter, leading to the accumulation of partially decomposed uncomplexed organic matter under shelterbelts. In contrast, broadleaf litter decomposes faster compared to the coniferous litter (Perry et al., 1987; Laganière et al., 2010b) and hence may produce greater dissolved organic carbon (DOC) flux from the surface to deeper soil layers. Hongve et al. (2000) observed that the leachate from deciduous litter contained significantly higher concentrations of DOC compared to spruce litter. Increased production of DOC facilitates its adsorption on soil-mineral surfaces, thus contributing to the higher proportion of mineral-associated fraction under these species (Woldeselassie et al., 2012). Besides litter quality, other factors may also affect the relative abundance of light and heavy fractions. Bu et al. (2012) observed a higher contribution of the light fraction C to SOC under coniferous vegetation and attributed it partially to greater amounts of fine root biomass under the conifers. Similarly, Laganière et al. (2011) attributed the higher proportion of uncomplexed organic matter under black spruce compared to aspen, to

microclimatic conditions, such as low temperature, high soil moisture and lower light penetration, which constrain microbial decomposition of litter, besides the litter quality.

5.7 Conclusions

Our study demonstrates that shelterbelts can increase the storage of SOC within the labile light fraction as well as the stable heavy fraction of soil compared to an agricultural field. A major portion of the SOC added was in the form of uncomplexed, plant derived debris (i.e. light fraction) but there was also a significant increase in the mineral-associated component of OM (i.e. heavy fraction) under the shelterbelts. The relative contribution of the density fractions to SOC sequestration varied with the shelterbelt species. Partially decomposed, plant-derived organic matter constituted a higher component of the SOC accumulated under white spruce and Scots pine, suggesting a lower decomposability of the coniferous litter, compared to the broadleaved species. On the other hand, greater SOC storage under hardwood species was associated with mineral soils and protected through adsorption to clay surfaces. Results also showed that majority of SOC accumulated at 10-30 cm soil depth was stabilized through association with minerals, while most of the soil C added in the surface layer (0-10 cm soil depth) was in the form of more labile light fraction. This observation underscores the importance of subsurface soil layers in long-term sequestration of C in soil. Overall, this study highlights the potential benefits of shelterbelts towards mitigation of greenhouse gases and improvement of soil quality through the addition of C to soils.

6. SPECTROSCOPIC INVESTIGATION OF SOIL ORGANIC CARBON COMPOSITION UNDER SHELTERBELT AGROFORESTRY SYSTEMS

6.1 Preface

Previous chapters have shown that shelterbelts affect the SOC storage in whole soils (Chapter 4) as well as its physical stabilization in light and heavy fractions (Chapter 5). Long-term stabilization and dynamics of SOC also depends on its inherent chemical stability to microbial degradation, which is a function of its molecular and structural composition. Shelterbelts may influence the molecular chemistry and chemical stabilization of SOC due to difference in litter quality and amount compared to agricultural crops. In this chapter, molecular composition of SOC was determined under shelterbelts and agricultural fields by using advanced molecular analytical techniques including attenuated total reflectance Fourier transform infrared (ATR-FTIR) spectroscopy and synchrotron-based C K-edge X-ray absorption near edge structure (XANES) spectroscopy.

6.2 Abstract

While the role of agroforestry systems in increasing soil organic carbon (SOC) storage has been studied, insufficient information is available on their effect on the chemical composition of SOC. The objective of this study was to determine the functional group chemistry of SOC under shelterbelts and compare it to adjacent agricultural fields by using attenuated total reflectance Fourier transform infrared (ATR-FTIR) and Carbon K-edge X-ray absorption near edge structure (XANES) spectroscopies. ATR-FTIR spectral analysis indicated larger proportions of conjugated carboxylic and aromatic carbon (C) groups for hybrid poplar, white spruce and caragana shelterbelts, phenolic C for hybrid poplar and Manitoba maple shelterbelts and aliphatic and aromatic C for Manitoba maple shelterbelts compared to the adjacent agricultural fields. Polysaccharide, ether and alcoholic C functional groups were generally lower in shelterbelts compared to agricultural fields, with the exception of hybrid poplar species. Analysis by C K-edge XANES spectroscopy showed the accumulation of aromatic C, ketones and carbohydrates in the surface soil layer (0-5 cm) under the shelterbelts compared to agricultural fields. Pearson correlation analysis indicated that the majority of SOC added under the shelterbelts was in the form of plant-derived aromatic, phenolic and carboxylic C groups. Results of this study suggested a strong influence of initial litter composition and quality on the composition of SOC under the shelterbelts. The higher proportion of microbially derived ketones indicated that SOC under shelterbelts was at an advanced stage of decomposition in the surface soil layers; potentially due to the differential placement of litter within soil profile under shelterbelts and agricultural fields. Overall, this study suggests that the incorporation of shelterbelts in agricultural fields leads to significant molecular-level changes in the composition of SOC, which may in turn influence SOC turnover rates.

6.3 Introduction

Soil organic carbon (SOC) is composed of diverse and heterogeneous organic substances that vary in structure and chemical complexity (Piccolo, 2002; Sutton and Sposito, 2005). Biological stability of SOC is dependent on its physical accessibility to microorganisms and their degradative enzymes, as well as on its inherent biochemical recalcitrance (Sollins et al., 1996; Six et al., 2002). Biochemical recalcitrance is the capacity of SOC to protect against decomposition through its chemical structure and it is dependent upon the abundance of recalcitrant structural units and their interstructural bond strength (Gleixner et al., 2001; Krull et al., 2003). While the role of the chemical structure of SOC in determining its turnover and storage has recently been debated (Krull et al., 2003; Schmidt et al., 2011; Dungait et al., 2012), it is nevertheless an important factor in regulating the dynamics of C in soil. Agroforestry practices, such as shelterbelts, are expected to influence not only the quantity of SOC (Nair et al., 2009), but also its quality and composition. Incorporation of shelterbelts into agricultural fields changes the quality of litter inputs (Lorenz and Lal, 2014), which may persist through the decomposition process leading to the differences in the molecular nature of SOM (Wickings et al., 2012). Shelterbelts also modify microclimatic conditions such as soil moisture and temperature (Kort, 1988; Scholten, 1988; Brandle et al., 2004), which may influence microbial decomposition, thus altering SOM composition (Davidson and Janssens, 2006; Hilli et al., 2008). Despite the importance of molecular composition in regulating C dynamics and sequestration (Krull et al., 2003), there is a lack of information on the effect of agroforestry practices on the composition of SOM.

Chemical and thermal degradative methods, as well as stable isotope techniques have been used to obtain information about the chemical composition and turnover rates of SOC

(Bernoux et al., 1998; Kögel-Knabner, 2000). Further progress in characterization of SOC and its decomposition pathways can be made through the use of advanced molecular-scale analytical techniques such as pyrolysis–gas chromatography /mass spectrometry (Py–GC/MS), nuclear magnetic resonance (NMR) spectroscopy and near-infrared (NIR) and mid-infrared (MIR) spectroscopy (Kögel-Knabner, 2000, 2002). Fourier transform infrared (FTIR) spectroscopy is a form of vibrational spectroscopy that allows for the quick and non-destructive estimation of soil properties such as soil fertility (Du and Zhou, 2009), mineral composition (Janik et al., 1995), particle size and aggregate distribution (Madari et al., 2006), and soil water content and retention (Rossel et al., 2006; Janik et al., 2007). FTIR spectroscopy may also be used for the determination of principal chemical forms of organic compounds, through the vibrational characteristics of their structural chemical bonds (Artz et al., 2008). Previous studies have used this technique for the characterization of organic matter in leaf litter (Haberhauer et al., 1998; Haberhauer and Gerzabek, 1999; Mascarenhas et al., 2000), whole soils (Ellerbrock et al., 1999, 2005; Gerzabek et al., 2006) and humic acid extracts (Solomon et al., 2005). Carbon K-edge X-ray absorption near edge structure (XANES) spectroscopy is another powerful spectroscopic technique, that employs synchrotron-based soft x-rays (photon energy less than 2000 eV) for excitation of core level electrons to unoccupied or partially occupied molecular orbitals, thus producing unique absorption spectra for the elements (Lehmann et al., 2009). These absorption spectra can be used to assess the speciation and functional group chemistry of the specific elements such as carbon (C) (Lehmann and Solomon, 2010). The knowledge of the structural characteristics of C and its speciation, obtained through techniques such as ATR-FTIR and C K-edge XANES, can be used to determine the role of structural moieties to the inherent recalcitrance of organic matter (Lehmann et al., 2005) as well as to investigate the effect of land

use and management practices on the composition and dynamics of organic C at molecular scale in the soils (Solomon et al., 2005, 2007).

This study is based on the hypothesis that the structural composition of SOC may vary between the shelterbelts and agricultural fields due to the differences in amount and quality of litter inputs. The objective of this study was, therefore, to determine and compare the structural composition of SOC of shelterbelts and adjacent agricultural fields at the molecular scale using ATR-FTIR and C K-edge XANES techniques.

6.4 Materials and Methods

6.4.1 Site selection and soil sampling

Sampling was performed for six major shelterbelt species - green ash (*Fraxinus pennsylvanica*), hybrid poplar (*Populus* spp.), Manitoba maple (*Acer negundo*), white spruce (*Picea glauca*), Scots pine (*Pinus sylvestris*) and caragana (*Caragana arborescens*).

Saskatchewan has 106 ecodistricts, as defined by the National Ecological Framework for Canada, and they were grouped into 31 homogeneous clusters, based on the similarity between 42 climate, site and soil variables obtained from the National Ecological Framework for Canada and Soil Landscapes of Canada (SLC v3.2) datasets. Among these clusters, the ones with the highest number of trees shipped for shelterbelt planting of a particular species were chosen for sampling of that species, based on the Prairie Farm Rehabilitation Administration (PFRA) tree orders database. A randomized branch sampling (RBS) procedure was applied within the chosen clusters to select sampling sites for each species. In this way, 59 sampling sites were chosen, consisting of 10 sites each for hybrid poplar, Manitoba maple and caragana, 11 sites for Scots pine and nine sites for green ash and white spruce shelterbelts. The procedure for selection of sampling sites has been described in more detail in Amichev et al. (2016).

At each site, soil samples were obtained at three replicate locations, 20 m apart, along a transect in the shelterbelt and in adjacent agricultural field. Sampling within the agricultural fields was performed at more than twice the height of shelterbelt trees, ranging from 50-100 m apart from shelterbelt, to avoid the influence of shelterbelts. Soil samples were collected at 0-5, 5-10, 10-30 and 30-50 cm depths using a hand auger (6.58 cm dia.), air-dried at room temperature and ground to less than 250 μm in size prior to laboratory analysis.

6.4.2 Analysis by attenuated total reflectance Fourier transform infrared (ATR-FTIR) spectroscopy

Chemical composition of SOC for shelterbelts and agricultural fields was investigated by using attenuated total reflectance Fourier transform infrared (ATR-FTIR) spectroscopy. A Bruker Optics Equinox 55 FTIR spectrometer equipped with a deuterated triglycine sulphate (DTGS) detector was used for ATR-FTIR spectra acquisition of the finely ground whole soil samples. The spectra were collected by averaging 128 scans at 4 cm^{-1} resolution over a spectral range of 4000-400 cm^{-1} and were corrected against the spectrum with ambient air as background. Baseline correction of the spectra was performed using OPUS (ver. 6.5, Bruker Optik GmbH, Ettlingen, Germany) spectral processing software package.

The ATR-FTIR spectra of the mineral soils under shelterbelts and agricultural fields showed a number of characteristic major absorbance bands representing the molecular structure of SOC (Fig. 6.1). Absorbance of the broad band at about 3600-3000 cm^{-1} arises from O-H stretching and is strongly influenced by water content (Ellerbrock et al., 2005), which may vary between the analyzed soil samples. Hence, the relative intensity of this band was not considered in the present study. The spectral region between 2700-1800 cm^{-1} was excluded from the analysis because the information attributable to organic matter is masked by C-O noise from

CO_{2(g)} (Dobarco, 2014). Similarly, the bands from 900-400 cm⁻¹ are predominantly attributed to soil minerals (Haberhauer et al., 2000). Hence, the wavenumber range of 1800-900 cm⁻¹ was considered for the analysis of SOC functional groups in this study. As there is a strong overlap among the bands of organic functional groups within this wavenumber range, the individual bands were resolved by spectral deconvolution. To resolve the spectra into individual bands, a series of Gaussian curves were fit to the infrared spectra using the Fityk software package (version 1.2.1; Wojdyr, 2010), following the script provided in Appendix G. Spectral deconvolution could be performed for only 54 of the 59 sites, as the ATR-FTIR spectra of the other 5 sites were of poor quality. Analyzed sites included 11 sites for Scots pine, 10 sites for Manitoba maple, nine sites for hybrid poplar and green ash, eight sites for caragana and seven sites for white spruce shelterbelts. The curve parameters were constrained to ensure equal FWHM (full width at half maximum) of the curves so that the curves were of equal width. Individual spectral band identification was performed by using the second-degree spectral derivatives of the ATR-FTIR bands, along with the available knowledge of characteristic infrared peak positions of SOC as reported in the literature. The relative absorbance intensity (rA) of the deconvoluted bands was calculated by dividing the area of individual bands within the 1800-900 cm⁻¹ wavenumber region (i.e. 917, 986, 1037, 1103, 1162, 1250, 1370, 1434, 1509, 1584, 1644, 1703 cm⁻¹) with the sum of total area of all the bands in this region (e.g., $rA_{1509} = A_{1509} / \sum A_{(917-1703\text{cm}^{-1})}$). The intensity of absorption bands depends on the amount of absorbing functional groups such that high absorption intensity indicates high content of the corresponding functional group and vice versa (Ellerbrock et al., 1999). Thus, the relative intensity of the bands was used as a semi-quantitative estimate of the relative proportion of C functional group within the total SOC of the soil sample.

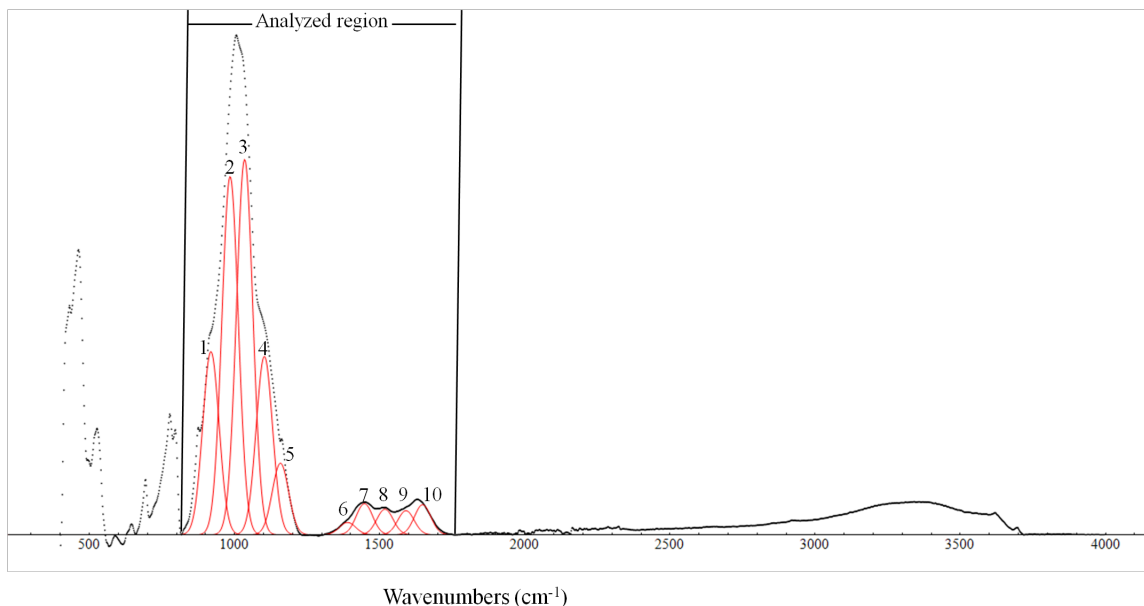


Fig. 6.1 A representative ATR-FTIR spectra of whole soil showing the fitted Gaussian peaks representing major C functional groups within the wavenumber range of 1800-900 cm^{-1} . Peaks are identified as follows: 1-917 cm^{-1} ; 2-986 cm^{-1} ; 3 – 1037 cm^{-1} ; 4-1103 cm^{-1} ; 5-1162 cm^{-1} ; 6-1370 cm^{-1} ; 7-1434 cm^{-1} ; 8-1509 cm^{-1} ; 9-1584 cm^{-1} ; 10-1644 cm^{-1} .

6.4.3 Analysis by Carbon K-edge X-ray absorption near edge structure (XANES) spectroscopy

Carbon K-edge X-ray absorption near edge structure (XANES) spectroscopy was used to investigate the SOC composition of three shelterbelt sites belonging to hybrid poplar, Scots pine and caragana shelterbelt species and their adjacent agricultural fields. The sites to be analyzed by C K-edge XANES were selected on the basis of maximum amount of SOC sequestered (described in Chapter 4) for their respective shelterbelt species. Soil samples from 0-5, 10-30 and 30-50 cm depths for shelterbelts and adjacent agricultural fields were analyzed for these three sites. Prior to the spectral analysis, samples were ground using ball-mill and a subsample of each soil was hydrated in deionized water, deposited onto Au-coated Si wafers and air-dried at room temperature. Carbon K-edge XANES spectra were measured at the spherical grating

monochromator (SGM) beamline 11ID-1 at the Canadian Light Source (CLS, Saskatoon, SK, Canada). Data were corrected by a linear regression fit through the pre-edge region followed by normalization of the spectra using custom macros in IGOR Pro (ver. 6.2, WaveMetrics Inc., Lake Oswego, OR, USA) and Athena (ver. 0.8.56; Ravel and Newville, 2005) software packages.

The C K-edge XANES spectra were deconvoluted by performing curve fitting, following the script provided in Appendix H, using Fityk software package. The arctangent function was fit for the ionization step at 290 eV. A series of Gaussian curves were fit for the main ($1s-\pi^*$) spectral features in the fine structure region (280-310 eV). The curve parameters were constrained to ensure equal FWHM for the main spectral peaks. Additionally, two Gaussian curves were fit for σ transitions without any constraint on the curve parameters. The deconvoluted C (1s) XANES spectra of a representative sample showing the main ($1s-\pi^*$) peaks at 284.1, 285.1, 286.2, 287.3, 288.4, 289.4 and 290.6 eV, as well as two σ transition peaks and the arctangent function is shown in Fig. 6.2. Average peak positions of the deconvoluted spectral bands of the analyzed soil samples are listed in Appendix I.

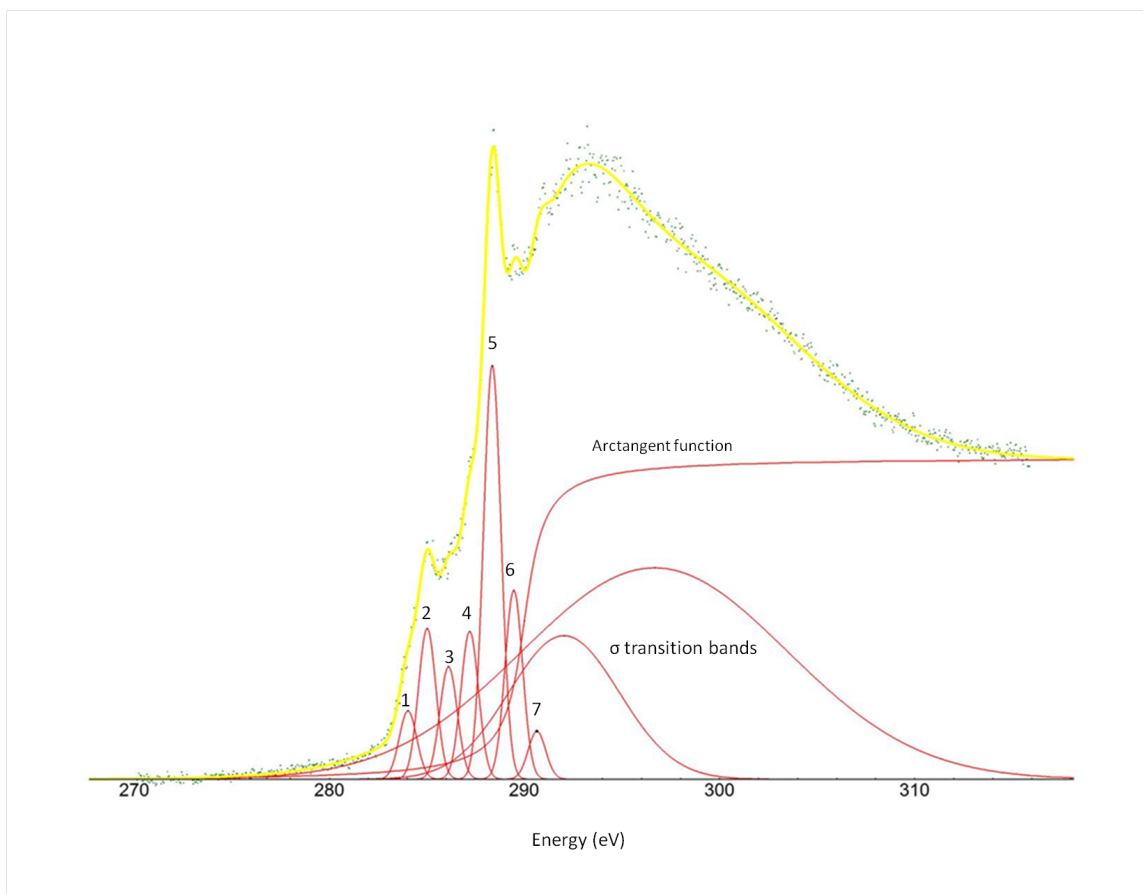


Fig. 6.2 A typical deconvoluted C K-edge XANES spectra of whole soil showing the main ($1s-\pi^*$) peaks (1-7), transition peaks and the arctangent function. Peaks are identified as the following; 1-284.1 eV (unsaturated C); 2- 285.1 eV (Aromatic-C); 3 – 286.2 eV (Ketones); 4 – 287.3 eV (Aliphatic-C); 5 – 288.4 eV (Carboxylic-C); 6 – 289.4 eV (Polysaccharides); 7 – 290.6 eV (Carbonates).

6.4.4 Statistical analysis

Data were analyzed using a two-way mixed analysis of variance (ANOVA) procedure, with the land cover (i.e. shelterbelts vs. fields) analyzed as the within-subjects factor. In the presence of a significant interaction, simple main effects were analyzed. In addition, Pearson correlation analysis was performed to determine the relationship between the increase in ATR-FTIR band intensities and the increase in SOC concentration under shelterbelts and fields. For the statistical analysis, a p-value of 0.1 was used to assess the significance. This was done to

reduce the risk of failing to detect existing differences between land use types (type II error), since a significant natural within-site variation is expected. Statistical analysis was performed using IBM SPSS Statistics version 23 (IBM Inc., Armonk, NY, USA).

6.5 Results

6.5.1 Deconvolution of ATR-FTIR spectra

ATR-FTIR spectra of the mineral soils showed a number of characteristic absorbance peaks for the investigation of structural composition of SOC for shelterbelts and agricultural fields (Fig. 6.1). The broad intense band at about 3600-3000 cm^{-1} represents the stretching vibrations of H-bonded hydroxyl (O-H) groups of alcohols, phenols and water molecules (Ellerbrock et al., 1999). The weak C-H vibration bands at about 2850 and 2920 cm^{-1} were superimposed as a shoulder on the broad O-H band and are formed due to vibrations of asymmetric and symmetric aliphatic (CH_3 and CH_2) groups (Haberhauer et al., 1998; Calderón et al., 2013). However, distinct peaks within this range were not visible for all the soil spectra in the current study. The absorbance band near 1703 cm^{-1} formed a shoulder on the broad band at 1644 cm^{-1} , and is attributed to carboxylic acids and carbonyls bands in esters (Sarkhot et al., 2007). This absorbance band was also not present in all soil spectra, suggesting loss of easily decomposable esters from the soil (Calderón et al., 2011). The absorbance band near 1644 cm^{-1} is attributed to C=O stretching of carboxylates, amides and conjugated ketones, as well as to aromatic C (C=C) vibrations (Haberhauer et al., 1998; Calderón et al., 2013). Similarly, the band around 1584 cm^{-1} is assigned to aromatic C=C stretching of the phenyl ring as well as C=O carboxylate stretching (Baes and Bloom, 1989; Calderón et al., 2013). The absorbance bands at 1644 and 1584 cm^{-1} are combination bands representing contributions from lignin, proteins and humic acids (Calderón et al., 2011). Calderón et al. (2011) observed that the incubation of soils

increases the absorbance of bands at 1570, 1630 and 1650 cm^{-1} , suggesting that these bands represent a relatively recalcitrant form of C. Absorbance band at 1509 cm^{-1} is assigned to aromatic C-H and C=C vibrations (Bornemann et al., 2010), while the absorbance band at 1434 cm^{-1} is assigned to aliphatic (C-H) bending of CH_2 and CH_3 groups (Lehmann et al., 2005; Calderón et al., 2013). The absorbance band at 1370 cm^{-1} is a combination band, and is primarily attributed to C-H absorption in aliphatics (Janik et al., 2007), as well as to CO- CH_3 vibrations in lignin-derived phenols (Tatzber et al., 2007b; Bornemann et al., 2010). Calderón et al. (2006) observed an increase in the band at 1510 cm^{-1} during the decomposition of manure, indicating that it may represent more processed forms of C. Similarly, alkyl C-H moieties represented by bands at 1370 and 1434 cm^{-1} have been observed to increase during the composting of cattle manure (Inbar et al., 1989) and SOM mineralization (Solomon et al., 2005, 2007). These bands, thus, may represent the stabilized, recalcitrant aliphatic biopolymers preserved in soil (Lorenz et al., 2007). However, the inorganic carbonate band at 1430 cm^{-1} may lead to interference (Tatzber et al., 2007a), and thus, care must be taken in the quantitative interpretation of these bands. The bands at 1162, 1103 and 1037 cm^{-1} are assigned to C-O stretch of polysaccharides, and of other groups such as alcohols, ether and esters (Janik et al., 2007; Spaccini and Piccolo, 2007; Dobarco, 2014). Calderón et al. (2013) found this region (1030-1160 cm^{-1}) to be sensitive to the addition of cellulose. These bands may overlap with Si-O stretching of silicate bands from mineral particles at 1050 cm^{-1} (Haberhauer et al., 2000). The bands below 1000 cm^{-1} are associated with a mixture of organic and inorganic compounds such as clay and quartz minerals (Haberhauer et al., 2000; Calderón et al., 2011).

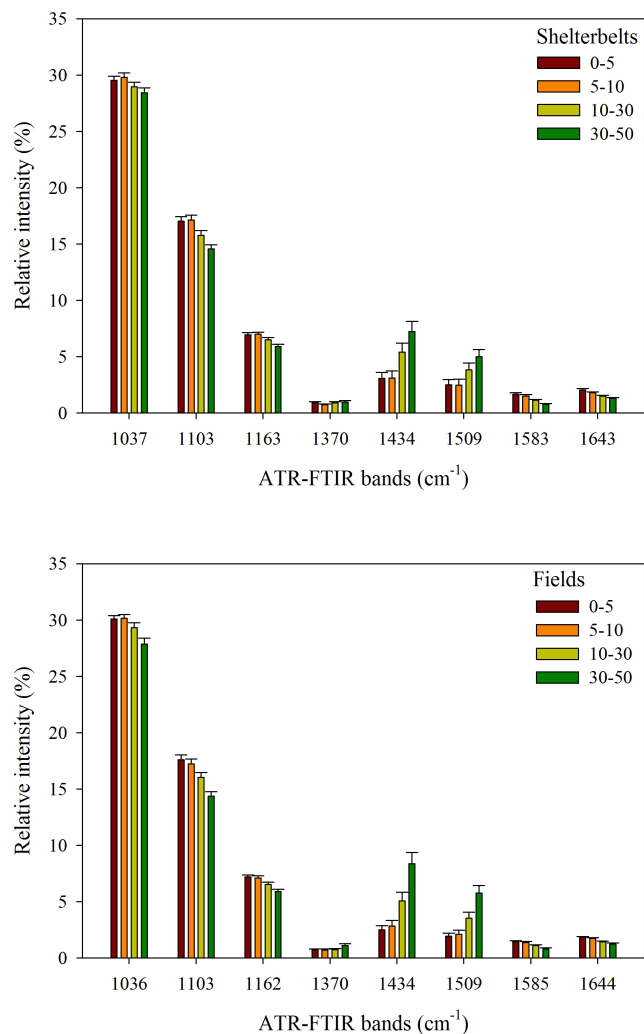


Fig. 6.3 Mean relative absorbance intensities of different ATR-FTIR bands at 0-5, 10-30 and 30-50 cm soil depths for (A) shelterbelts and (B) agricultural fields.

6.5.2 Changes in SOC composition with depth and land use

Relative intensities of ATR-FTIR absorbance bands were generally consistent and followed a similar pattern across the shelterbelts and agricultural fields (Fig. 6.3). ATR-FTIR bands representing the C-O bond of polysaccharides, polycyclic and ether functional groups (1037, 1103, 1162 cm⁻¹) showed decreases with soil depth. Similarly, there was a decrease with depth for ATR-FTIR bands attributed to aromatic (C=C) bond of phenyl ring structure as well as

conjugated carbonyl (C=O) bonds, that are part of carboxylic acids, ketones, aldehydes and esters (1584 and 1644 cm^{-1}). ATR-FTIR bands associated with aromatic vibrations (1509 cm^{-1}) as well as aliphatic (C-H) deformation of CH_2 and CH_3 groups (1434 cm^{-1}) showed an increase with depth under both land use types (Fig. 6.3).

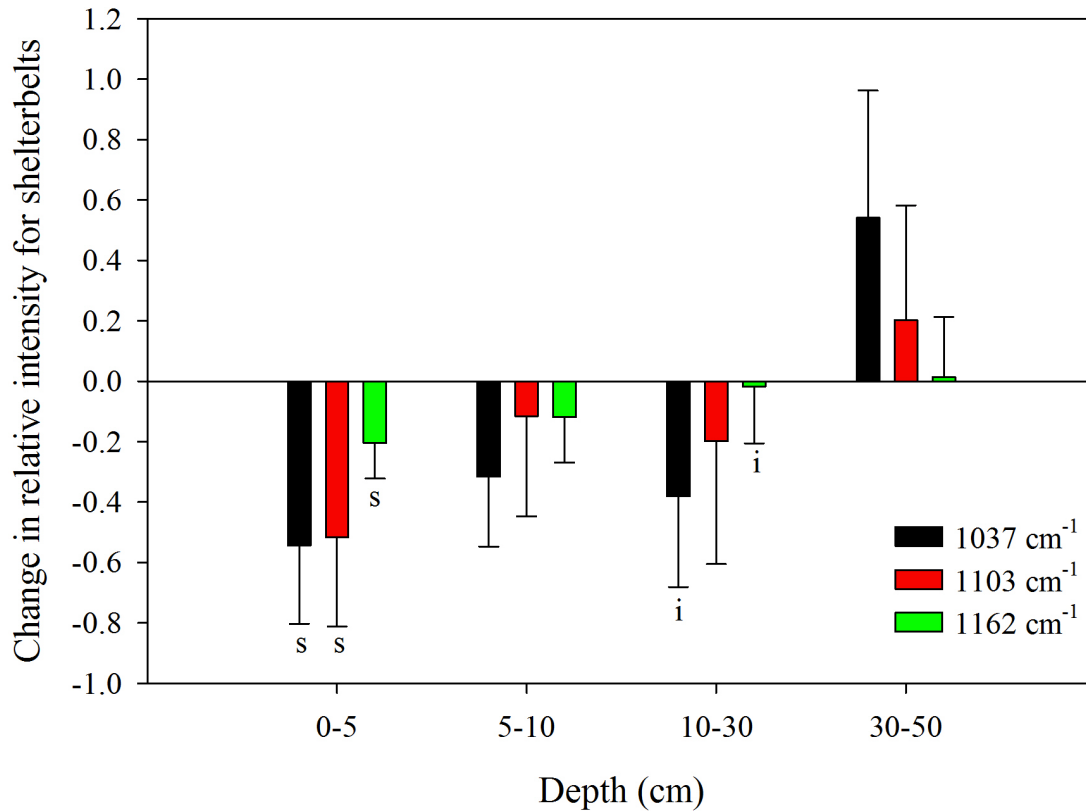


Fig. 6.4 Change in the relative absorbance intensities of ATR-FTIR bands at 1034, 1103 and 1162 cm^{-1} for shelterbelts compared to agricultural fields at 0-5, 5-10, 10-30 and 30-50 cm soil depths. 's' on the top of the bar indicates statistically significant effect of land use and 'i' indicates significant interaction between land use and species at $p < 0.1$.

Despite these similar trends, there were significant differences in relative intensities of ATR-FTIR bands between shelterbelts and agricultural fields (Table 6.1). There was a significant decrease in the relative intensity of 1037, 1103 and 1162 cm^{-1} bands for the shelterbelts compared to the agricultural fields at the 0-5 cm soil depth, indicating a decrease in polysaccharide and ether functional groups under the shelterbelts (Fig. 6.4). Changes in the relative proportion of polysaccharide functional groups (1037 cm^{-1}) was also affected by shelterbelt species, as indicated by a significant interaction effect at the 10-30 cm soil depth (Table 6.1; Fig. 6.4). Manitoba maple, green ash and white spruce showed a trend of decreasing relative intensity of 1037 cm^{-1} band for shelterbelts compared to agricultural fields at all soil depths; however, the difference was statistically significant only at the 0-5 cm depth for Manitoba maple, and at the 10-30 cm depth for green ash and white spruce (Fig. 6.5). Conversely, hybrid poplar showed a significant increase in the relative intensity of 1037 cm^{-1} band for shelterbelts compared to agricultural fields at the 10-30 cm depth. Similarly, for 1103 and 1162 cm^{-1} bands, there was a trend of increasing relative intensity for hybrid poplar shelterbelts compared to agricultural fields, with a statistically significant increase for the 1162 cm^{-1} band at the 10-30 cm depth (Fig. 6.5). Other shelterbelt species, however, showed a trend of decreasing relative intensity of the 1103 and 1162 cm^{-1} bands compared to agricultural fields, with a significant decrease for Scots pine at the 0-5 cm soil depth for both of these bands. These data showed a general trend of decreasing polysaccharides and ethers in Manitoba maple, green ash, white spruce and Scots pine shelterbelts compared to agricultural fields. Conversely, these C functional groups are higher in hybrid poplar shelterbelts compared to adjacent fields, especially at the 10-30 cm soil depth.

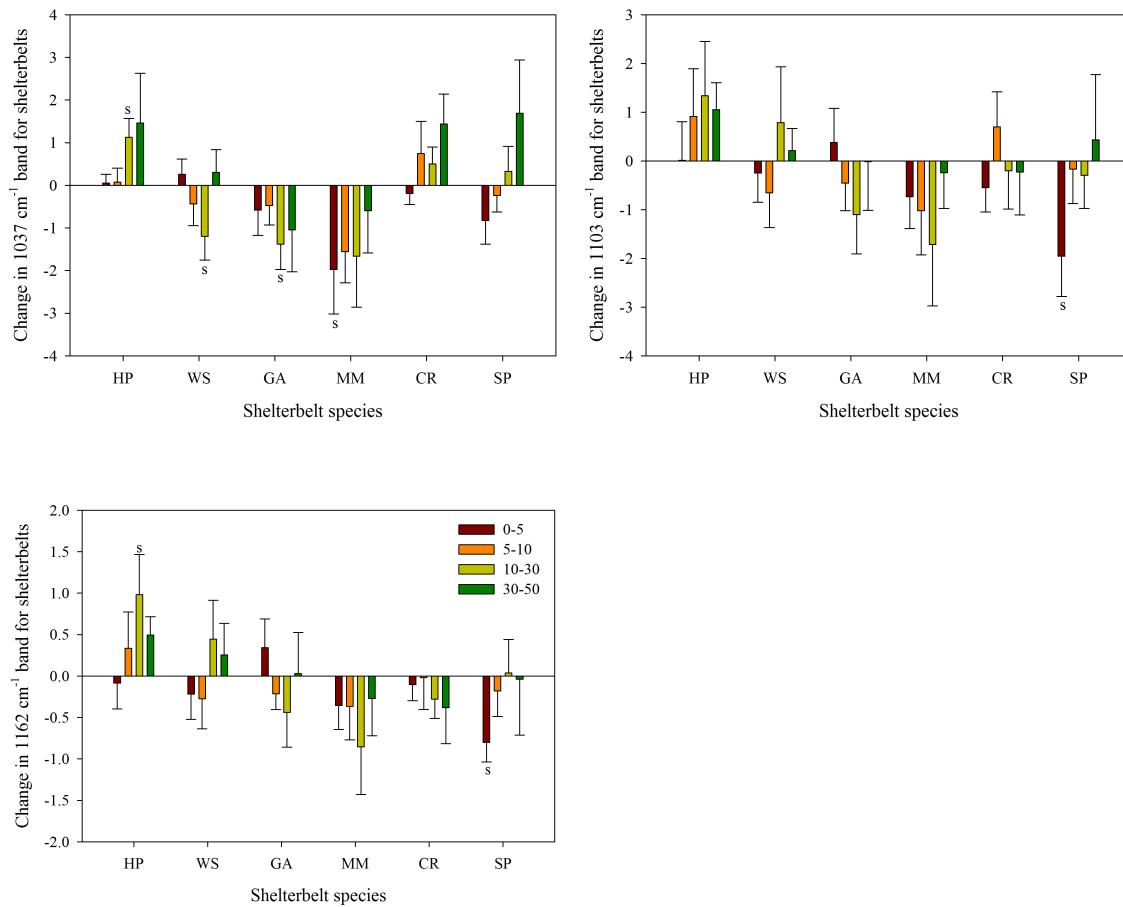


Fig. 6.5 Change in the relative absorbance intensities of the ATR-FTIR bands at 1034, 1103 and 1162 cm⁻¹ for different shelterbelt species (HP- Hybrid poplar; WS – White spruce; GA – Green ash; MM – Manitoba maple; CR- Caragana; SP – Scots pine) compared to agricultural fields at 0-5, 5-10, 10-30 and 30-50 cm soil depths. ‘s’ on the top of the bar indicates statistical significance at p < 0.1.

Table 6.1 Two-way mixed analysis of variance (ANOVA) of the effect of land use (i.e. shelterbelts and fields) and interaction between land use and species on the relative intensity of absorbance of ATR-FTIR bands at 0-5, 5-10, 10-30 and 30-50 cm soil depths.

ATR-FTIR bands (cm ⁻¹)		Soil Depth (cm)							
		0-5		5-10		10-30		30-50	
		F	p-value	F	p-value	F	p-value	F	p-value
1037	Landuse	4.41	0.04	1.88	0.18	1.62	0.21	1.65	0.21
	Interaction	1.67	0.16	1.94	0.11	2.61	0.04	1.36	0.26
1103	Landuse	3.03	0.09	0.12	0.73	0.24	0.63	0.28	0.60
	Interaction	1.44	0.23	0.93	0.47	1.33	0.27	0.29	0.92
1162	Landuse	3.01	0.09	0.63	0.43	0.01	0.92	0.01	0.94
	Interaction	1.92	0.11	0.49	0.78	2.10	0.08	0.44	0.82
1370	Landuse	3.68	0.06	0.32	0.58	2.35	0.13	1.01	0.32
	Interaction	2.09	0.08	1.49	0.21	0.93	0.47	0.71	0.62
1434	Landuse	0.95	0.33	0.09	0.77	0.17	0.68	1.27	0.27
	Interaction	3.57	0.01	1.97	0.10	1.63	0.17	0.89	0.50
1509	Landuse	1.87	0.18	0.41	0.53	0.26	0.62	1.35	0.25
	Interaction	2.50	0.04	2.06	0.09	1.69	0.16	1.03	0.41
1584	Landuse	7.25	0.01	3.75	0.06	0.38	0.54	0.84	0.36
	Interaction	1.80	0.13	1.42	0.23	2.46	0.05	1.74	0.15
1644	Landuse	7.90	0.01	1.24	0.27	1.14	0.29	0.56	0.46
	Interaction	1.16	0.34	1.12	0.36	0.68	0.64	1.35	0.26

Changes in aromatic, aliphatic and phenolic C moieties (represented by ATR-FTIR bands in the 1370-1510 cm⁻¹ region) under shelterbelts varied with the shelterbelt species, as indicated by the significant interactions between land use and shelterbelt species at the 0-5 cm (for 1370, 1434 and 1509 cm⁻¹ bands) and the 5-10 cm (for 1509 cm⁻¹) soil depth (Fig. 6.6; Table 6.1). The band at 1370 cm⁻¹, representing phenolic and aliphatic C groups, showed a significant increase for hybrid poplar and Manitoba maple shelterbelts compared to fields at the 0-5 cm depth, while the other species did not show significant changes at any soil depth (Fig. 6.7). Similarly, Manitoba maple shelterbelts also showed a higher relative intensity for the 1434 and 1509 cm⁻¹ bands compared to the adjacent field at 0-5 cm depth, with a similar but statistically insignificant trend at lower soil depths (Fig. 6.7). Conversely, hybrid poplar and caragana shelterbelts showed

a trend of lower relative intensities of 1434 and 1509 cm^{-1} bands compared to adjacent fields at all depths, with a statistically significant decrease in the 1434 cm^{-1} band for hybrid poplar at the 0-5 cm depth. These observations suggest that there was a relative increase in aromatic and aliphatic C functional groups, represented by 1434 and 1509 cm^{-1} bands, under Manitoba maple shelterbelts; while these C functional groups decreased compared to adjacent fields under hybrid poplar shelterbelts.

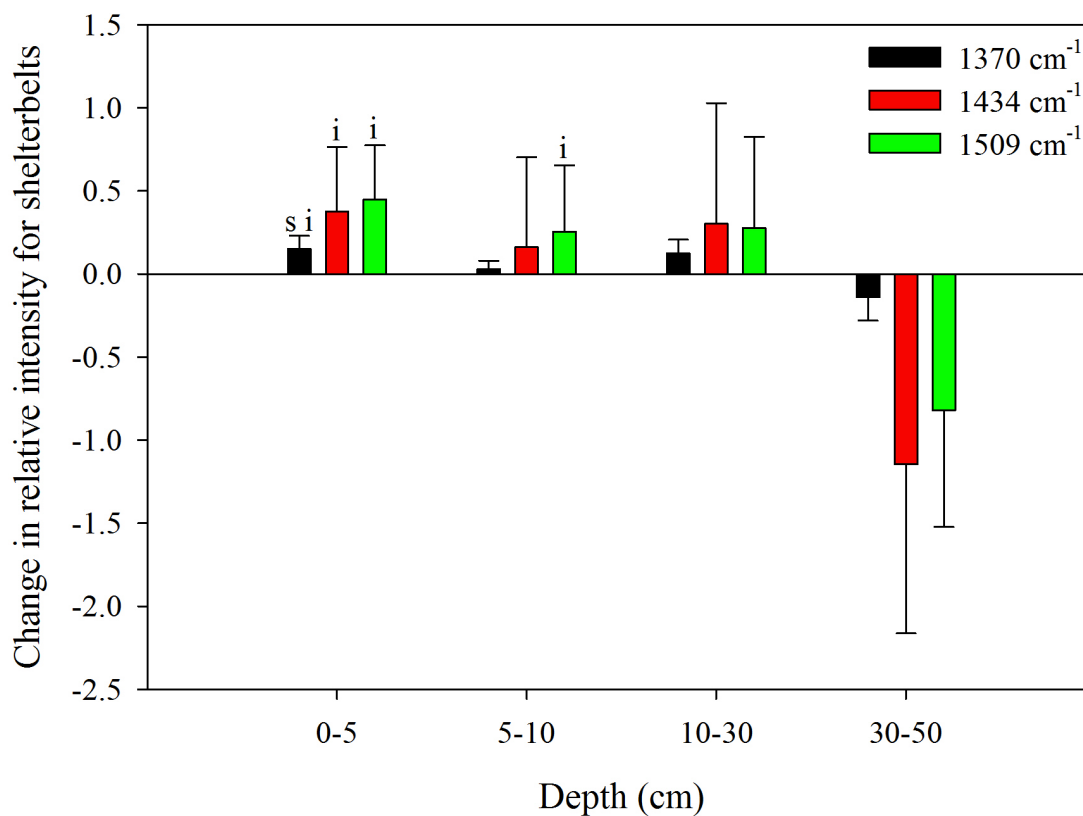


Fig. 6.6 Change in the relative absorbance intensities of ATR-FTIR bands at 1370, 1434 and 1509 cm^{-1} for shelterbelts compared to agricultural fields at 0-5, 5-10, 10-30 and 30-50 cm soil depths. 's' on the top of the bar indicates statistically significant effect of land use and 'i' indicates significant interaction between land use and species at $p < 0.1$.

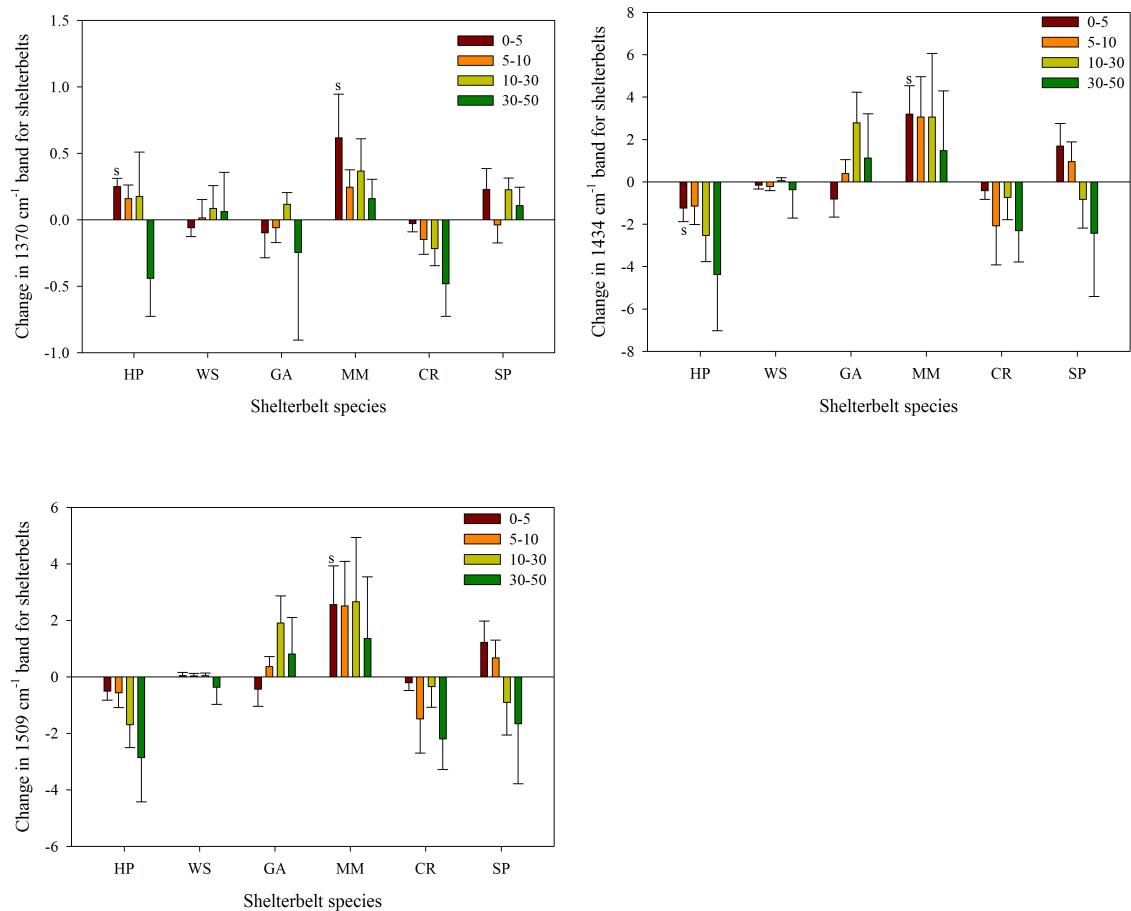


Fig. 6.7 Change in the relative absorbance intensities of the ATR-FTIR bands at 1370, 1434 and 1509 cm^{-1} for different shelterbelt species (HP- Hybrid poplar; WS – White spruce; GA – Green ash; MM – Manitoba maple; CR- Caragana; SP – Scots pine) compared to agricultural fields at 0-5, 5-10, 10-30 and 30-50 cm soil depths. ‘s’ on the top of the bar indicates statistical significance at $p < 0.1$.

The relative intensities of the 1584 and 1644 cm^{-1} bands were higher for shelterbelts compared to agricultural fields at the 0-5 cm soil depth, and at the 0-5 and 5-10 cm soil depths, respectively (Fig. 6.8). Moving down the soil profile, the difference in relative intensities of these bands between shelterbelts and fields decreased, and was statistically insignificant in the deeper layers. In terms of species, the relative intensity of the 1584 cm^{-1} band was higher for hybrid poplar at the 0-5, 5-10 and 10-30 cm soil depths and for white spruce shelterbelts at the 0-5 and 5-10 cm soil depths compared to agricultural fields (Fig. 6.9). Green ash shelterbelts showed a significant decrease in the relative intensity of the 1584 cm^{-1} band at the 10-30 cm soil depth. Similarly, there was a trend of increasing relative intensity of the 1644 cm^{-1} band for hybrid poplar, white spruce and caragana shelterbelts, with a statistically significant increase compared to agricultural fields at the 0-5 cm soil depth. These bands are attributed to aromatic and conjugated carboxylic groups, indicating the enrichment of these C functional groups in surface layers of hybrid poplar and white spruce shelterbelts compared to adjacent fields.

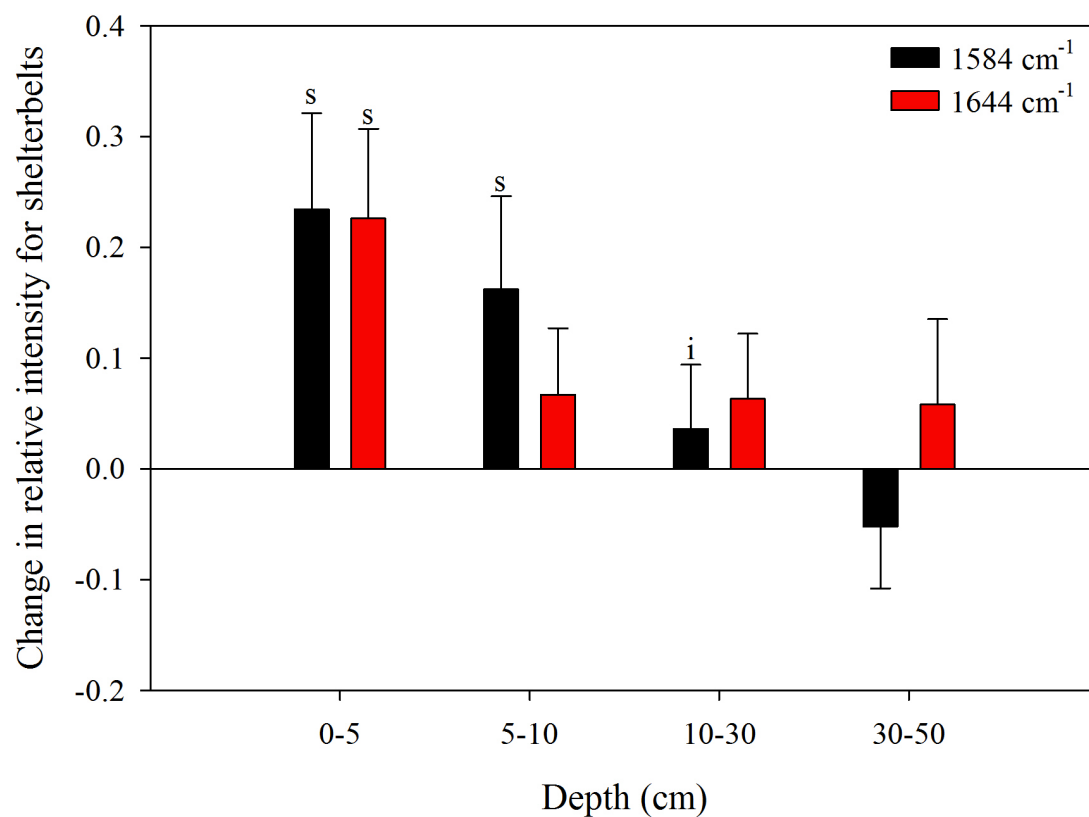


Fig. 6.8 Change in the relative absorbance intensities of ATR-FTIR bands at 1584 and 1644 cm⁻¹ for shelterbelts compared to agricultural fields at 0-5, 5-10, 10-30 and 30-50 cm soil depths. 's' on the top of the bar indicates statistically significant effect of land use and 'i' indicates significant interaction between land use and species at $p < 0.1$.

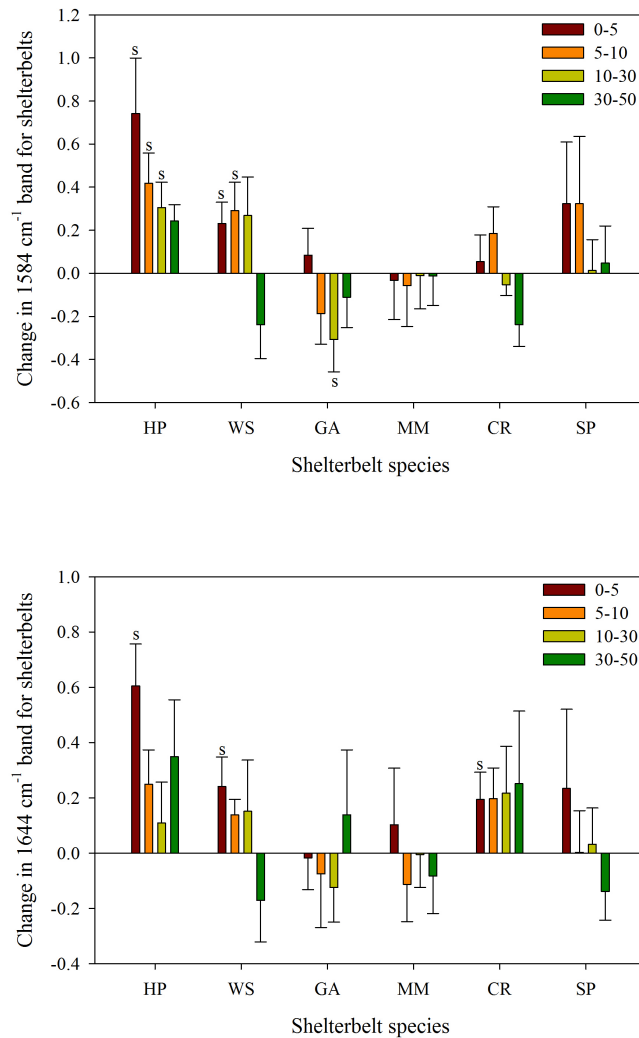


Fig. 6.9 Change in the relative absorbance intensities of the ATR-FTIR bands at 1584 and 1684 cm^{-1} for different shelterbelt species (HP- Hybrid poplar; WS – White spruce; GA – Green ash; MM – Manitoba maple; CR- Caragana; SP – Scots pine) compared to agricultural fields at 0-5, 5-10, 10-30 and 30-50 cm soil depths. ‘s’ on the top of the bar indicates statistical significance at $p < 0.1$.

Increases in the relative intensities of phenolic (1370 cm^{-1}), aromatic and conjugated carboxylic (1584 and 1644 cm^{-1}) functional groups were significantly correlated to the increase in soil organic carbon (SOC) concentration under the shelterbelts compared to the agricultural fields (Table 6.2). An increase in relative intensity of the 1370 and 1644 cm^{-1} bands was positively correlated to the increase in SOC concentration at the 0-5 and 5-10 cm soil depths, while the increase in relative intensity of 1584 cm^{-1} bands was positively related to the increase in SOC concentration at the 0-5, 5-10 and 10-30 cm soil depths (Table 6.2). The other bands at 1037 , 1103 , 1162 , 1434 and 1509 cm^{-1} were not significantly related to an increase in SOC concentration at any depth.

Table 6.2 Pearson correlations between the increase in relative intensity of absorbance of ATR-FTIR bands and increase in SOC concentrations (g kg^{-1}) at 0-5, 5-10, 10-30 and 30-50 cm soil depths.

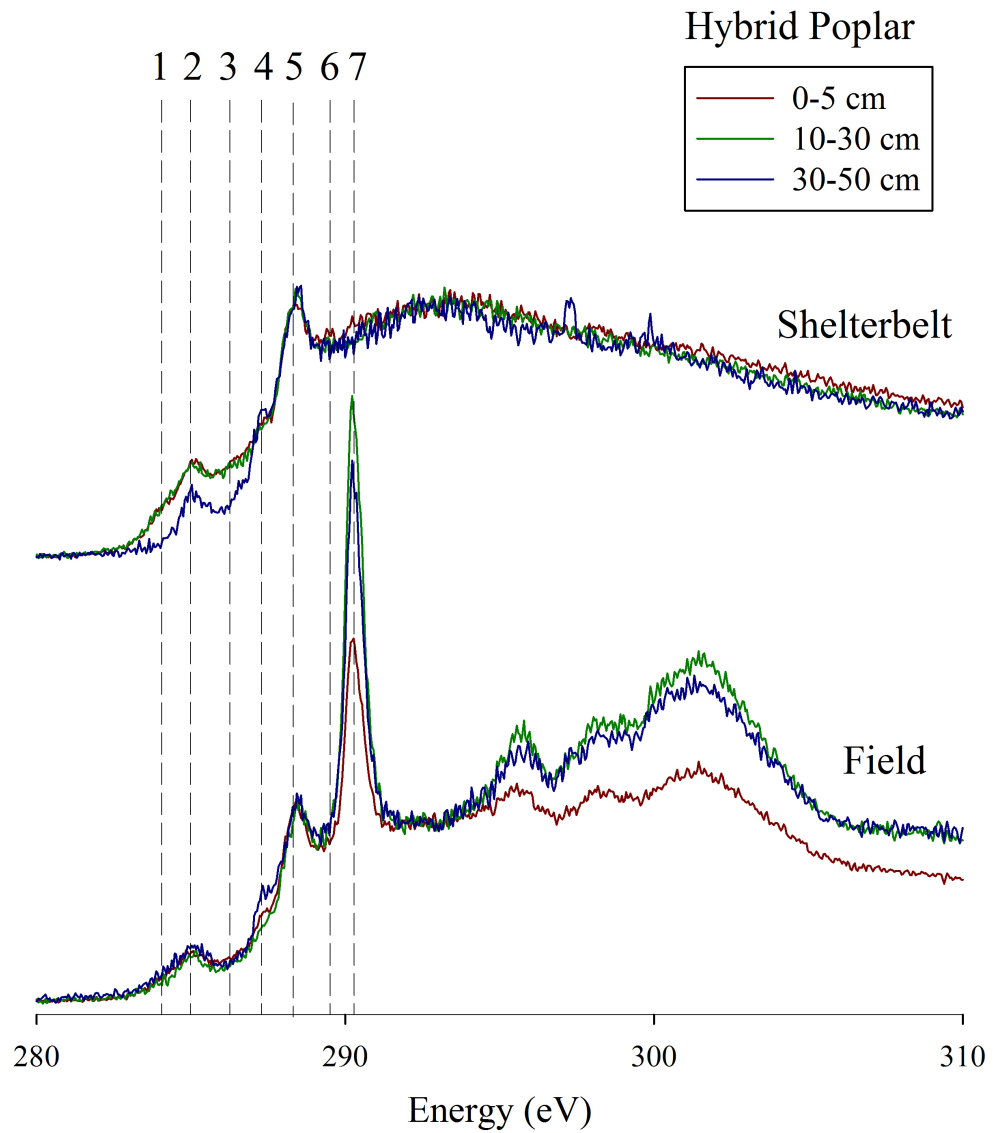
Soil depth (cm)	Increase in relative intensity of ATR-FTIR bands (cm^{-1})							
	1037	1103	1162	1370	1434	1509	1584	1644
0-5	-0.216	0.106	0.132	0.402*	-0.080	0.049	0.746*	0.654*
5-10	-0.107	0.061	0.126	0.308*	-0.067	0.059	0.401*	0.495*
10-30	-0.115	-0.089	-0.087	0.265	0.108	0.191	0.677*	0.216
30-50	-0.146	0.019	0.006	-0.042	0.129	0.184	0.028	0.041

*Correlations significant at 0.05 level

6.5.3 SOC composition resolved by C K-edge XANES spectroscopy

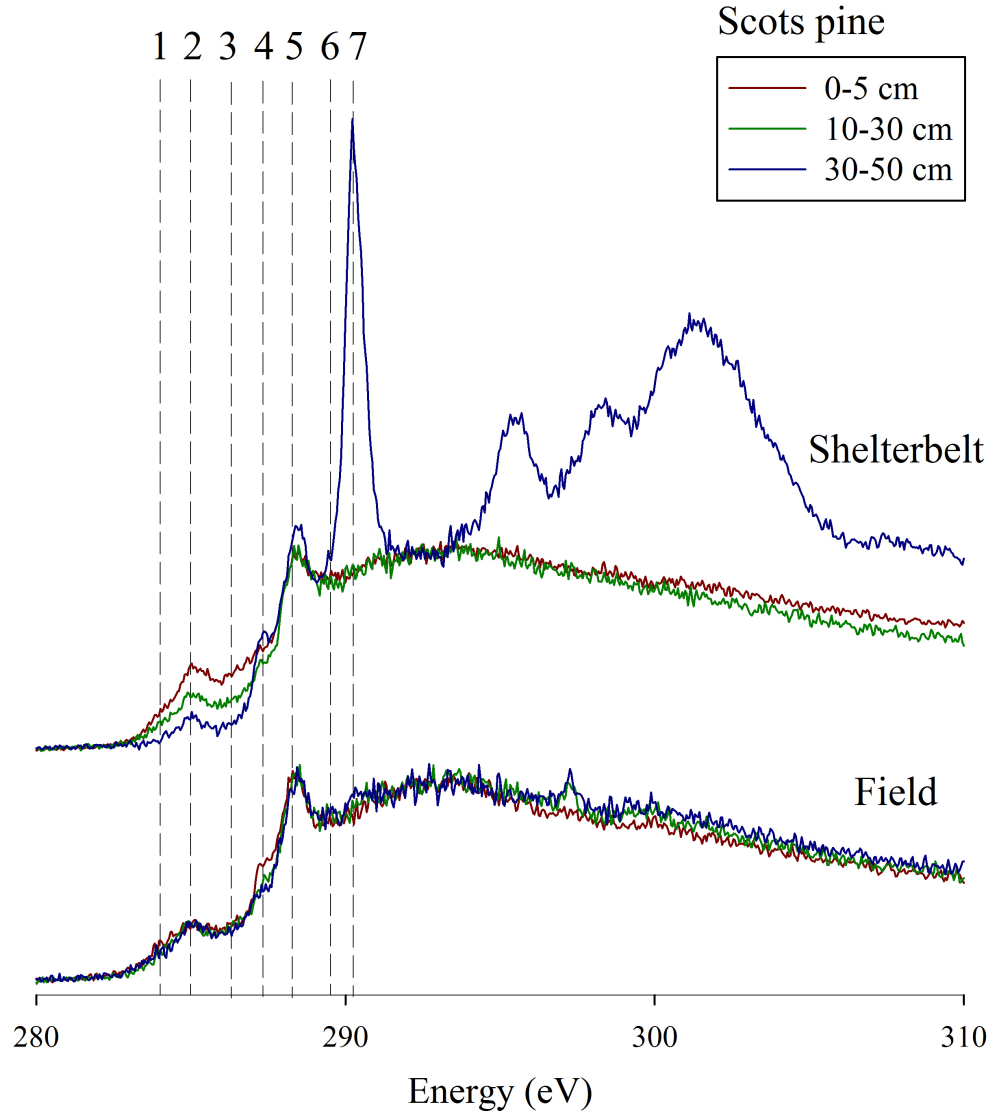
The deconvoluted C (1s) XANES spectra of a representative sample showing the main ($1s-\pi^*$) peaks, transition peaks and the arctangent function is shown in Fig. 6.2. Spectral features at the C K-edge were assigned according to the literature (Myneni, 2002; Urquhart and Ade, 2002; Gillespie et al., 2014a), to determine the molecular composition of SOC under shelterbelts and agricultural fields. The C K-edge XANES spectra of mineral soils of shelterbelts and fields

showed a strong absorbance at 288.4 eV, attributed to carboxylic-C and at 285.1 eV, attributed to aromatic-C (Fig. 6.10). Absorbance bands at 284.1 eV attributed to unsaturated-C, as well as at 286.2 eV for ketones, 287.3 eV for aliphatic-C and at 289.4 eV for carbohydrate-C were also observed in the soil samples across both land use types. A strong inorganic carbonate band at 290.6 eV was observed for Scots pine shelterbelts at the 30-50 cm soil depth (Fig. 6.10b), and for agricultural fields adjacent to hybrid poplar shelterbelts at the 0-5, 10-30 and 30-50 cm soil depths (Fig. 6.10a).



1 - Unsaturated; 2 - Aromatic; 3 - Ketone; 4 - Aliphatic
 5 - Carboxyl; 6 - Carbohydrate; 7 - Carbonate

Fig. 6.10a Carbon K-edge XANES spectra of the whole soil samples of hybrid poplar shelterbelt and adjacent agricultural field at 0-5, 10-30 and 30-50 cm soil depths.



1 - Unsaturated; 2 - Aromatic; 3 - Ketone; 4 - Aliphatic
 5 - Carboxyl; 6 - Carbohydrate; 7 - Carbonate

Fig. 6.10b Carbon K-edge XANES spectra of the whole soil samples of Scots pine shelterbelt and adjacent agricultural field at 0-5, 10-30 and 30-50 cm soil depths.

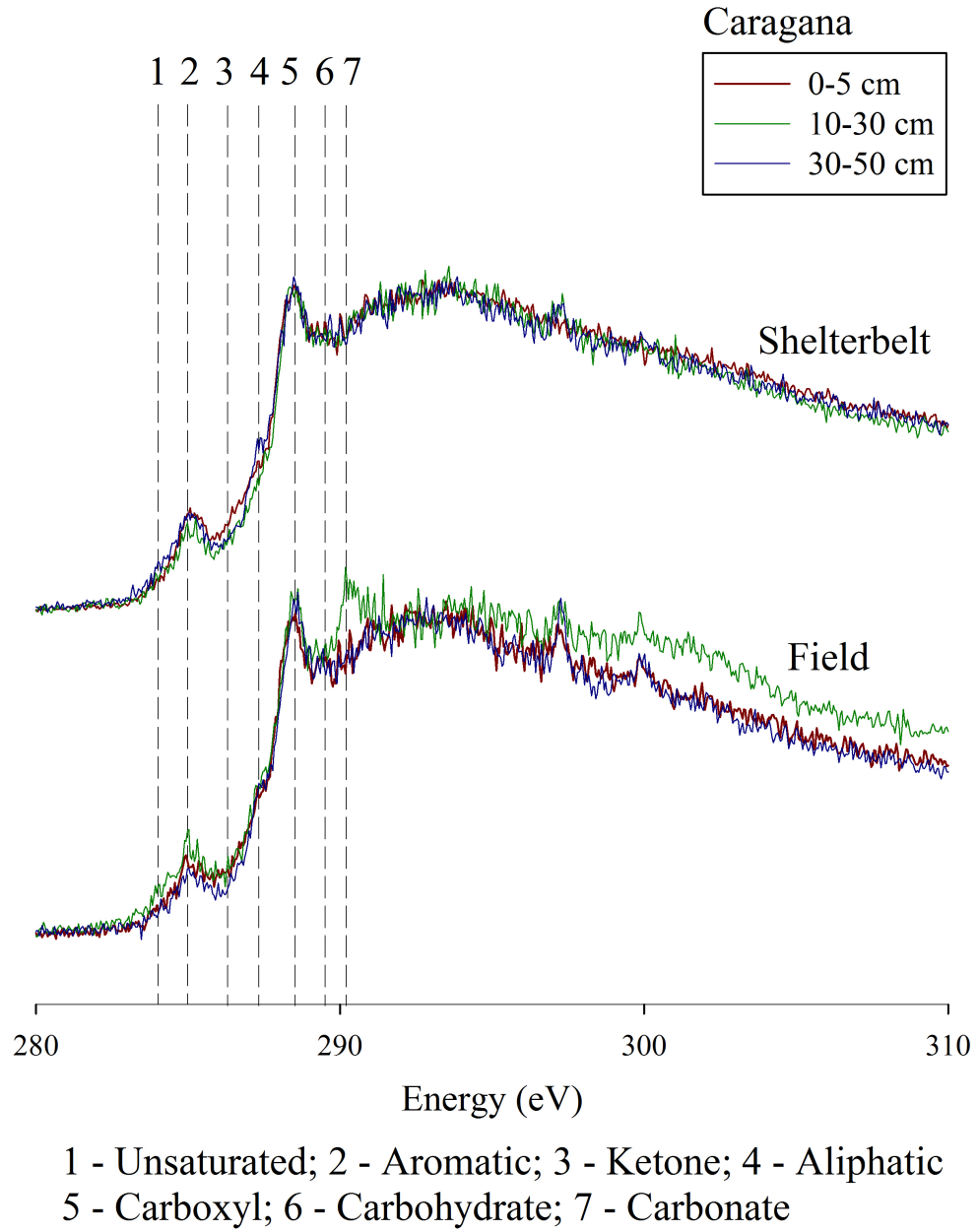


Fig. 6.10c Carbon K-edge XANES spectra of the whole soil samples of caragana shelterbelt and adjacent agricultural field at 0-5, 10-30 and 30-50 cm soil depths.

Table 6.3 C K-edge XANES absorbance intensities (arbitrary units [a.u.]) of the various organic C functional groups identified by C K-edge XANES spectroscopy for shelterbelts and agricultural fields at 0-5, 10-30 and 30-50 cm soil depths.

Depth/Species	Land cover	Unsaturation	Aromatic	Ketone	Aliphatic	Carboxylic	Carbohydrate
0-5 cm							
Hybrid Poplar	Shelterbelt	0.14	0.33	0.25	0.36	0.88	0.61
	Field	0.09	0.18	0.13	0.28	0.77	0.47
Scots Pine	Shelterbelt	0.14	0.38	0.25	0.34	0.83	0.59
	Field	0.12	0.20	0.16	0.40	0.86	0.49
Caragana	Shelterbelt	0.05	0.29	0.16	0.29	0.92	0.63
	Field	0.03	0.16	0.08	0.26	0.86	0.58
10-30 cm							
Hybrid Poplar	Shelterbelt	0.13	0.29	0.24	0.33	0.87	0.53
	Field	0.11	0.25	0.20	0.38	0.89	0.67
Scots Pine	Shelterbelt	0.07	0.21	0.12	0.25	0.84	0.53
	Field	0.08	0.21	0.15	0.30	0.84	0.51
Caragana	Shelterbelt	0.06	0.19	0.11	0.23	0.83	0.55
	Field	0.08	0.20	0.08	0.29	0.82	0.50
30-50 cm							
Hybrid Poplar	Shelterbelt	0.00	0.19	0.10	0.41	0.88	0.57
	Field	0.17	0.29	0.20	0.53	0.91	0.70
Scots Pine	Shelterbelt	0.06	0.15	0.12	0.51	0.96	0.65
	Field	0.08	0.22	0.11	0.28	0.86	0.53
Caragana	Shelterbelt	0.07	0.23	0.10	0.36	0.88	0.62
	Field	0.01	0.11	0.02	0.29	0.83	0.54

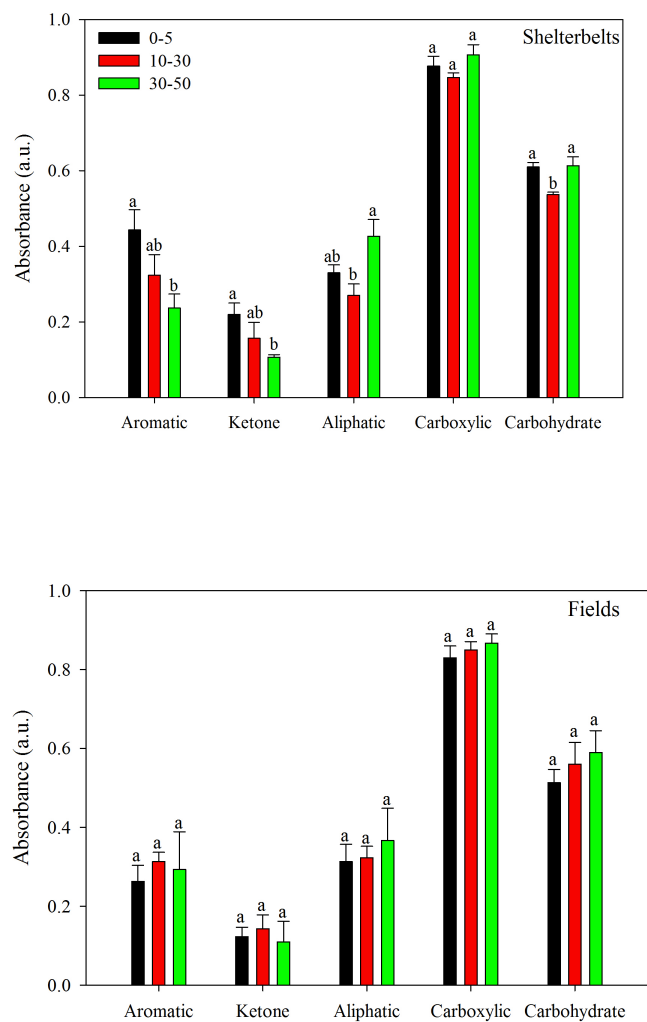


Fig. 6.11 Mean C K-edge XANES absorbance intensities (arbitrary units [a.u.]) of different C functional groups at 0-5, 10-30 and 30-50 cm soil depths for (A) shelterbelts and (B) agricultural fields. Different letters above bars for each functional group indicate significant difference at $p < 0.1$.

The C K-edge XANES spectra were resolved by peak-fitting to obtain the relative intensities of spectral bands, as shown in Table 6.3. Across both land use types, carboxylic-C (288.4 eV) had the highest absorbance (0.86 ± 0.04 normalized absorbance, arbitrary units [a.u.]), thus indicating that it was the most dominant organic C moiety. It was followed by carbohydrate-C (289.4 eV; 0.57 ± 0.06 a.u.), aliphatic-C (287.3 eV; 0.34 ± 0.08 a.u.), aromatic-C (284.1 and 285.1 eV; 0.31 ± 0.1 a.u.), and ketones (286.2 eV; 0.14 ± 0.06 a.u.). Absorbance of aromatic-C and ketones decreased significantly with soil depth under the shelterbelts; while the absorbance of aliphatic-C functional group was significantly higher at the 30-50 cm soil depth (Fig. 6.11). There was no significant difference between the absorbance of different C functional groups with soil depth in the case of agricultural fields (Fig. 6.11). These trends can also be noticed from the C K-edge XANES spectra of shelterbelts and agricultural fields stacked by soil depth (Figs. 6.10 a-c).

Absorbance of C XANES spectral features was compared between shelterbelts and agricultural fields to determine the differences in structural composition of SOC between the land use types (Table 6.3). There was a significant increase in the relative absorbance of aromatic-C, ketones and carbohydrate-C functional groups for shelterbelts compared to agricultural fields at 0-5 cm soil depth (Fig. 6.12). At the 10-30 cm soil depth, aliphatic-C was higher in the agricultural fields compared to shelterbelts, while there was no significant difference between the relative absorbance of C functional groups of shelterbelts and fields at the 30-50 cm depth (Fig. 6.12).

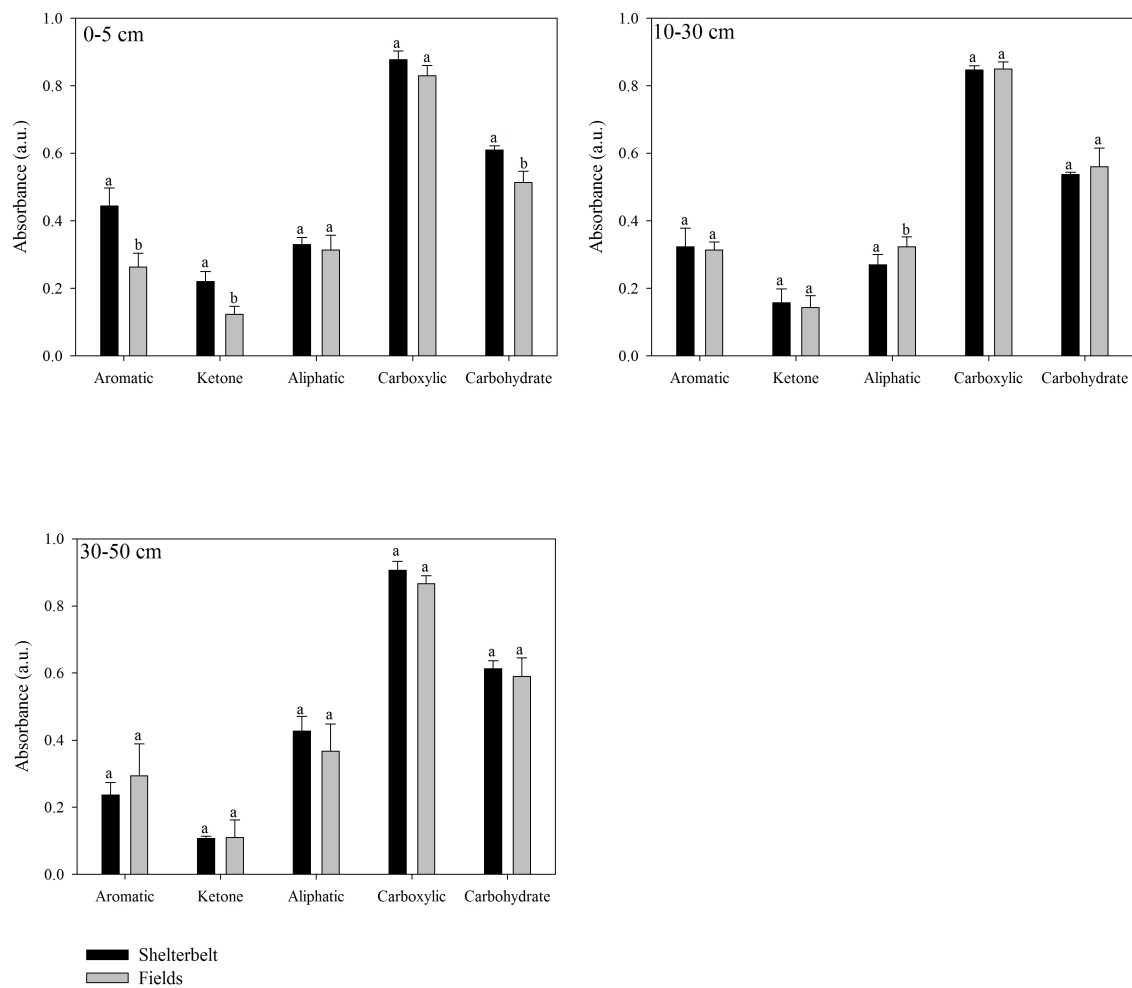


Fig. 6.12 Mean C K-edge XANES absorbance intensities (arbitrary units [a.u.]) of different C functional groups under shelterbelts and agricultural fields at 0-5, 10-30 and 30-50 cm soil depths, respectively. Different letters above bars for each functional group indicate significant difference at $p < 0.1$.

6.6 Discussion

6.6.1 SOC composition resolved by ATR-FTIR spectroscopy

6.6.1.1 General composition and depth distribution

Major ATR-FTIR absorbance bands across shelterbelts and agricultural fields showed identical peak positions and comparable absorbance intensities and trends with soil depth (Fig. 6.3), indicating similar molecular composition of SOC across shelterbelts and agricultural fields. This observation is in agreement with previous studies, which have found similar molecular composition of SOC across a wide range of vegetative, soil and environmental conditions (Mahieu et al., 1999; Lehmann et al., 2008). There was a trend of decreasing relative intensity of carbonyl (C-O) bonds of polysaccharide, alcohol and ether groups (1037 , 1103 and 1162 cm^{-1}), as well as of conjugated carboxylic and aromatic bonds of lignin and proteins (1584 and 1644 cm^{-1}) with soil depth for both shelterbelts and agricultural fields (Fig. 6.3). In contrast, relative intensities of bands attributed to aromatic C-H and C=C bonds (1509 cm^{-1}) and aliphatic C-H deformations of CH_2 or CH_3 groups (1434 cm^{-1}) increased with soil depth across both land use types (Fig. 6.3). These observations are in agreement with previous studies that reported a decrease in the amount of polysaccharides and plant-derived lignin, and an increase in the amount of alkyl-C forms with soil depth (Baldock et al., 1997; Dai et al., 2001; Rumpel et al., 2004).

6.6.1.2 Effect of shelterbelts on SOC composition

Despite the similarities in broad chemical composition of SOC, there were significant differences in the relative abundance of certain C functional groups. Shelterbelts generally showed a decrease in the content of C-O groups of polysaccharide, poly-alcoholic and ether groups compared to adjacent fields (Fig. 6.5), with the exception of hybrid poplar species.

Concomitantly, there was enrichment of lignin-derived phenols (HP, MM; Fig. 6.7a), aliphatic and aromatic C (MM; Figs. 6.7 b and c) and conjugated carboxylic and aromatic groups (HP, WS, CR; Fig. 6.9) under the shelterbelts compared to the agricultural fields. Composition of SOC in upper soil horizons is strongly influenced by the plant litter deposited on the surface soil (Lorenz and Lal, 2005, 2014). Previous studies have found that tree litter is enriched in lignin-derived C moieties such as aromatic and phenolic C, while residues of agricultural crops such as wheat (*Triticum aestivum*), alfalfa (*Medicago sativa*), soybean (*Glycine max*) and sorghum (*Sorghum bicolor*) have a lower content of lignin and higher content of polysaccharides such as cellulose and hemicellulose (Fründ and Lüdemann, 1989; Lorenz and Lal, 2005). Helfrich et al. (2006) observed spruce (*Picea abies*) litter to be enriched in aromatic, phenolic and alkyl-C functional forms compared to maize (*Zea mays*) litter that was higher in polysaccharides, leading to an increase in alkyl-C and decrease of O-alkyl C forms in particulate organic matter under spruce stands compared to maize fields. Thus, the differences in SOC composition of shelterbelts and agricultural fields may be attributed to the differences in composition of lignin-dominated woody litter of shelterbelt trees versus crop residues high in polysaccharides for agricultural fields.

The degree of decomposition of plant litter inputs also influences the chemical composition of SOM (Swift et al., 1979). Tree litter under shelterbelts forms a humus layer above the soil profile, in contrast to the cultivated fields, where the majority of crop residues are incorporated directly into the soil. Labile components of tree litter such as carbohydrates are preferentially mineralized in the course of humification in the humus layer (Kögel-Knabner et al., 1988). Studies on humification of tree litter have observed a decrease in the relative content of O-alkyl C, and an increase in alkyl-C content during the decomposition of humus (Kögel et

al., 1988; Kögel-Knabner et al., 1988; Zech et al., 1992). Thus, the organic matter reaching the mineral soil horizons under shelterbelts is depleted in labile C moieties such as polysaccharides, and enriched in the recalcitrant aliphatic and aromatic C moieties. Studies such as Guggenberger et al. (1994), Solomon et al. (2000) and Helfrich et al. (2006) have reported a higher concentration of carbohydrates in agricultural soils compared to woodlands despite lower SOC content, due to the direct input of crop residues in the soils of agricultural fields.

The increase in SOC content of shelterbelts compared to agricultural fields was positively related to an increase in the content of conjugated groups including aromatics, carboxylic acids and ketones (1584 and 1644 cm^{-1}), as well as phenolic C groups (1370 cm^{-1} ; Table 6.2). These C functional groups are associated with lignocellulosic plant material (Faix, 1992; Sills and Gossett, 2012; Xu et al., 2013), indicating that the majority of SOC added under shelterbelts represents plant-derived organic matter. These results are in agreement with Martens et al. (2004), who identified the soil C sequestered in long-term forest soils to be of plant origin through the use of carbohydrate and phenolic acid biomarkers.

6.6.1.3 Influence of shelterbelt species on SOC composition

Changes in SOC composition of shelterbelts compared to fields was also influenced by shelterbelt species. Hybrid poplar shelterbelts showed an increase in simple carbohydrates and poly-alcoholic groups (Fig. 6.5) and conjugated aromatic and carboxylic groups (Fig. 6.9) compared to adjacent fields. White spruce and Scots pine showed a decrease in C-O bonds, but an increase in conjugated groups compared to the agricultural fields. Recalcitrant aliphatic and aromatic C functional groups were higher in Manitoba maple shelterbelts and lower in hybrid poplar shelterbelts, in comparison to agricultural fields (Fig. 6.7). This is unsurprising, as the type and quality of vegetation inputs are known to influence soil organic matter composition (Quideau et al., 2001). High content of cellulose and hemicellulose, represented by C-O stretch

of polysaccharides, and of proteins and lignin, represented by conjugated aromatic and carboxylic groups, suggests limited alteration of original plant material under hybrid poplar shelterbelts. Slower leaf decomposition rate of poplar species such as trembling aspen (*Populus tremuloides*; decay rate (k) < 0.005) has been reported compared to other tree species including green ash (*Fraxinus americana*; $k > 0.01$; Peterson and Cummins, 1974). These results are also in accordance with the study by Dobarco (2014), who found a higher content of polysaccharides and C-O groups of ethers, esters under trembling aspen stands compared to coniferous species. Hannam et al. (2004) found lower amounts of oxidative degradation products represented by carbonyl-C, and higher amount of aromatic-C under trembling aspen stands compared to white spruce. In contrast, abundance of microbially derived recalcitrant aliphatic C and loss of cellulose and hemicellulose functional groups under Manitoba maple shelterbelts indicates rapid degradation of the plant litter material. Manitoba maple has fast-decomposing leaf litter (Swan and Palmer, 2006), due to its high nutrient concentration, compared to coniferous needle litter, which is high in lignin content, and decomposes slowly (Berg and Staaf, 1980; Perry et al., 1987). While these observations indicate a strong influence of litter decomposition rate on the chemical composition of stored SOC, other characteristics of litter such as C:N ratio, concentration of nutrients such as nitrogen, phosphorus, calcium and content of biopolymers such as tannin and suberin may also influence SOC composition (Webster and Benfield, 1986; Ostrofsky, 1993; Berg, 2000); this merits further investigation.

6.6.2 SOC composition resolved by C K-edge XANES spectroscopy

C K-edge XANES spectra indicated that the SOC composition across both land use types was dominated by carboxylic-C, followed by carbohydrate-C (Table 6.3). These were followed by moderate amounts of aliphatic-C, aromatic-C and ketone functional groups. Identification of

these organic carbon forms is in agreement with the molecular characterization of SOC in whole soils (Lehmann et al., 2008), soil colloidal particles (Schumacher et al., 2005) and organic matter extracts (Solomon et al., 2005, 2007) using C XANES spectroscopy. There was a decrease in the content of aromatic C with soil depth (Fig. 6.11a), which may be attributed to the decrease in lignin-derived compounds with soil depth (Dai et al., 2001; Rumpel et al., 2004). A decrease in ketones with depth indicated that the degree of microbial alteration of SOC decreased with soil depth, and is in accordance with the observation by Purton et al. (2015) on SOM chemistry in soil profiles. In contrast, recalcitrant aliphatic compounds increased at the 30-50 cm soil depth, which is consistent with ATR-FTIR results. For the agricultural fields, SOC composition did not change with depth (Fig. 6.11b), which may be due to homogenization of the cultivated soil due to tillage (Martens et al., 2004; Purton et al., 2015).

Aromatic C and ketone content was higher under shelterbelts compared to agricultural fields at the 0-5 cm soil depth (Fig. 6.12). Aromatic signals originate from lignin, and represent plant-derived organic matter (Baldock et al., 1989). Higher contents of these lignin-derived C moieties under shelterbelts are expected, since the woody tree litter is enriched in lignin compared to crop litter (Lorenz and Lal, 2005). Ketones are derived from the oxidation of fatty acid and aromatic compounds (Dent et al., 2004; Gottschalk, 2012), and have been identified as indicators of microbially transformed SOM depleted of labile C forms (Gillespie et al., 2014a, 2014b). The higher content of ketones in surface soil layers of shelterbelts compared to agricultural fields, indicates that SOM in surface layers of shelterbelts is at an advanced stage of decomposition compared to agricultural fields, which is in agreement with the findings of ATR-FTIR spectra. C K-edge XANES spectra also showed an increase in carbohydrate-C forms under shelterbelts compared to cropped fields (Fig. 6.12), which is contrary to the results obtained by

ATR-FTIR spectra that showed a lower proportion of polysaccharides under shelterbelts compared to agricultural fields. This discrepancy may be due to the fact that the shelterbelt sites analyzed by C K-edge XANES spectroscopy were selected on the basis of maximum amount of SOC sequestration, and hence are expected to have a higher input of fresh plant residues (described in chapter 4) compared to other sites. Increased litter input may have led to higher amounts of holocellulose-derived carbohydrates for these shelterbelt sites compared to fields.

6.6.3 Land use effects on SOC composition and dynamics

ATR-FTIR and C K-edge XANES spectroscopic analyses indicated higher abundance of aromatic, conjugated carboxylic and aliphatic C functional groups for different shelterbelt species compared to adjacent agricultural fields. Aliphatic and aromatic C functional groups are generally considered resistant to microbial degradation, due to their cross linked and polymeric structures, respectively (Gleixner et al., 2001; Lorenz et al., 2007). In contrast, polysaccharide C, which is rapidly broken down for energy metabolism by microorganisms (Gleixner et al., 2001; Krull et al., 2003), was relatively higher for agricultural fields. Thus, SOC stored under shelterbelts may have higher chemical resistance to degradation compared to agricultural fields, in case of changes in management or climatic conditions. The relative importance of SOC composition in determining its long-term stability, however, has recently been questioned (Marschner et al., 2008; Dungait et al., 2012), with the studies, instead, indicating the major control of microbial ecology (Ekschmitt et al., 2005) or organo-mineral interactions (Mikutta et al., 2006; Kögel-Knabner et al., 2008) on SOC decomposition rate. Nevertheless, shifts in structural composition of SOC can influence physical stabilization mechanisms through changes in stereo-chemical and hydrophobic characteristics (Kleber et al., 2007; Bachmann et al., 2008), as well as regulate ecological responses to environmental changes such as in CO₂ content and

temperature (Feng and Simpson, 2011; Simpson and Simpson, 2012). Thus, changes in molecular characteristics and speciation may affect SOC storage and dynamics, and should be considered in the determination of SOC sequestration potential.

6.6.4 Application of ATR-FTIR spectroscopy to determine SOC composition

Peak heights of unresolved FTIR spectra have generally been used in earlier attempts to study SOC composition using FTIR spectroscopy (Haberhauer et al., 1998; Ellerbrock et al., 1999; Solomon et al., 2005). In this study, we used a spectral deconvolution technique, which involved fitting of a series of Gaussian curves to ATR-FTIR spectral features, to separate overlapped or hidden peaks and determine their relative intensities. Separation of individual absorbance bands, using spectral deconvolution, can be especially useful in FTIR spectroscopic analysis of SOC, since a strong overlap in the absorption frequencies of different SOC functional groups in the mid-infrared region has been recognized (Janik et al., 2007; Calderón et al., 2013). Peak positions of the deconvoluted spectral bands (listed in Appendix J) were in agreement with the vibrational frequencies assigned to different soil C functional groups in the literature (described in section 6.5.1), demonstrating that the resolved spectral bands represented chemical information associated with SOC. Similarly, variation in chemical composition of SOC between land use types, as determined by ATR-FTIR and C K-edge XANES spectroscopy, was generally consistent between both techniques, thus indicating that ATR-FTIR spectroscopy, in conjunction with Gaussian curve-fitting analysis, can be effectively used to study the chemistry of soil C under different land use types.

6.7 Conclusions

The SOC composition of shelterbelts and adjacent agricultural fields as measured by ATR-FTIR and C K-edge XANES spectroscopic analyses showed that SOC chemistry under

shelterbelts was dominated by the more processed forms of C including aromatic and conjugated carboxyl groups in the case of hybrid poplar and white spruce, and aromatic and aliphatic C moieties for Manitoba maple. In contrast, agricultural field soils were enriched in easily decomposable C forms such as polysaccharides, esters and ethers compared to shelterbelts. These trends were attributed to differences in initial chemical composition of litter and its degree of decomposition affected by litter placement between shelterbelts and agricultural fields. Relative enrichment of microbially synthesized secondary SOC sources such as ketones under the shelterbelts indicated that SOC under shelterbelts was at an advanced stage of decomposition. SOC composition was also affected by the litter quality of fast- and slow-decomposing shelterbelt species.

Our study demonstrates that shelterbelts may change the chemical composition of SOC in the mineral soil horizons compared to adjacent agricultural fields, which may further affect biochemical recalcitrance of SOC to microbial degradation. Thus, the effect of shelterbelt establishment on SOC sequestration should be assessed not only in terms of change in C stocks but also with respect to changes in SOC speciation and quality. This study also demonstrated the application of ATR-FTIR spectroscopy, in conjunction with Gaussian curve fitting, for the effective determination of SOC composition.

7. SYNTHESIS AND CONCLUSIONS

Agroforestry systems, such as shelterbelts, have a strong potential for soil C sequestration; however, major knowledge gaps exist about C storage and dynamics under such systems. The effect of shelterbelts on the magnitude of SOC stocks compared to cultivated fields and other agroforestry systems remains unclear (Lorenz and Lal, 2014; Nair et al., 2009a), especially in the deeper soil horizons, which are especially relevant under such tree-based systems due to their deeper root depth compared to agricultural crops (Lorenz and Lal, 2005). Shelterbelt characteristics such as stand species, structure and design may alter biomass and litter production, which in turn, influences the SOC sequestration rate (Woldeselassie, 2009). The response of SOC sequestration potential to these biophysical shelterbelt characteristics has not been investigated. Similarly, the effect of shelterbelt planting on the processes and mechanisms affecting the stabilization and dynamics of SOC is not yet clear. Combined application of different techniques to simultaneously study physical and chemical processes regulating SOC stabilization is desired in order to get a comprehensive understanding of SOC dynamics under shelterbelts.

The research presented in this thesis addresses these knowledge gaps by measuring the amount of SOC sequestered in the whole soil, and the heavy and light fractions of soil for six major shelterbelt species of Saskatchewan compared to their adjacent agricultural fields. Additionally, the influence of shelterbelts on molecular composition of SOC was determined by using ATR-FTIR and C K-edge XANES techniques. SOC is a complex and heterogeneous

medium, and hence, the application of these advance molecular techniques is useful for its characterization. Using a paired site design controlling for differences in climate and soil properties allowed us to study changes in SOC storage, physical stabilization and chemical composition due to planting of shelterbelts in agricultural fields.

7.1 Summary of findings

Reliable estimation of SOC sequestration potential is dependent on the availability of accurate methods for separation and measurement of inorganic and organic C constituents of soil. In chapter 3, frequently used SOC measurement procedures, including in-situ HCl-fumigation method (Harris et al., 2001), in-situ HCl-addition method and thermal decomposition method (Wang and Anderson, 1998) were compared to determine their suitability for SOC measurement in carbonate-rich soils of Saskatchewan. Results indicated that the measurement procedure based on HCl-acid fumigation, followed by elemental C analysis via automated C analyzer, was the most efficient method for determination of OC in soils. Hence, this method was used for the estimation of SOC content in the subsequent studies for whole soil samples (Chapter 4), and the light and heavy fractions (Chapter 5) of soil.

Our study on soil C sequestration potential (Chapter 4) revealed a significant increase in SOC concentration for the shelterbelts compared to agricultural fields throughout the soil profile (measured up to 50 cm depth). Consequently, shelterbelts had higher SOC stocks (119.1 Mg C ha⁻¹) compared to agricultural fields (100.5 Mg C ha⁻¹) in the mineral soil profile, in addition to 3-8 Mg C ha⁻¹ stored in the litter layer under shelterbelts. SOC stocks for shelterbelts increased in the form of both mineral-free plant debris (called light fraction) and mineral-stabilized organic matter (called heavy fraction) (Chapter 5). The increase in SOC is attributed primarily to higher litter inputs in trees compared to agricultural crops, as well as to reduced soil erosion and lack of

soil disturbance from agronomic practices (Sauer et al., 2007). The increase in SOC stocks was higher in the 10-30 cm soil depth (13 Mg C ha⁻¹), compared to the surface soil layer (0-10 cm depth; 4 Mg C ha⁻¹) and 30-50 cm soil layer (1.4 Mg C ha⁻¹). Furthermore, results from Chapter 5 suggested higher contributions of the mineral-associated SOC fraction towards SOC addition in the deeper soil layers (10-30 and 30-50 cm soil depths), compared to higher contributions from uncomplexed plant debris in the surface soil layer (0-10 cm soil depth). All of these findings allude to different sources of plant litter inputs (i.e. plant shoots vs. roots) with soil depth, and also support the observation that root-derived C is more likely to be stabilized by organo-mineral interactions than shoot-derived C, primarily due to the close association with soil matrix, and higher mineral-sorption capacity of root-exudates, such as organic acids (Jones, 1998; Rasse et al., 2005). Moreover, these results emphasize the importance of subsurface soil layers in SOC storage and long-term stabilization through their association with minerals. This observation is in line with recent review studies such as Jobbágy and Jackson (2000) and Lorenz and Lal (2005) that suggest the higher capacity of deeper soil horizons to sequester SOC with increased turnover times. Average yearly accrual of SOC for shelterbelts was estimated to be around 0.7 Mg C ha⁻¹ year⁻¹; however, younger shelterbelts (< 20 years of age) generally showed a decrease in C stocks due to SOC mineralisation during plantation establishment (Hansen, 1993). Thus, significant accrual of SOC due to shelterbelt planting may be observed only at decadal time-scales.

Average SOC sequestered under shelterbelts varied with the tree species – hybrid poplar (38 Mg ha⁻¹), white spruce (21 Mg ha⁻¹), Scots pine (20 Mg ha⁻¹), green ash (15 Mg ha⁻¹), Manitoba maple (11 Mg ha⁻¹) and caragana (6 Mg ha⁻¹). Differences in C sequestration potential were attributed to variations in canopy age and structure among the species, which consisted of

larger trees with higher diameter, height and crown width among hybrid poplar and coniferous species, and smaller trees and lesser litter production in green ash, Manitoba maple and caragana. Canopy structure influences the biomass and litter production and inputs (Woldeselassie, 2009), also indicated by a positive relationship between stand characteristics and litterfall density. It may also affect SOC storage and loss indirectly by influencing soil microclimate and understory vegetation (Moeur, 1997). Shelterbelt species also affected the physical stabilization of SOC through organo-mineral associations. After adjusting for variations in SOC stocks, a higher increase in uncomplexed plant-derived debris was observed for Scots pine and white spruce shelterbelts, while hybrid poplar, green ash, Manitoba maple and caragana showed a higher increase in mineral-associated SOC. Differences in organo-mineral stabilization may be explained by higher decomposition rates of foliar litter of deciduous species compared to coniferous needle litter (Prescott et al., 2000). Decomposition of foliar deciduous litter leads to higher production of dissolved organic carbon (DOC), which adsorbs onto the mineral surface of deeper soil horizons, while the slow-decomposing coniferous needle litter layer collects on the surface as partially decomposed debris. Previous studies have also found higher proportions of uncomplexed organic matter under coniferous species such as spruce compared to broadleaf species (Bu et al., 2012; Laganière et al., 2011). In summary, biophysical characteristics of shelterbelts including biomass and litter production affected the quantity of SOC, while the litter quality influenced its partitioning into partially-decomposed and mineral-associated fractions.

In chapter 6, the changes in molecular composition of SOC due to shelterbelt planting were studied through analytical techniques including ATR-FTIR and C K-edge XANES spectroscopy. Molecular composition of SOC was strongly influenced by litter chemistry and its degree of decomposition. Tree litter, which is rich in lignin and cutin-derived C moieties

including aromatic, phenolic and alkyl-C (Helfrich et al., 2006), led to the higher abundance of these functional groups under shelterbelts. In comparison, agricultural fields had a higher abundance of polysaccharide C functional groups, due to a higher content of cellulose and hemicellulose in crop residues (Lorenz and Lal, 2005). Chemical composition of SOC was also regulated by the degree of decomposition of input litter. Tree litter under shelterbelts was at a higher stage of decomposition due to increased decomposition in the humus layer. Thus, SOC under shelterbelts was rich in processed C forms including aliphatic and aromatic C forms. This finding was further confirmed by C XANES results indicating higher abundance of ketones, which are considered to be microbial biomarkers of decomposition (Gillespie et al., 2014a, 2014b).

Observations regarding the processes regulating SOC composition are in agreement with the currently accepted paradigms of litter decomposition, including ‘initial litter quality’ and ‘chemical convergence’ hypotheses. Chemical convergence hypothesis postulates that chemical composition of OM is determined by the degree of decomposition of litter, proceeding with preferential loss of easily decomposable compounds (e.g. water soluble compounds and carbohydrates) and selective preservation of recalcitrant C moieties (e.g. alkyl and aromatic C in lignin, tannin and suberin; Fierer et al., 2009; Kögel-Knabner, 2002), thus, converging towards a common chemistry. However, it states that the chemistry in early decomposition stages may be determined by initial litter quality, which is also strongly emphasized in the ‘initial litter quality’ hypothesis. Initial litter quality hypothesis states that differences in initial litter chemistry persist throughout the process of decay to SOM, irrespective of the extent of litter processing (Wickings et al., 2012). The strong effect of initial litter quality in this study may also have been seen due to the continuous supply of fresh litter from the shelterbelts during each growing cycle. Microbial

activity or biomass were not examined within this study, however, the differences in SOC chemical composition between different shelterbelt species and agricultural fields may also be caused through differences in microbial community structure among land use types (Yannikos et al., 2014; Strickland et al., 2009).

7.2 Future research directions

The research presented in this thesis presented information pertaining to the strong potential of shelterbelt agroforestry systems for SOC sequestration. Since SOC sequestration potential depends on shelterbelt characteristics such as species, stand overstory characteristics and litter quality and quantity, the next step would be to identify the processes and practices that can help maximize the SOC potential of shelterbelts. Shelterbelt designs and management practices that maximize biomass accumulation and reduce growth constraints such as pest and disease should be determined. Similarly, viability of management practices that promote higher soil C inputs and reduce its decomposition rate such as reduced thinning and pruning of trees, higher stand-density etc. should be investigated. The potential of tree species and cultivars with deeper and thicker root systems (Kell, 2011; Lorenz and Lal, 2005) and higher contents of resistant aliphatic biopolymers including cutin, cutan and suberin (Lorenz et al., 2007), in increasing SOC storage and stabilization in the deeper soil horizons should be determined. Simultaneously, further research is also required to study the fate and role of these aliphatic precursors in tree litter towards the increase in the recalcitrance of SOC. The capacity of promising shelterbelt species to provide ecological, agronomic and C sequestration benefits under different future climate change scenarios needs to be assessed.

While this study determined soil C sequestration potential of shelterbelts at the field scale, future research investigation should expand their scope to assess the sequestration

potential of shelterbelts at the provincial and national-scale, by estimating the soil C sequestration potential and land area occupied under different shelterbelt species, soil types and ecoregions. Similarly, soil C sequestration potential of other agroforestry systems – including alley cropping, silvopasture, riparian buffers and forest farming – should also be estimated, in order to develop national-scale inventories on the full scope of agroforestry practices to sequester C and mitigate greenhouse gases. Social and economic barriers to adoption and retention of shelterbelts on farmyards and crop fields should be identified, in order to reverse the recent trend of shelterbelt removal from agricultural fields (Rempel, 2015). Such information can help guide the policy decisions on increasing shelterbelt establishment and providing incentives to producers for adoption of shelterbelts.

Finally, this study showed the effective application of analytical techniques including ATR-FTIR and synchrotron-based C K-edge XANES spectroscopy, combined with curve-fitting, for effective determination of changes in SOC composition with land use. However, improvement in the identification of spectral bands and their validation is desired in order to increase their effectiveness (Calderón et al., 2013). Similarly, additional research is required, especially for ATR-FTIR spectroscopy, to remove the interference of minerals and carbonates in studying the SOC composition.

REFERENCES

- Albrecht, A. and S.T. Kandji. 2003. Carbon sequestration in tropical agroforestry systems. *Agric., Ecosyst. Environ.* 99: 15-27.
- Amelung, W. and W. Zech. 1996. Organic species in ped surface and core fractions along a climosequence in the prairie, North America. *Geoderma* 74: 193-206.
- Amichev, B.Y. 2007. Biogeochemistry of Carbon on Disturbed Forest Landscapes. Ph. D. Dissertation, University Libraries, Virginia Polytechnic Institute and State University, Blacksburg, VA.
- Amichev, B.Y., M.J. Bentham, D. Cerkowniak, J. Kort, S. Kulshreshtha, C.P. Laroque, et al. 2015. Mapping and quantification of planted tree and shrub shelterbelts in Saskatchewan, Canada. *Agroforest. Syst.* 89: 49-65.
- Amichev, B.Y., M.J. Bentham, W.A. Kurz, C.P. Laroque, S. Kulshreshtha, J.M. Piwowar, et al. 2016. Carbon sequestration by white spruce shelterbelts in Saskatchewan, Canada: 3PG and CBM-CFS3 model simulations. *Ecol. Modell.* 325: 35-46.
- Aneja, M.K., S. Sharma, F. Fleischmann, S. Stich, W. Heller, G. Bahnweg, et al. 2006. Microbial colonization of beech and spruce litter—influence of decomposition site and plant litter species on the diversity of microbial community. *Microb. Ecol.* 52: 127-135.
- Artz, R.R., S.J. Chapman, A.J. Robertson, J.M. Potts, F. Laggoun-Défarge, S. Gogo, et al. 2008. FTIR spectroscopy can be used as a screening tool for organic matter quality in regenerating cutover peatlands. *Soil Biol. Biochem.* 40: 515-527.
- Aslan-Sungur, G., F. Evrendilek, N. Karakaya, K. Gungor and S. Kilic. 2013. Integrating ATR-FTIR and data-driven models to predict total soil carbon and nitrogen towards sustainable watershed management. *Res. J. Chem. Environ* 17: 5-11.
- Baah-Acheamfour, M., C.N. Carlyle, E.W. Bork and S.X. Chang. 2014. Trees increase soil carbon and its stability in three agroforestry systems in central Alberta, Canada. *For. Ecol. Manage.* 328: 131-139.
- Baah-Acheamfour, M., S.X. Chang, C.N. Carlyle and E.W. Bork. 2015. Carbon pool size and stability are affected by trees and grassland cover types within agroforestry systems of western Canada. *Agric., Ecosyst. Environ.* 213: 105-113.
- Baes, A. and P. Bloom. 1989. Diffuse reflectance and transmission Fourier transform infrared (DRIFT) spectroscopy of humic and fulvic acids. *Soil Sci. Soc. Am. J.* 53: 695-700.
- Baisden, W., R. Amundson, A. Cook and D. Brenner. 2002. Turnover and storage of C and N in five density fractions from California annual grassland surface soils. *Global Biogeochem. Cycles* 16: 117-132.

- Baldock, J., J. Oades, A. Vassallo and M. Wilson. 1989. Incorporation of uniformly labeled ^{13}C glucose carbon into the organic fraction of a soil-carbon balance and CP MAS ^{13}C NMR Measurements. *Aust. J. Soil Res.* 27: 725-746.
- Baldock, J., J.M. Oades, P. Nelson, T. Skene, A. Golchin and P. Clarke. 1997. Assessing the extent of decomposition of natural organic materials using solid-state ^{13}C NMR spectroscopy. *Aust. J. Soil Res.* 35: 1061-1083.
- Baldock, J.A. 2007. Composition and cycling of organic carbon in soil. In: P. Marschner and Z. Rengel, editors, *Nutrient cycling in terrestrial ecosystems*. Springer Berlin Heidelberg, Berlin, Heidelberg. p. 1-35.
- Baldock, J.A. and J. Skjemstad. 2000. Role of the soil matrix and minerals in protecting natural organic materials against biological attack. *Org. Geochem.* 31: 697-710.
- Balazy, S. 2002. Ecological guidelines for the management of afforestations in rural areas. In: Ryszkowski, L., editors, *Landscape ecology in agroecosystems management*. CRC Press, Boca Raton, FL, p. 299-316.
- Balesdent, J., E. Besnard, D. Arrouays and C. Chenu. 1998. The dynamics of carbon in particle-size fractions of soil in a forest-cultivation sequence. *Plant and Soil* 201: 49-57.
- Bambrick, A.D., J.K. Whalen, R.L. Bradley, A. Cogliastro, A.M. Gordon, A. Olivier, et al. 2010. Spatial heterogeneity of soil organic carbon in tree-based intercropping systems in Quebec and Ontario, Canada. *Agroforest. Syst.* 79: 343-353.
- Bartlett, J. and H. Doner. 1988. Decomposition of lysine and leucine in soil aggregates: adsorption and compartmentalization. *Soil Biol. Biochem.* 20: 755-759.
- Batjes, N.H. 1996. Total carbon and nitrogen in the soils of the world. *Eur. J. Soil Sci.* 47: 151-163.
- Baumann, K., P. Marschner, R.J. Smernik and J.A. Baldock. 2009. Residue chemistry and microbial community structure during decomposition of eucalypt, wheat and vetch residues. *Soil Biol. Biochem.* 41: 1966-1975.
- Beauchemin, S., D. Hesterberg, J. Chou, M. Beauchemin, R.R. Simard and D.E. Sayers. 2003. Speciation of phosphorus in phosphorus-enriched agricultural soils using X-ray absorption near-edge structure spectroscopy and chemical fractionation. *J. Environ. Qual.* 32: 1809-1819.
- Beck, C.W. 1950. Differential thermal analysis curves of carbonate materials. *American Mineralogist* 35: 985-1013.
- Beer, J. 1988. Litter production and nutrient cycling in coffee (*Coffea arabica*) or cacao (*Theobroma cacao*) plantations with shade trees. *Agroforest. Syst.* 7: 103-114.
- Berg, B. 2000. Litter decomposition and organic matter turnover in northern forest soils. *For. Ecol. Manage.* 133: 13-22.
- Berg, B. and C. McClaugherty. 2014. *Plant litter. Decomposition, humus formation, carbon sequestration*. 3rd ed. Springer, Heidelberg, DE.
- Berg, B. and H. Staaf. 1980. Decomposition rate and chemical changes of Scots pine needle litter. II. Influence of chemical composition. *Ecol. Bull.* 32: 373-390.

- Bernoux, M., C.C. Cerri, C. Neill and J.F. de Moraes. 1998. The use of stable carbon isotopes for estimating soil organic matter turnover rates. *Geoderma* 82: 43-58.
- Blanco-Canqui, H., R. Lal, F. Sartori and R. Miller. 2007. Changes in organic carbon and physical properties of soil aggregates under fiber farming. *Soil Sci.* 172: 553-564.
- Bolinder, M., D. Angers and J. Dubuc. 1997. Estimating shoot to root ratios and annual carbon inputs in soils for cereal crops. *Agric., Ecosyst. Environ.* 63: 61-66.
- Bonsal, B.R., E.E. Wheaton, A.C. Chipanshi, C. Lin, D.J. Sauchyn and L. Wen. 2011. Drought research in Canada: a review. *Atmosphere-Ocean* 49: 303-319.
- Boone, R.D. 1994. Light-fraction soil organic matter: Origin and contribution to net nitrogen mineralization. *Soil Biol. Biochem.* 26: 1459-1468.
- Bornemann, L., G. Welp and W. Amelung. 2010. Particulate organic matter at the field scale: Rapid acquisition using mid-infrared spectroscopy. *Soil Sci. Soc. Am. J.* 74: 1147-1156.
- Boyce, C.K., G.D. Cody, M. Feser, C. Jacobsen, A.H. Knoll and S. Wirick. 2002. Organic chemical differentiation within fossil plant cell walls detected with X-ray spectromicroscopy. *Geology* 30: 1039-1042.
- Brandle, J.R., Hodges, L., Tyndall, J. and Sudmeyer, R.A. 2000. Windbreak practices. In: Garrett H. E., editor, *North American Agroforestry, an integrated science and practice*. American Society of Agronomy. Madison, WI. p. 79-118.
- Brandle, J.R., L. Hodges and X.H. Zhou. 2004. Windbreaks in North American agricultural systems. In: P. K. R. Nair, M. R. Rao and L. E. Buck, editors, *New vistas in agroforestry: A compendium for 1st world congress of agroforestry, 2004*. Springer Netherlands, Dordrecht. p. 65-78.
- Brandle, J.R., B.B. Johnson and D.D. Dearmont. 1984. Windbreak economics: The case of winter wheat production in eastern Nebraska. *J. Soil Water Conserv.* 39: 339-343.
- Brandle, J.R., T.D. Wardle and G.F. Bratton. 1992. Opportunities to increase tree planting in shelterbelts and the potential impacts on carbon storage and conservation. In: N. Sampson and F. Hair, editors, *Forests and global change, vol. 1. Opportunities for increasing forest cover*. American Forests, Washington, DC. p. 157-176.
- Bremer, E., H.H. Janzen and A.M. Johnston. 1994. Sensitivity of total, light fraction and mineralizable organic matter to management practices in a Lethbridge soil. *Can. J. Soil Sci.* 74: 131-138.
- Brunetti, G., K. Farrag, C. Plaza and N. Senesi. 2012. Advanced techniques for characterization of organic matter from anaerobically digested grapemarc distillery effluents and amended soils. *Environ. Monit. Assess.* 184: 2079-2089.
- Bu, X., H. Ruan, L. Wang, W. Ma, J. Ding and X. Yu. 2012. Soil organic matter in density fractions as related to vegetation changes along an altitude gradient in the Wuyi Mountains, southeastern China. *Appl. Soil Eco.* 52: 42-47.
- Byers, S.C., E.L. Mills and P.L. Stewart. 1978. A comparison of methods of determining organic carbon in marine sediments, with suggestions for a standard method. *Hydrobiologia* 58: 43-47.
- Cable, T.T. 1999. Nonagricultural benefits of windbreaks in Kansas. *Great Plains Res.* 9: 41-53.

- Calderón, F., M. Haddix, R. Conant, K. Magrini-Bair and E. Paul. 2013. Diffuse-reflectance Fourier-transform mid-infrared spectroscopy as a method of characterizing changes in soil organic matter. *Soil Sci. Soc. Am. J.* 77: 1591-1600.
- Calderón, F.J., G.W. McCarty and J.B. Reeves. 2006. Pyrolysis-MS and FT-IR analysis of fresh and decomposed dairy manure. *J. Anal. Appl. Pyrolysis* 76: 14-23.
- Calderón, F.J., J.B. Reeves, H.P. Collins and E.A. Paul. 2011. Chemical differences in soil organic matter fractions determined by diffuse-reflectance mid-infrared spectroscopy. *Soil Sci. Soc. Am. J.* 75: 568-579.
- Cambardella, C. and E. Elliott. 1992. Particulate soil organic-matter changes across a grassland cultivation sequence. *Soil Sci. Soc. Am. J.* 56: 777-783.
- Canadell, J.G., M.U.F. Kirschbaum, W.A. Kurz, M-J. Sanz, B. Schlamadinger and Y. Yamagata. 2007. Factoring out natural and indirect human effects on terrestrial carbon sources and sinks. *Environ. Sci. Policy* 10: 370-384.
- Cerli, C., L. Celi, K. Kalbitz, G. Guggenberger and K. Kaiser. 2012. Separation of light and heavy organic matter fractions in soil — Testing for proper density cut-off and dispersion level. *Geoderma* 170: 403-416.
- Chang, C.W., D.A. Laird, M.J. Mausbach and C.R. Hurburgh. 2001. Near-infrared reflectance spectroscopy—principal components regression analyses of soil properties. *Soil Sci. Soc. Am. J.* 65: 480-490.
- Christensen, B.T. 2001. Physical fractionation of soil and structural and functional complexity in organic matter turnover. *Eur. J. Soil Sci.* 52: 345-353.
- Christensen, B.T. 1996. Matching measurable soil organic matter fractions with conceptual pools in simulation models of carbon turnover: Revision of model structure. In: D. S. Powlson, P. Smith and J. U. Smith, editors, *Evaluation of soil organic matter models: Using existing long-term datasets*. Springer Berlin Heidelberg, Berlin, Heidelberg. p. 143-159.
- Christensen, B.T. 1992. Physical fractionation of soil and organic matter in primary particle size and density separates. In: B. A. Stewart, editor *Advances in soil science*. Springer New York, New York, NY. p. 1-90.
- Chang, F., S. Kao and K. Liu. 1991. Analysis of organic and carbonate carbon in sediment. *Acta Oceanogr. Taiwan* 27: 140-150.
- Clarke, R. 1995. *Controlling carbon dioxide emissions: the tradeable permit system*. United Nations, Geneva (Switzerland).
- Cody, G., H. Ade, S. Wirick, G. Mitchell and A. Davis. 1998. Determination of chemical-structural changes in vitrinite accompanying luminescence alteration using C-NEXAFS analysis. *Org. Geochem.* 28: 441-455.
- Cody, G., R. Botto, H. Ade and S. Wirick. 1996. The application of soft X-ray microscopy to the in-situ analysis of sporinite in coal. *Int. J. Coal Geo.* 32: 69-86.
- Cole, V., C. Cerri, K. Minami, A. Moiser, N. Rosenberg and D. Sauerbeck. 1996. Agricultural options for mitigation of greenhouse gas emissions. In: R. Watson, M. Zinyowera and R. Moss,

- editors, *Climate change 1995. Impacts, adaptations and mitigation of climate change: Scientific-technical analyses*. Cambridge University Press, Cambridge. p. 745-771.
- Coleman, D.M., J.G. Isebrands, N.D. Tolsted and R.V. Tolbert. 2004. Comparing Soil Carbon of Short Rotation Poplar Plantations with Agricultural Crops and Woodlots in North Central United States. *Environ. Manage.* 33: S299-S308.
- Conceição, P.C., M. Boeni, J. Dieckow, C. Bayer, L. Martin-Neto and J. Mielniczuk. 2007. Efficiency of sodium polytungstate in density fractionation of soil organic matter. *R. Bras. Ci. Solo* 31: 1301-1310.
- Cook, P.S. and T.T. Cable. 1995. The scenic beauty of shelterbelts on the Great Plains. *Landscape Urban Plan.* 32: 63-69.
- Correll, D.L. 1997. Buffer zones and water quality protection: general principles. In: Haycock, N.E., Burt, T.P., Goulding, K.W.T., Pinay, G., editors, *Buffer Zones: Their Processes and Potential Water Protection*. Quest Environmental, Harpenden, UK, p. 7-20.
- Crow, S.E., C.W. Swanston, K. Lajtha, J.R. Brooks and H. Keirstead. 2007. Density fractionation of forest soils: methodological questions and interpretation of incubation results and turnover time in an ecosystem context. *Biogeochemistry* 85: 69-90.
- Cutter, G. A. and Radford-Knoery, J. (1991) Determination of Carbon, Nitrogen, Sulfur, and Inorganic Sulfur Species in Marine Particles, In: D. C. Hurd and D. W. Spencer, editors, *Marine particles: Analysis and characterization*, American Geophysical Union, Washington, D.C. p. 57-63.
- Dai, K.O.H., C.E. Johnson and C.T. Driscoll. 2001. Organic matter chemistry and dynamics in clear-cut and unmanaged hardwood forest ecosystems. *Biogeochemistry* 54: 51-83.
- Dalal, R. and R. Mayer. 1986. Long term trends in fertility of soils under continuous cultivation and cereal cropping in southern Queensland. IV. Loss of organic carbon from different density functions. *Soil Res.* 24: 301-309.
- Davidson, J.M., F. Gray and D.I. Pinson. 1967. Changes in organic matter and bulk density with depth under two cropping systems. *Agron. J.* 59: 375-378.
- Davidson, E.A. and I.A. Janssens. 2006. Temperature sensitivity of soil carbon decomposition and feedbacks to climate change. *Nature* 440: 165-173.
- Davis, J. and J. Norman. 1988. Effects of shelter on plant water use. *Agric., Ecosyst. Environ.* 22: 393-402.
- DeBellis, T., G. Kernaghan, R. Bradley and P. Widden. 2006. Relationships between stand composition and ectomycorrhizal community structure in boreal mixed-wood forests. *Microbial Ecol.* 52: 114-126.
- Demyan, M., F. Rasche, E. Schulz, M. Breulmann, T. Müller and G. Cadisch. 2012. Use of specific peaks obtained by diffuse reflectance Fourier transform mid-infrared spectroscopy to study the composition of organic matter in a Haplic Chernozem. *Eur. J. Soil Sci.* 63: 189-199.
- Dent, B.B., S.L. Forbes and B.H. Stuart. 2004. Review of human decomposition processes in soil. *Environ. Geol.* 45: 576-585.

- Davis, M., A. Nordmeyer, D. Henley and M. Watt. 2007. Ecosystem carbon accretion 10 years after afforestation of depleted subhumid grassland planted with three densities of *Pinus nigra*. *Glob. Change Biol.* 13: 1414-1422.
- Dhillon, G.S., B.Y. Amichev, R. de Freitas and K. Van Rees. 2015. Accurate and precise measurement of organic carbon content in carbonate-rich soils. *Commun. Soil Sci. Plant Anal.* 46: 2707-2720.
- Dick, W., R. Blevins, W. Frye, S. Peters, D. Christenson, F. Pierce, et al. 1998. Impacts of agricultural management practices on C sequestration in forest-derived soils of the eastern Corn Belt. *Soil Tillage Res.* 47: 235-244.
- Dobarco, R.M. 2014. Influence of Stand Composition on Soil Organic Carbon Stabilization and Biochemistry in Aspen and Conifer Forests of Utah. Ph.D. thesis. Utah State Univ., Utah.
- Drew, R. 1982. The effects of irrigation and of shelter from wind on emergence of carrot and cabbage seedlings. *J. Hortic. Sci.* 57: 215-219.
- Dronen, S.I. 1988. 13. Layout and design criteria for livestock windbreaks. *Agric., Ecosyst. Environ.* 22: 231-240.
- Du, C. and J. Zhou. 2009. Evaluation of soil fertility using infrared spectroscopy: a review. *Environ. Chem. Lett.* 7: 97-113.
- Dumanski, J., R. Desjardins, C. Tarnocai, C. Monreal, E. Gregorich, V. Kirkwood, et al. 1998. Possibilities for future carbon sequestration in Canadian agriculture in relation to land use changes. *Clim. Change* 40: 81-103.
- Dungait, J.A., D.W. Hopkins, A.S. Gregory and A.P. Whitmore. 2012. Soil organic matter turnover is governed by accessibility not recalcitrance. *Glob. Change Biol.* 18: 1781-1796.
- Dunlop, A. 2000. Spatial and temporal aspects of Saskatchewan field shelterbelts, 1949-98. M.Sc. thesis. University of Saskatchewan, Saskatoon.
- Ekschmitt, K., M. Liu, S. Vetter, O. Fox and V. Wolters. 2005. Strategies used by soil biota to overcome soil organic matter stability—why is dead organic matter left over in the soil? *Geoderma* 128: 167-176.
- Ellerbrock, R. and H. Gerke. 2004. Characterizing organic matter of soil aggregate coatings and biopores by Fourier transform infrared spectroscopy. *Eur. J. Soil Sci.* 55: 219-228.
- Ellerbrock, R., H. Gerke, J. Bachmann and M.-O. Goebel. 2005. Composition of organic matter fractions for explaining wettability of three forest soils. *Soil Sci. Soc. Am. J.* 69: 57-66.
- Ellerbrock, R.H., A. Höhn and H.H. Gerke. 1999. Characterization of soil organic matter from a sandy soil in relation to management practice using FT-IR spectroscopy. *Plant and Soil* 213: 55-61.
- Elliott, E.T. and C.A. Cambardella. 1991. Proceedings of the International Workshop on Modern Techniques in Soil Ecology Relevant to Organic Matter Breakdown, Nutrient Cycling and Soil Biological Processes Physical separation of soil organic matter. *Agric. Ecosyst. Environ.* 34: 407-419.

- Eusterhues, K., C. Rumpel and I. Kögel-Knabner. 2005. Organo-mineral associations in sandy acid forest soils: importance of specific surface area, iron oxides and micropores. *Eur. J. Soil Sci.* 56: 753-763.
- Faix, O. 1992. Fourier Transform Infrared Spectroscopy. In: S. Y. Lin and C. W. Dence, editors, *Methods in Lignin Chemistry*. Springer Berlin Heidelberg, Berlin, Heidelberg. p. 83-109.
- Fassbender, H. and L. Alpizar. 1987. Criteria for the evaluation of organic matter and nutrient cycling in agroforestry systems. In: J. Beer, H. Fassbender and J. Heuveldop, editors, *Advances in agroforestry research*. CATIE, Turrialba, Costa Rica. p. 91-103.
- Feller, C. and M. Beare. 1997. Physical control of soil organic matter dynamics in the tropics. *Geoderma* 79: 69-116.
- Feller C. E., R. Fritsch, C. Poss and C. Valentin. 1991. Effect of the texture on the storage and dynamics of organic matter in some low activity clay soils (West Africa, particularly). *Cahier ORSTOM série Pedologie* 26: 25-36.
- Feng, X. and M.J. Simpson. 2011. Molecular-level methods for monitoring soil organic matter responses to global climate change. *J. Environ. Monit.* 13: 1246-1254.
- Ferguson, A. C., L. Lenz, J.A. Menzies J.A. and G. Stone. 1977. Horticulture. In *Principles and Practices of Commercial Farming*. University of Manitoba.
- Fierer, N., A.S. Grandy, J. Six and E.A. Paul. 2009. Searching for unifying principles in soil ecology. *Soil Biol. Biochem.* 41: 2249-2256.
- Filley, T.R., T.W. Boutton, J.D. Liao, J.D. Jastrow and D.E. Gamblin. 2008. Chemical changes to nonaggregated particulate soil organic matter following grassland-to-woodland transition in a subtropical savanna. *J. Geophys. Res.: Biogeosci.* 113 (G3).
- Folland, C.K., T. Karl and K.Y. Vinnikov. 1990. Observed climate variations and change. In: J. T. Houghton, G. J. Jenkins and J. J. Ephraums, editors, *Climate change: the IPCC scientific assessment*. Univeristy Press, Cambridge. p. 195-238.
- Follett, R.F. 2001. Soil management concepts and carbon sequestration in cropland soils. *Soil Till. Res.* 61: 77-92.
- Follett, R.F. and J.M. Kimble. 2000. *The potential of US grazing lands to sequester carbon and mitigate the greenhouse effect*. CRC Press, Boca raton, FL.
- Frank, A. and W. Willis. 1978. Effect of winter and summer windbreaks on soil water gain and spring wheat yield. *Soil Sci. Soc. Am. J.* 42: 950-953.
- Froelich, P. 1980. Analysis of organic carbon in marine sediments. *Limnol. Oceanogr* 25: 564-572.
- Fründ, R. and H.-D. Lüdemann. 1989. ¹³C-NMR Spectroscopy of Lignins and Lignocellulosic Materials. In: A. Chesson and E. R. Ørskov, editors, *Physico-Chemical Characterisation of Plant Residues for Industrial and Feed Use*. Springer Netherlands, Dordrecht. p. 110-117.
- Gale, W. and C. Cambardella. 2000. Carbon dynamics of surface residue-and root-derived organic matter under simulated no-till. *Soil Sci. Soc. Am. J.* 64: 190-195.

- Garten, C., S.D. Wullschleger and A.T. Classen. 2011. Review and model-based analysis of factors influencing soil carbon sequestration under hybrid poplar. *Biomass Bioenergy* 35: 214-226.
- Garten, C.T. 2002. Soil carbon storage beneath recently established tree plantations in Tennessee and South Carolina, USA. *Biomass Bioenergy* 23: 93-102.
- Garten Jr., C.T., W.M. Post III, P.J. Hanson and L.W. Cooper. 1999. Forest soil carbon inventories and dynamics along an elevation gradient in the southern Appalachian Mountains. *Biogeochemistry* 45: 115-145.
- Gehman, H., Jr. 1962. Organic matter in limestones. *Geochim. Cosmochim. Acta* 26: 885-897.
- Gerzabek, M., R. Antil, I. Kögel-Knabner, H. Knicker, H. Kirchmann and G. Haberhauer. 2006. How are soil use and management reflected by soil organic matter characteristics: a spectroscopic approach. *Eur. J. Soil Sci.* 57: 485-494.
- Gillespie, A., H. Sanei, A. Diochon, B. Ellert, T. Regier, D. Chevrier, et al. 2014a. Perennially and annually frozen soil carbon differ in their susceptibility to decomposition: analysis of Subarctic earth hummocks by bioassay, XANES and pyrolysis. *Soil Biol. Biochem.* 68: 106-116.
- Gillespie, A., F. Walley, R. Farrell, P. Leinweber, K.-U. Eckhardt, T. Regier, et al. 2011. XANES and pyrolysis-FIMS evidence of organic matter composition in a hummocky landscape. *Soil Sci. Soc. Am. J.* 75: 1741-1755.
- Gillespie, A.W., A. Diochon, B.L. Ma, M.J. Morrison, L. Kellman, F.L. Walley, et al. 2014b. Nitrogen input quality changes the biochemical composition of soil organic matter stabilized in the fine fraction: a long-term study. *Biogeochemistry* 117: 337-350.
- Gleixner, G., C. Czimczik, C. Kramer, B. Lühker and M. Schmidt. 2001. Plant compounds and their turnover and stability as soil organic matter. In: E.D. Schulze, M. Heimann, S. P. Harrison, E. Holland, J. Lloyd, I. C. Prentice, et al., editors, *Global biogeochemical cycles in the climate system*. Academic Press, San Diego. p. 201-215.
- Golchin, A., J. Oades, J. Skjemstad and P. Clarke. 1994. Study of free and occluded particulate organic matter in soils by solid state ¹³C CP/MAS NMR spectroscopy and scanning electron microscopy. *Soil Res.* 32: 285-309.
- González, G. and T.R. Seastedt. 2001. Soil fauna and plant litter decomposition in tropical and subalpine forests. *Ecology* 82: 955-964.
- Gottschalk, G. 2012. *Bacterial metabolism*. 2nd ed. Springer Science & Business Media, New York, NY.
- Grandy, A.S. and J.C. Neff. 2008. Molecular C dynamics downstream: the biochemical decomposition sequence and its impact on soil organic matter structure and function. *Sci. Total Environ.* 404: 297-307.
- Gregorich, E., M. Beare, U. McKim and J. Skjemstad. 2006. Chemical and biological characteristics of physically uncomplexed organic matter. *Soil Sci. Soc. Am. J.* 70: 975-985.
- Gregorich, E.G., C.M. Monreal, M. Schnitzer and H.R. Schulten. 1996. Transformation of plant residues into soil organic matter: Chemical characterization of plant tissue, isolated soil fractions, and whole soils. *Soil Sci.* 161: 680-693

- Griffiths, P.R. and J.A. De Haseth. 2007. Fourier transform infrared spectrometry. John Wiley & Sons.
- Grigal, D. and L. Ohmann. 1992. Carbon storage in upland forests of the Lake States. *Soil Sci. Soc. Am. J.* 56: 935-943.
- Grigal, D.F. and W.E. Berguson. 1998. Soil carbon changes associated with short-rotation systems. *Biomass Bioenergy* 14: 371-377.
- Grogan, P. and R. Matthews. 2002. A modelling analysis of the potential for soil carbon sequestration under short rotation coppice willow bioenergy plantations. *Soil Use Manage.* 18: 175-183.
- Gu, B., J. Schmitt, Z. Chen, L. Liang and J.F. McCarthy. 1995. Adsorption and desorption of different organic matter fractions on iron oxide. *Geochim. Cosmochim. Acta* 59: 219-229.
- Grünzweig, J., I. Gelfand and D. Yakir. 2007. Biogeochemical factors contributing to enhanced carbon storage following afforestation of a semi-arid shrubland. *Biogeosci. Discuss.* 4: 2111-2145.
- Guggenberger, G., B.T. Christensen and W. Zech. 1994. Land-use effects on the composition of organic matter in particle-size separates of soil: I. Lignin and carbohydrate signature. *Eur. J. Soil Sci.* 45: 449-458.
- Guler, A., F. Evrendilek and N. Karakaya. 2011. Quantifying Spatial Variability of Peat Soil Carbon and Nitrogen using Infrared Spectroscopy, Statistical and Geo-Statistical Models. *Res. J. Chem. Environ.* Vol 15: 68-74.
- Haberhauer, G., B. Feigl, M. Gerzabek and C. Cerri. 2000. FT-IR spectroscopy of organic matter in tropical soils: changes induced through deforestation. *Appl. Spectrosc.* 54: 221-224.
- Haberhauer, G. and M. Gerzabek. 1999. Drift and transmission FT-IR spectroscopy of forest soils: an approach to determine decomposition processes of forest litter. *Vib. Spectrosc* 19: 413-417.
- Haberhauer, G., B. Rafferty, F. Strebl and M. Gerzabek. 1998. Comparison of the composition of forest soil litter derived from three different sites at various decompositional stages using FTIR spectroscopy. *Geoderma* 83: 331-342.
- Hamza, M. and W. Anderson. 2005. Soil compaction in cropping systems: A review of the nature, causes and possible solutions. *Soil Tillage Res.* 82: 121-145.
- Hansen, E.A. 1993. Soil carbon sequestration beneath hybrid poplar plantations in the north central United States. *Biomass Bioenergy* 5: 431-436.
- Hannam, K., S. Quideau, S.-W. Oh, B. Kishchuk and R. Wasylishen. 2004. Forest floor composition in aspen-and spruce-dominated stands of the boreal mixedwood forest. *Soil Sci. Soc. Am. J.* 68: 1735-1743.
- Harris, D., W.R. Horwath and C. van Kessel. 2001. Acid fumigation of soils to remove carbonates prior to total organic carbon or carbon-13 isotopic analysis. *Soil Sci. Soc. Am. J.* 65:1853-1856.
- Hassink, J. 1995. Decomposition rate constants of size and density fractions of soil organic matter. *Soil Sci. Soc. Am. J.* 59: 1631-1635.

- Hättenschwiler, S., A.V. Tiunov and S. Scheu. 2005. Biodiversity and litter decomposition in terrestrial ecosystems. *Annu. Rev. Ecol. Evol. Syst.* 36: 191-218.
- Hättenschwiler, S. and P.M. Vitousek. 2000. The role of polyphenols in terrestrial ecosystem nutrient cycling. *Trends Ecol. Evol.* 15: 238-243.
- Haynes, R.J. 2005. Labile organic matter fractions as central components of the quality of agricultural soils: An overview. *Adv. Agron.* 85: 221-268.
- Hedde, M., F. Bureau, M. Akpa-Vinceslas, M. Aubert and T. Decaëns. 2007. Beech leaf degradation in laboratory experiments: Effects of eight detritivorous invertebrate species. *Appl. Soil Ecol.* 35: 291-301.
- Hedges, J.I. and J.H. Stern. 1984. Carbon and nitrogen determinations of carbonate-containing solids. *Limnol. Oceanogr.* 29.
- Helfrich, M., B. Ludwig, P. Buurman and H. Flessa. 2006. Effect of land use on the composition of soil organic matter in density and aggregate fractions as revealed by solid-state ¹³C NMR spectroscopy. *Geoderma* 136: 331-341.
- Hilli, S., S. Stark and J. Derome. 2008. Carbon Quality and Stocks in Organic Horizons in Boreal Forest Soils. *Ecosystems* 11: 270-282.
- Hitchcock, A.P., J.J. Dynes, G. Johansson, J. Wang and G. Botton. 2008. Comparison of NEXAFS microscopy and TEM-EELS for studies of soft matter. *Micron* 39: 311-319.
- Hongve, D., P.A.W. Van Hees and U.S. Lundström. 2000. Dissolved components in precipitation water percolated through forest litter. *Eur. J. Soil Sci.* 51: 667-677.
- Hontoria, C., A. Saa and J. Rodríguez-Murillo. 1999. Relationships between soil organic carbon and site characteristics in peninsular Spain. *Soil Sci. Soc. Am. J.* 63: 614-621.
- Huang, P. 1990. Role of soil minerals in transformations of natural organics and xenobiotics in soil. In: J. M. Bollag and G. Stotzky, editors, *Soil biochemistry*. Marcel Dekker, New York, NY. p. 29-115.
- Hutchison, K.J., D. Hesterberg and J.W. Chou. 2001. Stability of reduced organic sulfur in humic acid as affected by aeration and pH. *Soil Sci. Soc. Am. J.* 65: 704-709.
- IBM Corp. 2013. IBM SPSS Statistics for Macintosh, Version 22.0. IBM Corp., Armonk, NY.
- IPCC 1995. *Climate change 1994: Radiative forcing of climate change and an evaluation of the IPCC IS92 emission scenarios*. Cambridge University Press, Cambridge, UK.
- IPCC 2001. *Climate Change: The Scientific Basis. Contribution of Working Group I to the Third Assessment Report of the Intergovernmental Panel on Climate Change*. Cambridge University Press, Cambridge, UK.
- Inbar, Y., Y. Chen and Y. Hadar. 1989. Solid-state carbon-13 nuclear magnetic resonance and infrared spectroscopy of composted organic matter. *Soil Sci. Soc. Am. J.* 53: 1695-1701.
- Jackson, R., J. Canadell, J.R. Ehleringer, H. Mooney, O. Sala and E. Schulze. 1996. A global analysis of root distributions for terrestrial biomes. *Oecologia* 108: 389-411.
- Jackson, R.B., H.A. Mooney and E.D. Schulze. 1997. A global budget for fine root biomass, surface area, and nutrient contents. *P. Natl. Acad. Sci. USA* 94: 7362-7366.

- Jacobsen, C., S. Wirrick, G. Flynn and C. Zimba. 2000. Soft X-ray spectroscopy from image sequences with sub-100 nm spatial resolution. *J. Microsc.* 197: 173-184.
- Janik, L.J., R.H. Merry, S. Forrester, D. Lanyon and A. Rawson. 2007. Rapid prediction of soil water retention using mid infrared spectroscopy. *Soil Sci. Soc. Am. J.* 71: 507-514.
- Janik, L.J., R.H. Merry and J. Skjemstad. 1998. Can mid infrared diffuse reflectance analysis replace soil extractions? *Anim. Prod. Sci.* 38: 681-696.
- Janik, L.J., J. Skjemstad and M.D. Raven. 1995. Characterization and analysis of soils using mid-infrared partial least-squares. 1. Correlations with XRF-determined major-element composition. *Aust. J. Soil Res.* 33: 621-636.
- Janik, L.J., J. Skjemstad, K. Shepherd and L. Spouncer. 2007. The prediction of soil carbon fractions using mid-infrared-partial least square analysis. *Aust. J. Soil Res.* 45: 73-81.
- Janzen, H.H., C.A. Campbell, S.A. Brandt, G.P. Lafond and L. Townley-Smith. 1992. Light-fraction organic matter in soils from long-term crop rotations. *Soil Sci. Soc. Am. J.* 56: 1799-1806.
- Jastrow, J.D., J.E. Amonette and V.L. Bailey. 2006. Mechanisms controlling soil carbon turnover and their potential application for enhancing carbon sequestration. *Climatic Change* 80: 5-23.
- Jenkinson, D. 1971. The accumulation of organic matter in soil left uncultivated. Rep. Rothamsted Exp. Stn. for 1970, Part 2. p. 113-137.
- Jenkinson, D. 1991. The Rothamsted long-term experiments: are they still of use? *Agron. J.* 83: 2-10.
- Jobbágy, E.G. and R.B. Jackson. 2000. The vertical distribution of soil organic carbon and its relation to climate and vegetation. *Ecol. Appl.* 10: 423-436.
- Johnson, D.W. 1992. Effects of forest management on soil carbon storage. In: J. Wisniewski and A. E. Lugo, editors, *Natural sinks of CO₂ : Palmas Del Mar, Puerto Rico, 24–27 February 1992*. Springer Netherlands, Dordrecht. p. 83-120.
- Johnson, R. and M. Beck. 1988. 17. Influences of shelterbelts on wildlife management and biology. *Agric., Ecosyst. Environ.* 22: 301-335.
- Jokic, A., J.N. Cutler, E. Ponomarenko, G. van der Kamp and D.W. Anderson. 2003. Organic carbon and sulphur compounds in wetland soils: insights on structure and transformation processes using K-edge XANES and NMR spectroscopy. *Geochim. Cosmochim. Acta* 67: 2585-2597.
- Jones, D.L. 1998. Organic acids in the rhizosphere – a critical review. *Plant Soil* 205: 25-44.
- Jones, D.L. and A.C. Edwards. 1998. Influence of sorption on the biological utilization of two simple carbon substrates. *Soil Biol. Biochem.* 30: 1895-1902.
- Jones, E. and B. Singh. 2014. Organo-mineral interactions in contrasting soils under natural vegetation. *Front. Environ. Sci.* 2: 2.
- Kaiser, K. and G. Guggenberger. 2000. The role of DOM sorption to mineral surfaces in the preservation of organic matter in soils. *Org. Geochem.* 31: 711-725.

- Kaiser, K. and G. Guggenberger. 2003. Mineral surfaces and soil organic matter. *Eur. J. Soil Sci.* 54: 219-236.
- Kang, B., H. Grimme and T. Lawson. 1985. Alley cropping sequentially cropped maize and cowpea with *Leucaena* on a sandy soil in Southern Nigeria. *Plant Soil* 85: 267-277.
- Kell, D.B. 2011. Breeding crop plants with deep roots: Their role in sustainable carbon, nutrient and water sequestration. *Ann. Bot.* 108: 407-418.
- Kell, D.B. 2012. Large-scale sequestration of atmospheric carbon via plant roots in natural and agricultural ecosystems: why and how. *Phil. Trans. R. Soc. B* 367: 1589-1597.
- Kelleher, B.P. and A.J. Simpson. 2006. Humic substances in soils: are they really chemically distinct? *Environ. Sci. & Technol.* 40: 4605-4611.
- Kikuma, J. and B. Tonner. 1996. XANES spectra of a variety of widely used organic polymers at the C K-edge. *J. Electron. Spectrosc. Relat. Phenom.* 82: 53-60.
- Kinyangi, J., D. Solomon, B. Liang, M. Lerotic, S. Wirick and J. Lehmann. 2006. Nanoscale biogeochemical complexity of the organomineral assemblage in soil. *Soil Sci. Soc. Am. J.* 70: 1708-1718.
- Kleber, M. and M.G. Johnson. 2010. Advances in understanding the molecular structure of soil organic matter: implications for interactions in the environment. In: D. L. Sparks, editor, *Advances in agronomy*. Academic press. p. 77-142.
- Kleber, M., P. Sollins and R. Sutton. 2007. A conceptual model of organo-mineral interactions in soils: self-assembly of organic molecular fragments into zonal structures on mineral surfaces. *Biogeochemistry* 85: 9-24.
- Kögel, I., R. Hempfling, W. Zech, P.G. Hatcher and H.-R. Schulden. 1988. Chemical composition of the organic matter in forest soils: 1. Forest litter. *Soil Sci.* 146: 124-136.
- Kögel-Knabner, I. 2000. Analytical approaches for characterizing soil organic matter. *Org. Geochem.* 31: 609-625.
- Kögel-Knabner, I. 2002. The macromolecular organic composition of plant and microbial residues as inputs to soil organic matter. *Soil Biol. Biochem.* 34: 139-162.
- Kögel-Knabner, I., J.W. de Leeuw and P.G. Hatcher. 1992. Nature and distribution of alkyl carbon in forest soil profiles: implications for the origin and humification of aliphatic biomacromolecules. *Sci. Total Environ.* 117: 175-185.
- Kögel-Knabner, I., W. Zech and P.G. Hatcher. 1988. Chemical composition of the organic matter in forest soils: The humus layer. *Z. Pflanzenernaehr. Bodenk.* 151: 331-340.
- Kögel-Knabner, I., G. Guggenberger, M. Kleber, E. Kandeler, K. Kalbitz, S. Scheu, et al. 2008. Organo-mineral associations in temperate soils: Integrating biology, mineralogy, and organic matter chemistry. *J. Plant Nutr. Soil Sci.* 171: 61-82.
- Kort, J. 1988. Benefits of windbreaks to field and forage crops. *Agric., Ecosyst. Environ.* 22: 165-190.
- Kort, J., G. Bank, J. Pomeroy and X. Fang. 2012. Effects of shelterbelts on snow distribution and sublimation. *Agroforest. Syst.* 86: 335-344.

- Kort, J. and P. Cherneski. 1989. Shelterbelt studies. 1989 Report of the PFRA Shelterbelt Centre. Indian Head, Saskatchewan.
- Kort, J. and R. Turnock. 1998. Carbon reservoir and biomass in Canadian prairie shelterbelts. *Agroforest. Syst.* 44: 175-186.
- Kravchenko, A. and G. Robertson. 2011. Whole-profile soil carbon stocks: The danger of assuming too much from analyses of too little. *Soil Sci. Soc. Am. J.* 75: 235-240.
- Kristensen, E. and F.Ø. Andersen. 1987. Determination of organic carbon in marine sediments: a comparison of two CHN-analyzer methods. *J. Exp. Mar. Biol. Ecol.* 109: 15-23.
- Krull, E.S., J.A. Baldock and J.O. Skjemstad. 2003. Importance of mechanisms and processes of the stabilisation of soil organic matter for modelling carbon turnover. *Funct. Plant Biol.* 30: 207-222.
- Kulshreshtha, S.N. and J. Rempel. 2014. Shelterbelts on Saskatchewan Farms: An assest or a nuisance. In: S. Lac and M. P. McHenry, editors, *Climate change and forest ecosystems*. Nova Publishers, New York. p. 37-55.
- Kuhlbusch, T.A.J. 1995. Method for determining black carbon in residues of vegetation fires. *Environ. Sci. Technol.* 29: 2695-2702.
- Kunhamu, T.K., B.M. Kumar and S. Samuel. 2011. Does tree management affect biomass and soil carbon stocks of *Acacia mangium* Willd. stands in Kerala, India? In: M. B. Kumar and R. P. K. Nair, editors, *Carbon sequestration potential of agroforestry systems: Opportunities and challenges*. Springer Netherlands, Dordrecht. p. 217-228.
- Ladd, J., M. Amato and J. Oades. 1985. Decomposition of plant material in Australian soils. III. Residual organic and microbial biomass C and N from isotope-labelled legume material and soil organic matter, decomposing under field conditions. *Soil Res.* 23: 603-611.
- Ladd, J., M. Amato, L.-K. Zhou and J. Schultz. 1994. Differential effects of rotation, plant residue and nitrogen fertilizer on microbial biomass and organic matter in an Australian Alfisol. *Soil Biol. Biochem.* 26: 821-831.
- Ladd, J., R. Foster and J. Skjemstad. 1993. Soil structure: carbon and nitrogen metabolism. *Geoderma* 56: 401-434.
- Laganiere, J., D.A. Angers and D. Pare. 2010a. Carbon accumulation in agricultural soils after afforestation: A meta-analysis. *Glob. Change Biol.* 16: 439-453.
- Laganière, J., D.A. Angers, D. Paré, Y. Bergeron and H.Y.H. Chen. 2011. Black spruce soils accumulate more uncomplexed organic matter than aspen soils. *Soil Sci. Soc. Am. J.* 75: 1125-1132.
- Laganière, J., D. Paré and R.L. Bradley. 2009. Linking the abundance of aspen with soil faunal communities and rates of belowground processes within single stands of mixed aspen-black spruce. *Appl. Soil Ecol.* 41: 19-28.
- Laganière, J., D. Pare and R.L. Bradley. 2010b. How does a tree species influence litter decomposition? Separating the relative contribution of litter quality, litter mixing, and forest floor conditions. *Can. J. For. Res.* 40: 465-475.
- Lal, R. 2004a. Soil carbon sequestration to mitigate climate change. *Geoderma* 123: 1-22.

- Lal, R. 2004b. Soil carbon sequestration impacts on global climate change and food security. *Science* 304: 1623-1627.
- Lal, R. 2008. Carbon sequestration. *Philosophical Transactions of the Royal Society of London B: Biological Sciences* 363: 815-830.
- Lamarche, J., R.L. Bradley, E. Hooper, B. Shipley, A.-M.S. Beaulieu and C. Beaulieu. 2007. Forest floor bacterial community composition and catabolic profiles in relation to landscape features in Québec's southern boreal forest. *Microbial Ecol.* 54: 10-20.
- Landi, A., A. Mermut and D. Anderson. 2003. Origin and rate of pedogenic carbonate accumulation in Saskatchewan soils, Canada. *Geoderma* 117: 143-156.
- Lehmann, J., B. Liang, D. Solomon, M. Lerotic, F. Luizão, J. Kinyangi, et al. 2005. Near-edge X-ray absorption fine structure (NEXAFS) spectroscopy for mapping nano-scale distribution of organic carbon forms in soil: Application to black carbon particles. *Global Biogeochem. Cycles* 19: GB1013.
- Lehmann, J. and D. Solomon. 2010. Organic carbon chemistry in soils observed by synchrotron-based spectroscopy. *Dev. Soil Sci.* 34: 289-312.
- Lehmann, J., D. Solomon, J. Brandes, H. Fleckenstein, C. Jacobson, J. Thieme, et al. 2009. Synchrotron-based near-edge X-ray spectroscopy of natural organic matter in soils and sediments. In: N. Senesi, P. Xing and P.M. Huang, editors, *Bio-physico-chemical processes involving natural nonliving organic matter in environmental systems*. IUPAC series on biophysico-chemical processes in environmental systems, pp. 729–781.
- Lehmann, J., D. Solomon, J. Kinyangi, L. Dathe, S. Wirick and C. Jacobsen. 2008. Spatial complexity of soil organic matter forms at nanometre scales. *Nat. Geosci.* 1: 238-242.
- Leifeld, J. and I. Kögel-Knabner. 2005. Soil organic matter fractions as early indicators for carbon stock changes under different land-use? *Geoderma* 124: 143-155.
- Leite, L.F.C., B.d.F. Iwata and A.S.F. Araújo. 2014. Soil organic matter pools in a tropical savanna under agroforestry system in Northeastern Brazil. *Rev. Árvore* 38: 711-723.
- Lokupitiya, E. and K. Paustian. 2006. Agricultural soil greenhouse gas emissions. *J. Environ. Qual.* 35: 1413-1427.
- Lombi, E. and J. Susini. 2009. Synchrotron-based techniques for plant and soil science: opportunities, challenges and future perspectives. *Plant and Soil* 320: 1-35.
- Lorenz, K. and R. Lal. 2005. The depth distribution of soil organic carbon in relation to land use and management and the potential of carbon sequestration in subsoil horizons. *Adv. Agron.* 88: 35-66.
- Lorenz, K., R. Lal, C.M. Preston and K.G. Nierop. 2007. Strengthening the soil organic carbon pool by increasing contributions from recalcitrant aliphatic bio (macro) molecules. *Geoderma* 142: 1-10.
- López-Ulloa, M., E. Veldkamp and G. De Koning. 2005. Soil carbon stabilization in converted tropical pastures and forests depends on soil type. *Soil Sci. Soc. Am. J.* 69: 1110-1117.

- Lorenz, K. and R. Lal. 2005. The depth distribution of soil organic carbon in relation to land use and management and the potential of carbon sequestration in subsoil horizons. *Adv. Agron.* 88: 35-66.
- Lorenz, K. and R. Lal. 2014. Soil organic carbon sequestration in agroforestry systems. A review. *Agron. Sustainable Dev.* 34: 443-454.
- Lorenz, K., R. Lal, C.M. Preston and K.G. Nierop. 2007. Strengthening the soil organic carbon pool by increasing contributions from recalcitrant aliphatic bio (macro) molecules. *Geoderma* 142: 1-10.
- MacKeague, J., J. Desjardins and M. Wolynetz. 1979. Minor elements in Canadian soils. Land Resource Research Institute Contribution (no. LLRI 27).
- Madari, B.E., J.B. Reeves, P.L. Machado, C.M. Guimarães, E. Torres and G.W. McCarty. 2006. Mid-and near-infrared spectroscopic assessment of soil compositional parameters and structural indices in two Ferralsols. *Geoderma* 136: 245-259.
- Mahieu, N., E. Randall and D. Powlson. 1999. Statistical analysis of published carbon-13 CPMAS NMR spectra of soil organic matter. *Soil Sci. Soc. Am. J.* 63: 307-319.
- Marschner, B., S. Brodowski, A. Dreves, G. Gleixner, A. Gude, P.M. Grootes, et al. 2008. How relevant is recalcitrance for the stabilization of organic matter in soils? *J. Plant Nutr. Soil Sci.* 171: 91-110.
- Martens, D.A., T.E. Reedy and D.T. Lewis. 2004. Soil organic carbon content and composition of 130-year crop, pasture and forest land-use managements. *Glob. Change Biol.* 10: 65-78.
- Mascarenhas, M., J. Dighton and G.A. Ar buckle. 2000. Characterization of plant carbohydrates and changes in leaf carbohydrate chemistry due to chemical and enzymatic degradation measured by microscopic ATR FT-IR spectroscopy. *Appl. Spectrosc.* 54: 681-686.
- Matějková, Š. and T. Šimon. 2012. Application of FTIR spectroscopy for evaluation of hydrophobic/hydrophilic organic components in arable soil. *Plant Soil Environ.* 58: 192-195.
- McCarty, G., J. Reeves, V. Reeves, R. Follett and J. Kimble. 2002. Mid-infrared and near-infrared diffuse reflectance spectroscopy for soil carbon measurement. *Soil Sci. Soc. Am. J.* 66: 640-646.
- McCulley, R.L., S. Archer, T. Boutton, F. Hons and D. Zuberer. 2004. Soil respiration and nutrient cycling in wooded communities developing in grassland. *Ecology* 85: 2804-2817.
- McNaughton, K. 1988. Effects of windbreaks on turbulent transport and microclimate. *Agric., Ecosyst. Environ.* 22: 17-39.
- Mensah, F., J. Schoenau and S. Malhi. 2003. Soil carbon changes in cultivated and excavated land converted to grasses in east-central Saskatchewan. *Biogeochemistry* 63: 85-92.
- Messing, I., A. Alriksson and W. Johansson. 1997. Soil physical properties of afforested and arable land. *Soil Use Manage.* 13: 209-217.
- Mikutta, R., M. Kleber, M.S. Torn and R. Jahn. 2006. Stabilization of soil organic matter: association with minerals or chemical recalcitrance? *Biogeochemistry* 77: 25-56.
- Mills, G.L. and J.G. Quinn. 1979. Determination of organic carbon in marine sediments by persulfate oxidation. *Chem. Geol.* 25: 155-162.

- Miltner, A. and W. Zech. 1998. Beech leaf litter lignin degradation and transformation as influenced by mineral phases. *Org. Geochem.* 28: 457-463.
- Mitchell, R.J., C.D. Campbell, S.J. Chapman and C.M. Cameron. 2010. The ecological engineering impact of a single tree species on the soil microbial community. *J. Ecol.* 98: 50-61.
- Mize, C.W., J.R. Brandle, M.M. Schoeneberger and G. Bentrup. 2008. Ecological development and function of shelterbelts in temperate North America. In: S. Jose and A. M. Gordon, editors, *Toward agroforestry design: An ecological approach*. Springer Netherlands, Dordrecht. p. 27-54.
- Moeur, M. 1997. Spatial models of competition and gap dynamics in old-growth *Tsuga heterophylla*/*Thuja plicata* forests. *For. Ecol. Manage.* 94: 175-186.
- Mokany, K., R. Raison and A.S. Prokushkin. 2006. Critical analysis of root: shoot ratios in terrestrial biomes. *Glob. Change Biol.* 12: 84-96.
- Montagnini, F. 2001. Strategies for the recovery of degraded ecosystems: Experiences from Latin America. *Interciencia* 26: 498-503.
- Montagnini, F. and P. Nair. 2004. Carbon sequestration: An underexploited environmental benefit of agroforestry systems. *Agroforest. Syst.* 61: 281-295.
- Mungai, N.W. and P.P. Motavalli. 2006. Litter quality effects on soil carbon and nitrogen dynamics in temperate alley cropping systems. *Appl. Soil Ecol.* 31: 32-42.
- Myneni, S.C. 2002. Soft X-ray spectroscopy and spectromicroscopy studies of organic molecules in the environment. *Rev. Mineral. Geochem.* 49: 485-579.
- Nair, P.R., R.J. Buresh, D.N. Mugendi and C.R. Latt. 1999. Nutrient cycling in tropical agroforestry systems: Myths and science. In: L. E. Buck, J. P. Lassoie and E. C. M. Fernandes, editors, *Agroforestry in sustainable agricultural systems*. CRC Press, Boca Raton, FL. p. 1-31.
- Nair, P.R. and V.D. Nair. 2003. Carbon storage in North American agroforestry systems. In: J. M. Kimble, R. Lal, R. Birdsey and L. S. Heath, editors, *The potential of US forest soils to sequester carbon and mitigate the greenhouse effect*. p. 333-346.
- Nair, P.R., V.D. Nair, B.M. Kumar and S.G. Haile. 2009a. Soil carbon sequestration in tropical agroforestry systems: A feasibility appraisal. *Environ. Sci. Policy* 12: 1099-1111.
- Nair, P.R., V.D. Nair, E.F. Gama-Rodrigues, R. Garcia, S.G. Haile, D.S. Howlett, et al. 2009b. Soil carbon in agroforestry systems: An unexplored treasure? Available from Nature Precedings <http://hdl.handle.net/10101/npre.2009.4061.1>
- Nair, P.R., V.D. Nair, B.M. Kumar and J.M. Showalter. 2010. Carbon sequestration in agroforestry systems. *Adv. Agron.* 108: 237-307.
- Nelson, D.W. and L.E. Sommers. 1982. Total carbon, organic carbon, and organic matter. In: A. L. Page, R. H. Miller and D. R. Keeney, editors, *Methods of Soil Analysis, Part 2. Chemical and Microbiological Properties*. ASA-SSSA, Madison, WI. p. 539-579.
- Nicholaichuk, W. and D.I. Norum. 1975. Snow management on the Canadian prairies. *Proc. symp. on snow management on the Great Plains, Great Plains Agric. Council. Publ., No. 73:118-127.*
- Nieuwenhuize, J., Y.E. Maas and J.J. Middelburg. 1994. Rapid analysis of organic carbon and nitrogen in particulate materials. *Marine Chemistry* 45: 217-224.

- Niu, X. and S.W. Duiker. 2006. Carbon sequestration potential by afforestation of marginal agricultural land in the Midwestern US. *For. Ecol. Manage.* 223: 415-427.
- Oades, J. 1988. The retention of organic matter in soils. *Biogeochemistry* 5: 35-70.
- Oades, J. 1995. An overview of processes affecting the cycling of organic carbon in soils. In: R. G. Zepp and C. Sonntag, editors, *The role of nonliving organic matter in the earth's carbon cycle.* John Wiley, New York. p. 293-303.
- Oelbermann, M., R.P. Voroney and A.M. Gordon. 2004. Carbon sequestration in tropical and temperate agroforestry systems: A review with examples from Costa Rica and southern Canada. *Agric., Ecosyst. Environ.* 104: 359-377.
- Oelbermann, M., R.P. Voroney, N.V. Thevathasan, A.M. Gordon, D.C. Kass and A.M. Schlönvoigt. 2006. Soil carbon dynamics and residue stabilization in a Costa Rican and southern Canadian alley cropping system. *Agroforest. Syst.* 68: 27-36.
- Ogbuehi, S. and J. Brandle. 1982. Influence of windbreak-shelter on soybean growth, canopy structure, and light relations. *Crop Science* 22: 269-273.
- Ostrofsky, M. 1993. Effect of tannins on leaf processing and conditioning rates in aquatic ecosystems: an empirical approach. *Can. J. Fish. Aquat. Sci.* 50: 1176-1180.
- Parikh, S.J., K.W. Goyne, A.J. Margenot, F.N. Mukome and F.J. Calderón. 2014. Soil chemical insights provided through vibrational spectroscopy. In: D. L. Sparks, editor, *Advances in agronomy.* Academic press, Waltham, MA. p. 1-148.
- Parton, W.J., D.S. Schimel, C. Cole and D. Ojima. 1987. Analysis of factors controlling soil organic matter levels in Great Plains grasslands. *Soil Sci. Soc. Am. J.* 51: 1173-1179.
- Paul, K., P. Polglase, J. Nyakuengama and P. Khanna. 2002. Change in soil carbon following afforestation. *For. Ecol. Manage.* 168: 241-257.
- Paulis, J. 2007. Measurable soil organic carbon fractions for modeling soil carbon sequestration. M.S. thesis. Univ. of Guelph, Guelph.
- Paustian, K., J. Six, E. Elliott and H. Hunt. 2000. Management options for reducing CO₂ emissions from agricultural soils. *Biogeochemistry* 48: 147-163
- Peichl, M., N.V. Thevathasan, A.M. Gordon, J. Huss and R.A. Abohassan. 2006. Carbon sequestration potentials in temperate tree-based intercropping systems, southern Ontario, Canada. *Agroforest. Syst.* 66: 243-257.
- Pelton, W. 1967. The effect of a windbreak on wind travel, evaporation and wheat yield. *Can. J. Plant Sci.* 47: 209-214.
- Perry, D.A., C. Choquette and P. Schroeder. 1987. Nitrogen dynamics in conifer-dominated forests with and without hardwoods. *Can. J. For. Res.* 17: 1434-1441.
- Peterson, R.C. and K.W. Cummins. 1974. Leaf processing in a woodland stream. *Freshwater Biol.* 4: 343-368.
- Prairie Farm Rehabilitation Administration. 1983. *Land degradation and soil conservation issues on the Canadian Prairies.* Agriculture Canada. Regina, SK.

- Piccolo, A. 2002. The supramolecular structure of humic substances: A novel understanding of humus chemistry and implications in soil science. *Adv. Agron.* 75: 57-134.
- Pocklington, R. and G. Hagell. 1975. The Quantitative Determination of Organic Carbon, Hydrogen, Nitrogen, and Lignin in Marine Sediments. Bedford Institute of Oceanography.
- Post, W.M., W.R. Emanuel, P.J. Zinke and A.G. Stangenberger. 1982. Soil carbon pools and world life zones. *Nature* 298: 156-159.
- Post, W.M. and K.C. Kwon. 2000. Soil carbon sequestration and land-use change: Processes and potential. *Glob. Change Biol.* 6: 317-327.
- Powlson, D.S., P.J. Gregory, W.R. Whalley, J.N. Quinton, D.W. Hopkins, A.P. Whitmore, et al. 2011. Soil management in relation to sustainable agriculture and ecosystem services. *Food Policy* 36, Supplement 1: S72-S87.
- Prescott, C.E., L.M. Zabek, C.L. Staley and R. Kabzems. 2000. Decomposition of broadleaf and needle litter in forests of British Columbia: Influences of litter type, forest type, and litter mixtures. *Can. J. For. Res.* 30: 1742-1750.
- Price, G. and A. Gordon. 1998. Spatial and temporal distribution of earthworms in a temperate intercropping system in southern Ontario, Canada. *Agroforest. Syst.* 44: 141-149.
- Priesack, E. and G. Kisser-Priesack. 1993. Modelling diffusion and microbial uptake of ¹³C-glucose in soil aggregates. *Geoderma* 56: 561-573.
- Purton, K., D. Pennock, P. Leinweber and F. Walley. 2015. Will changes in climate and land use affect soil organic matter composition? Evidence from an ecotonal climosequence. *Geoderma* 253: 48-60.
- Quam, V., L. Johnson, B. Wight and J.R. Brandle. 1994. Windbreaks for livestock operations. *Papers in Natural Resources*: 123.
- Quideau, S., O. Chadwick, A. Benesi, R. Graham and M. Anderson. 2001. A direct link between forest vegetation type and soil organic matter composition. *Geoderma* 104: 41-60.
- Randhawa, R. 2008. Evaluation of Dry-Soil Infrared Techniques for Soil Organic Carbon Characterization. M.Sc. thesis. Pennsylvania State Univ., Pennsylvania.
- Rao, M., P. Nair and C. Ong. 1998. Biophysical interactions in tropical agroforestry systems. *Agrofor. Syst.* 38: 3-50.
- Rasse, D.P., C. Rumpel and M.-F. Dignac. 2005. Is soil carbon mostly root carbon? Mechanisms for a specific stabilisation. *Plant Soil* 269: 341-356.
- Ravel, B. and M. Newville. 2005. ATHENA, ARTEMIS, HEPHAESTUS: data analysis for X-ray absorption spectroscopy using IFEFFIT. *J. Synchrotron Radiat.* 12: 537-541.
- Rempel, J. 2015. Costs, benefits, and barriers to the adoption and retention of shelterbelts in Prairie agriculture as identified by Saskatchewan producers. M.Sc. thesis. Univ. of Saskatchewan, Saskatoon.
- Richter, D.D., D. Markewitz, S.E. Trumbore and C.G. Wells. 1999. Rapid accumulation and turnover of soil carbon in a re-establishing forest. *Nature* 400: 56-58.

- Rizvi, S., M. Tahir, V. Rizvi, R. Kohli and A. Ansari. 1999. Allelopathic interactions in agroforestry systems. *Crit. Rev. Plant Sci.* 18: 773-796.
- Roberts, A.A., J.G. Palacas and I.C. Frost. 1973. Determination of organic carbon in modern carbonate sediments. *J. Sediment. Res.* 43:1157-1159.
- Rossel, R.V., D. Walvoort, A. McBratney, L.J. Janik and J. Skjemstad. 2006. Visible, near infrared, mid infrared or combined diffuse reflectance spectroscopy for simultaneous assessment of various soil properties. *Geoderma* 131: 59-75.
- Rothe, J., M.A. Denecke and K. Dardenne. 2000. Soft X-ray spectromicroscopy investigation of the interaction of aquatic humic acid and clay colloids. *J. Colloid Interface Sci.* 231: 91-97.
- Rumpel, C., K. Eusterhues and I. Kögel-Knabner. 2004. Location and chemical composition of stabilized organic carbon in topsoil and subsoil horizons of two acid forest soils. *Soil Biol. Biochem.* 36: 177-190.
- Saggar, S., A. Parshotam, G. Sparling, C. Feltham and P. Hart. 1996. ¹⁴C-labelled ryegrass turnover and residence times in soils varying in clay content and mineralogy. *Soil Biol. Biochem.* 28: 1677-1686.
- Saha, S.K., P.R. Nair, V.D. Nair and B.M. Kumar. 2009. Soil carbon stock in relation to plant diversity of homegardens in Kerala, India. *Agroforest. Syst.* 76: 53-65.
- Sarkhot, D.V., N. Comerford, E.J. Jokela, J.B. Reeves and W.G. Harris. 2007. Aggregation and aggregate carbon in a forested southeastern coastal plain spodosol. *Soil Sci. Soc. Am. J.* 71: 1779-1787.
- Sarkhot, D.V., E.J. Jokela and N.B. Comerford. 2008. Surface soil carbon size–density fractions altered by loblolly pine families and forest management intensity for a Spodosol in the southeastern US. *Plant Soil* 307: 99-111.
- Sartori, F., R. Lal, M.H. Ebinger and J.A. Eaton. 2007. Changes in soil carbon and nutrient pools along a chronosequence of poplar plantations in the Columbia Plateau, Oregon, USA. *Agric., Ecosyst. Environ.* 122: 325-339.
- Sauer, T.J., C.A. Cambardella and J.R. Brandle. 2007. Soil carbon and tree litter dynamics in a red cedar–scotch pine shelterbelt. *Agroforest. Syst.* 71: 163-174.
- Schäfer, T., N. Hertkorn, R. Artinger, F. Claret, and A. Bauer. 2003. Functional group analysis of natural organic colloids and clay association kinetics using C (1s) spectromicroscopy. *Journal de Physique IV (Proceedings)*, EDP sciences.
- Scheinost, A., R. Kretschmar, I. Christl, and C. Jacobsen. 2001. Carbon group chemistry of humic and fulvic acid: A comparison of C-1s NEXAFS and ¹³C-NMR spectroscopies. In: E.A. Ghabbour and G. Davies, editors, *Humic substances: structures, models and functions*. The Royal Society of Chemistry. Cambridge. UK. p. 39-50.
- Scheu, S. and J. Schauer mann. 1994. Decomposition of roots and twigs: Effects of wood type (beech and ash), diameter, site of exposure and macrofauna exclusion. *Plant Soil* 163: 13-24.
- Schimel, D.S., B. Braswell, E.A. Holland, R. McKeown, D. Ojima, T.H. Painter, et al. 1994. Climatic, edaphic, and biotic controls over storage and turnover of carbon in soils. *Global Biogeochem. Cy.* 8: 279-293.

- Schlesinger, W.H. and J.A. Andrews. 2000. Soil respiration and the global carbon cycle. *Biogeochemistry* 48: 7-20.
- Schmidt, M.W., M.S. Torn, S. Abiven, T. Dittmar, G. Guggenberger, I.A. Janssens, et al. 2011. Persistence of soil organic matter as an ecosystem property. *Nature* 478: 49-56.
- Schnitzer, M., D. McArthur, H.-R. Schulten, L. Kozak and P. Huang. 2006. Long-term cultivation effects on the quantity and quality of organic matter in selected Canadian prairie soils. *Geoderma* 130: 141-156.
- Schoeneberger, M.M. 2009. Agroforestry: Working trees for sequestering carbon on agricultural lands. *Agroforest. Syst.* 75: 27-37.
- Schoeneberger, M.M., G. Bentrup and C.A. Francis. 2001. Ecobelts: reconnecting agriculture and communities. In: C. Flora, editor, *Interactions between agroecosystems and rural human communities*. Adv. in Agroecology, CRC Press, Boca Raton, FL. p. 239-260.
- Scholten, H. 1988. Snow distribution on crop fields. *Agric., Ecosyst. Environ.* 22: 363-380.
- Schroeder, P. 1994. Carbon storage benefits of agroforestry systems. *Agroforest. Syst.* 27: 89-97.
- Schroth, G. 1998. A review of belowground interactions in agroforestry, focussing on mechanisms and management options. *Agroforest. Syst.* 43: 5-34.
- Schulten, H. 1996. Direct pyrolysis-mass spectrometry of soils: a novel tool in agriculture, ecology, forestry, and soil science. In: T. W. Boutton and S. Yamasaki, editors, *Mass Spectrometry of Soils*, Marcel Dekker, New York, p. 373-436.
- Schumacher, M., I. Christl, A.C. Scheinost, C. Jacobsen and R. Kretzschmar. 2005. Chemical heterogeneity of organic soil colloids investigated by scanning transmission X-ray microscopy and C-1s NEXAFS microspectroscopy. *Environ. Sci. Technol.* 39: 9094-9100.
- Sexstone, A.J., N.P. Revsbech, T.B. Parkin and J.M. Tiedje. 1985. Direct measurement of oxygen profiles and denitrification rates in soil aggregates. *Soil Sci. Soc. Am. J.* 49: 645-651.
- Shaw, D.L. 1988. 19. The design and use of living snow fences in North America. *Agric., Ecosyst. Environ.* 22: 351-362.
- Sileshi, G., F.K. Akinnifesi, O.C. Ajayi, S. Chakeredza, M. Kaonga and P. Matakala. 2007. Contributions of agroforestry to ecosystem services in the Miombo eco-region of eastern and southern Africa. *Afr. J. Environ. Sci. Technol.* 1: 68-80.
- Sills, D.L. and J.M. Gossett. 2012. Using FTIR to predict saccharification from enzymatic hydrolysis of alkali-pretreated biomasses. *Biotechnol. Bioeng.* 109: 353-362.
- Šimon, T. 2007. Quantitative and qualitative characterization of soil organic matter in the long-term fallow experiment with different fertilization and tillage. *Arch. Agron. Soil Sci.* 53: 241-251.
- Simpson, M.J. and A.J. Simpson. 2012. The chemical ecology of soil organic matter molecular constituents. *J. Chem. Ecol.* 38: 768-784.
- Six, J., R.T. Conant, E.A. Paul and K. Paustian. 2002. Stabilization mechanisms of soil organic matter: Implications for C-saturation of soils. *Plant Soil* 241: 155-176.

- Six, J., P. Schultz, J. Jastrow and R. Merckx. 1999. Recycling of sodium polytungstate used in soil organic matter studies. *Soil Biol. Biochem.* 31: 1193-1196.
- Skjemstad, J., R. LeFeuvre and R. Prebble. 1990. Turnover of soil organic matter under pasture as determined by ¹³C natural abundance. *Soil Res.* 28: 267-276.
- Skjemstad, J.O. and J.A. Taylor. 1999. Does the Walkley-Black Method determine soil charcoal? *Commun. Soil Sci. Plant Anal.* 30: 2299-2310.
- Smith, P. 2004. Soils as carbon sinks: the global context. *Soil Use Manage.* 20: 212-218.
- Smith, P., C. Fang, J.J.C. Dawson and J.B. Moncrieff. 2008. Impact of global warming on soil organic carbon. *Adv. Agron.* 97:1-43.
- Smith, P., D.S. Powlson, J.U. Smith, P. Falloon and K. Coleman. 2000. Meeting Europe's climate change commitments: quantitative estimates of the potential for carbon mitigation by agriculture. *Glob. Change Biol.* 6: 525-539.
- Sohi, S.P., N. Mahieu, J.R. Arah, D.S. Powlson, B. Madari and J.L. Gaunt. 2001. A procedure for isolating soil organic matter fractions suitable for modeling. *Soil Sci. Soc. Am. J.* 65: 1121-1128.
- Sollins, P., P. Homann and B.A. Caldwell. 1996. Stabilization and destabilization of soil organic matter: Mechanisms and controls. *Geoderma* 74: 65-105.
- Solomon, D., J. Lehmann, J. Kinyangi, W. Amelung, I. Lobe, A. Pell, et al. 2007. Long-term impacts of anthropogenic perturbations on dynamics and speciation of organic carbon in tropical forest and subtropical grassland ecosystems. *Glob. Change Biol.* 13: 511-530.
- Solomon, D., J. Lehmann, J. Kinyangi, B. Liang and T. Schäfer. 2005. Carbon K-edge NEXAFS and FTIR-ATR spectroscopic investigation of organic carbon speciation in soils. *Soil Sci. Soc. Am. J.* 69: 107-119.
- Solomon, D., J. Lehmann and W. Zech. 2000. Land use effects on soil organic matter properties of chromic luvisols in semi-arid northern Tanzania: carbon, nitrogen, lignin and carbohydrates. *Agric., Ecosyst. Environ.* 78: 203-213.
- Spaccini, R. and A. Piccolo. 2007. Molecular characterization of compost at increasing stages of maturity. 1. Chemical fractionation and infrared spectroscopy. *J. Agric. Food. Chem.* 55: 2293-2302.
- Spielvogel, S., J. Prietzel and I. Kögel-Knabner. 2008. Soil organic matter stabilization in acidic forest soils is preferential and soil type-specific. *Eur. J. Soil Sci.* 59: 674-692.
- Spycher, G., P. Sollins and S. Rose. 1983. Carbon and nitrogen in the light fraction of a forest soil: vertical distribution and seasonal patterns. *Soil Sci.* 135: 79-87.
- Stenberg, B., R.A.V. Rossel, A.M. Mouazen and J. Wetterlind. 2010. Chapter five-visible and near infrared spectroscopy in soil science. *Adv. Agron.* 107: 163-215.
- Stöhr, J. 1992. NEXAFS spectroscopy. Springer-Verlag Berlin.
- Strickland, M.S., C. Lauber, N. Fierer and M.A. Bradford. 2009. Testing the functional significance of microbial community composition. *Ecology* 90: 441-451.

- Sutton, R. and G. Sposito. 2005. Molecular structure in soil humic substances: The new view. *Environ. Sci. Tech.* 39: 9009-9015.
- Swan, C.M. and M.A. Palmer. 2006. Composition of speciose leaf litter alters stream detritivore growth, feeding activity and leaf breakdown. *Oecologia* 147: 469-478.
- Swanston, C.W., B.A. Caldwell, P.S. Homann, L. Ganio and P. Sollins. 2002. Carbon dynamics during a long-term incubation of separate and recombined density fractions from seven forest soils. *Soil Biol. Biochem.* 34: 1121-1130.
- Swift, M.J., O.W. Heal and J.M. Anderson. 1979. *Decomposition in terrestrial ecosystems.* Blackwell Scientific Publications, Oxford.
- Tatzber, M., M. Stemmer, H. Spiegel, C. Katzlberger, G. Haberhauer and M. Gerzabek. 2007a. An alternative method to measure carbonate in soils by FT-IR spectroscopy. *Environ. Chem. Lett.* 5: 9-12
- Tatzber, M., M. Stemmer, H. Spiegel, C. Katzlberger, G. Haberhauer, A. Mentler, et al. 2007b. FTIR-spectroscopic characterization of humic acids and humin fractions obtained by advanced NaOH, Na₄P₂O₇, and Na₂CO₃ extraction procedures. *J. Plant Nutr. Soil Sci.* 170: 522-529.
- Teklay, T. and S.X. Chang. 2008. Temporal changes in soil carbon and nitrogen storage in a hybrid poplar chronosequence in northern Alberta. *Geoderma* 144: 613-619.
- Thevathasan, N. and A. Gordon. 2004. Ecology of tree intercropping systems in the North temperate region: Experiences from southern Ontario, Canada. *Agroforest. Syst.* 61: 257-268.
- Thevathasan, N.V. and A.M. Gordon. 1995. Moisture and fertility interactions in a potted poplar-barley intercropping. *Agroforest. Syst.* 29: 275-283.
- Thevathasan, N.V., A.M. Gordon, R. Bradley, A. Cogliastro, P. Folkard, R. Grant, et al. 2012. Agroforestry research and development in Canada: The way forward. In: P. K. R. Nair and D. Garrity, editors, *Agroforestry-The Future of Global Land Use.* Springer Netherlands. p. 247-283.
- Thomsen, I.K., P. Schjønning, B. Jensen, K. Kristensen and B.T. Christensen. 1999. Turnover of organic matter in differently textured soils: II. Microbial activity as influenced by soil water regimes. *Geoderma* 89: 199-218.
- Tietenberg, T., M. Grubb, A. Michaelowa, B. Swift and Z. Zhang. 1999. *International rules for greenhouse gas emissions trading: Defining the principles, modalities, rules and guidelines for verification, reporting and accountability.* United Nations, New York (NY), Geneva (Switzerland).
- Torn, M., C. Swanston, C. Castanha and S. Trumbore. 2009. Storage and turnover of organic matter in soil. In: N. Senesi, B. Xing and P. M. Huang, editors, *Biophysico-chemical processes involving natural nonliving organic matter in environmental systems.* Wiley, Hoboken. p. 219-272.
- Udawatta, R.P. and S. Jose. 2011. Carbon sequestration potential of agroforestry practices in temperate North America. In: M. B. Kumar and R. P. K. Nair, editors, *Carbon sequestration potential of agroforestry systems: Opportunities and challenges.* Springer Netherlands, Dordrecht. p. 17-42.

- Upson, M. and P. Burgess. 2013. Soil organic carbon and root distribution in a temperate arable agroforestry system. *Plant Soil* 373: 43-58.
- Urquhart, S. and H. Ade. 2002. Trends in the carbonyl core (C 1s, O 1s)→ π^* C=O transition in the near-edge X-ray absorption fine structure spectra of organic molecules. *J. Phys. Chem. B* 106: 8531-8538.
- Van Iperen, J. and W. Helder. 1985. A method for the determination of organic carbon in calcareous marine sediments. *Mar. Geol.* 64: 179-187.
- Verardo, D.J., P.N. Froelich and A. McIntyre. 1990. Determination of organic carbon and nitrogen in marine sediments using the Carlo Erba NA-1500 Analyzer. *Deep Sea Res., Part I.* 37: 157-165.
- Vesterdal, L., N. Clarke, B.D. Sigurdsson and P. Gundersen. 2013. Do tree species influence soil carbon stocks in temperate and boreal forests? *For. Ecol. Manage.* 309: 4-18.
- von Lützow, M., I. Kögel-Knabner, K. Ekschmitt, H. Flessa, G. Guggenberger, E. Matzner, et al. 2007. SOM fractionation methods: Relevance to functional pools and to stabilization mechanisms. *Soil Biol. Biochem.* 39: 2183-2207.
- von Lützow, M., I. Kögel-Knabner, K. Ekschmitt, E. Matzner, G. Guggenberger, B. Marschner, et al. 2006. Stabilization of organic matter in temperate soils: Mechanisms and their relevance under different soil conditions – a review. *Eur. J. Soil Sci.* 57: 426-445.
- Walkley, A. and I.A. Black. 1934. An examination of the Degtjareff method for determining soil organic matter, and a proposed modification of the chromic acid titration method. *Soil Sci.* 37: 29-38.
- Wan, J., T. Tyliszczak and T.K. Tokunaga. 2007. Organic carbon distribution, speciation, and elemental correlations within soil microaggregates: applications of STXM and NEXAFS spectroscopy. *Geochim. Cosmochim. Acta* 71: 5439-5449.
- Wander, M. 2004. Soil organic matter fractions and their relevance to soil function. In: F. Magdoff and R. R. Weil, editors, *Soil organic matter in sustainable agriculture*. CRC Press, Boca Raton, FL. p. 67–102.
- Wang, D. and D. Anderson. 1998. Direct Measurement of Organic Carbon Content in Soils by the Leco CR-12 Carbon Analyzer. *Commun. Soil Sci. Plant Anal.* 29: 15-21.
- Wang, F., X. Xu, B. Zou, Z. Guo, Z. Li and W. Zhu. 2013. Biomass accumulation and carbon sequestration in four different aged *Casuarina equisetifolia* coastal shelterbelt plantations in south China. *PloS ONE* 8: e77449.
- Waples, D.W. and J.R. Sloan. 1980. Carbon and nitrogen diagenesis in deep sea sediments. *Geochim. Cosmochim. Acta* 44: 1463-1470.
- Watanabe, A., S. Kawasaki, S. Kitamura and S. Yoshida. 2007. Temporal changes in humic acids in cultivated soils with continuous manure application. *Soil Sci. Plant Nutr.* 53: 535-544.
- Watters, J. 2002. Tree planting in rural Saskatchewan, 1870-1914. M.Sc. thesis, Univ. of Saskatchewan, Saskatoon.
- Webster, J. and E. Benfield. 1986. Vascular plant breakdown in freshwater ecosystems. *Annu. Rev. Ecol. Syst.* 17: 567-594.

- Weliky, K., P. Muller, K. Fischer and E. Suess. 1983. Problems with accurate carbon measurements in marine sediments and particulate matter in seawater. A new approach. *Limnol. Oceanogr* 28: 1252-1259.
- West, T.O. and W.M. Post. 2002. Soil organic carbon sequestration rates by tillage and crop rotation. *Soil Sci. Soc. Am. J.* 66: 1930-1946.
- Whalen, J.K., P.J. Bottomley and D.D. Myrold. 2000. Carbon and nitrogen mineralization from light- and heavy-fraction additions to soil. *Soil Biol. Biochem.* 32: 1345-1352.
- Wheaton, E. 1992. Prairie dust storms—a neglected hazard. *Nat. Hazards* 5: 53-63.
- Wickings, K., A.S. Grandy, S.C. Reed and C.C. Cleveland. 2012. The origin of litter chemical complexity during decomposition. *Ecol. Lett.* 15: 1180-1188.
- Wiseman, G., J. Kort and D. Walker. 2009. Quantification of shelterbelt characteristics using high-resolution imagery. *Agric., Ecosyst. Environ.* 131: 111-117.
- Wojdyr, M. 2010. Fityk: a general-purpose peak fitting program. *J. Appl. Crystallogr.* 43: 1126-1128.
- Woldeselassie, M., H. Van Miegroet, M.-C. Gruselle and N. Hambly. 2012. Storage and stability of soil organic carbon in aspen and conifer forest soils of northern Utah. *Soil Sci. Soc. Am. J.* 76: 2230-2240.
- Woldeselassie, M.K. 2009. Soil organic carbon and site characteristics in aspen and evaluation of the potential effects of conifer encroachment on soil properties in Northern Utah. Ph.D. thesis. Utah State Univ., Logan.
- Wotherspoon, A., N.V. Thevathasan, A.M. Gordon and R.P. Voroney. 2014. Carbon sequestration potential of five tree species in a 25-year-old temperate tree-based intercropping system in southern Ontario, Canada. *Agroforest. Syst.* 88: 631-643.
- Wu, T., J.J. Schoenau, F. Li, P. Qian, S.S. Malhi, Y. Shi, et al. 2004. Influence of cultivation and fertilization on total organic carbon and carbon fractions in soils from the Loess Plateau of China. *Soil Tillage Res.* 77: 59-68.
- Wu, Z., P. Dijkstra, G.W. Koch, J. Peñuelas and B.A. Hungate. 2011. Responses of terrestrial ecosystems to temperature and precipitation change: a meta-analysis of experimental manipulation. *Glob. Change Biol.* 17: 927-942.
- Xu, F., J. Yu, T. Tesso, F. Dowell and D. Wang. 2013. Qualitative and quantitative analysis of lignocellulosic biomass using infrared techniques: a mini-review. *Appl. Energy* 104: 801-809.
- Yamamuro, M. and H. Kayanne. 1995. Rapid direct determination of organic and nitrogen in carbonate-bearing sediments with a Yanaco MT-5 CHN analyzer. *Limnol. Oceanogr* 40: 1001-1005.
- Yang, H. and A.M. Mouazen. 2012. Vis/near and mid-infrared spectroscopy for predicting soil N and C at a farm scale. In: T. Theophanides, editor, *Infrared Spectroscopy-Life and Biomedical Sciences*. Intech Press, Rijeka, Croatia. p.185-210.
- Yannikos, N., P. Leinweber, B.L. Helgason, C. Baum, F.L. Walley and K.C. Van Rees. 2014. Impact of Populus trees on the composition of organic matter and the soil microbial community in Orthic Gray Luvisols in Saskatchewan (Canada). *Soil Biol. Biochem.* 70: 5-11.

Youkhana, A. and T. Idol. 2011. Addition of *Leucaena*-KX2 mulch in a shaded coffee agroforestry system increases both stable and labile soil C fractions. *Soil Biol. Biochem.* 43: 961-966

Young, A. 1997. *Agroforestry for soil management*. CAB International, Wallingford, UK.

Zech, W., F. Ziegler, I. Kögel-Knabner and L. Haumaier. 1992. Humic substances distribution and transformation in forest soils. *Sci. Total Environ.* 117: 155-174.

APPENDICES

Appendix A. Major stand characteristics of the sampling sites with hybrid poplar shelterbelt plantation

Site ID	Age of Shelterbelt (years)	Shelterbelt length (m)	Shelterbelt area (m ²)	Avg. crown width (m)	Avg. tree height (m)	Mortality rate (%)	No. of rows	Other tree species
HP1	18	27	601	2.3	12.9	0	5	Silver maple, White spruce, Manitoba maple, Lilac
HP2	20	119	1658	8.6	16.0	9	3	Siberian elm, Willow
HP3	20	104	1527	4.8	7.6	28	3	Spruce, Acute willow, Lilac
HP4	29	71	1524	11.9	11.1	37	5	Hybrid poplar, Manitoba maple, White spruce
HP5	31	69	545	7.9	17.9	9	1	None
HP6	34	80	1104	13.8	9.3	40	1	None
HP7	35	59	1252	7.4	12.9	28	6	Caragana, Maple, White spruce
HP8	36	26	385	10.6	16.3	3	4	Caragana, Maple
HP9	38	73	993	7.5	18.5	12	3	Acute willow, Siberian elm, Green elm, Hybrid poplar, White spruce
HP10	45	41	622	12.7	23.2	13	2	Siberian elm

Appendix B. Major stand characteristics of the sampling sites with white spruce shelterbelt plantation

Site ID	Age of Shelterbelt (years)	Shelterbelt length (m)	Shelterbelt area (m ²)	Avg. crown width (m)	Avg. tree height (m)	Mortality rate (%)	No. of rows	Other tree species
WS2	12	115	446	1.8	5.0	19	2	None
WS3	12	86	1849	3.5	4.9	0	3	American Elm
WS4	20	43	322	4.5	7.3	17	2	None
WS5	24	52	296	5.7	1.5	73	1	Manitoba maple
WS6	27	32	274	5.5	6.2	14	3	Manitoba maple
WS7	30	131	1040	4.7	9.1	0	2	Colorado spruce
WS8	32	60	354	5.9	8.3	0	1	None
WS9	32	75	512	6.8	8.4	27	1	None
WS10	58	149	1651	3.9	19.4	55	3	Hybrid poplar

Appendix C. Major stand characteristics of the sampling sites with green ash shelterbelt plantation

Site ID	Age of Shelterbelt (years)	Shelterbelt length (m)	Shelterbelt area (m ²)	Avg. crown width (m)	Avg. tree height (m)	Mortality rate (%)	No. of rows	Other tree species
GA1	5	81	2747	3.0	3.8	0	3	Caragana, Siberian elm, Lilac, Manitoba maple
GA2	7	84	521	1.2	1.8	4	2	Acute willow
GA3	8	17	904	3.2	4.1	0	11	Scots pine, Dogwood, Buffalo berry, Lilac
GA4	12	69	2522	6.6	9.3	13	4	Manitoba maple, Colorado spruce, Lilac
GA5	13	56	977	5.1	7.4	0	3	Colorado spruce, Lilac
GA6	24	18	99	5.6	7.6	25	1	None
GA7	31	52	923	4.3	10.0	0	4	Colorado spruce, Lilac, Manitoba maple
GA8	32	304	2690	4.1	8.2	16	3	Caragana, Colorado spruce
GA9	44	15	182	7.4	9.3	29	3	Caragana, Colorado spruce, Elm

Appendix D. Major stand characteristics of the sampling sites with Manitoba maple shelterbelt plantation

Site ID	Age of Shelterbelt (years)	Shelterbelt length (m)	Shelterbelt area (m ²)	Avg. crown width (m)	Avg. tree height (m)	Mortality rate (%)	No. of rows	Other tree species
MM1	5	55	729	4.0	3.8	8	3	Colorado spruce, Lilac
MM2	6	55	152	2.8	3.1	5	1	None
MM3	10	207	6351	2.7	2.3	32	8	Willow, Bur oak, Choke cherry, Scots pine, Dog wood, Sea buckthorn
MM4	11	62	383	3.4	3.8	27	3	Manitoba maple, Lilac
MM5	19	35	266	7.6	5.9	9	1	None
MM6	20	89	2426	9.5	8.0	3	4	Colorado spruce
MM7	24	32	570	5.7	6.0	4	5	Chokecherry, Manitoba maple
MM8	30	28	255	2.7	2.6	65	4	Siberian elm, Colorado spruce
MM9	46	25	195	5.4	5.2	0	2	Caragana
MM10	46	42	290	5.9	3.2	19	2	Caragana

Appendix E. Major stand characteristics of the sampling sites with Scots pine shelterbelt plantation

Site ID	Age of Shelterbelt (years)	Shelterbelt length (m)	Shelterbelt area (m ²)	Avg. crown width (m)	Avg. tree height (m)	Mortality rate (%)	No. of rows	Other tree species
SP1	7	26	259	3.3	4.5	0	2	White spruce, Green ash, Colorado spruce
SP2	19	22	210	6.2	10.0	0	3	Colorado spruce, American elm
SP3	18	38	546	6.2	5.5	25	2	Green ash, Scots pine
SP4	20	22	151	6.7	8.1	29	1	Colorado spruce, Tamarack, Maple
SP5	27	18	335	4.0	10.4	0	5	Spruce, Caragana, Scots pine
SP6	29	25	365	6.4	5.1	40	3	White spruce, Siberian elm
SP7	30	62	621	6.0	6.4	22	3	Colorado spruce
SP8	32	39	288	5.6	8.0	7	2	Colorado Blue Spruce
SP9	39	53	441	8.4	10.7	0	1	None
SP10	60	61	859	5.5	15.1	17	4	Siberian elm, Hybrid poplar, Scots pine
SP11	63	37	342	4.0	13.2	6	5	Caragana, American elm, Manitoba maple

Appendix F. Major stand characteristics of the sampling sites with caragana shelterbelt plantation

Site ID	Age of Shelterbelt (years)	Shelterbelt length (m)	Shelterbelt area (m ²)	Avg. crown width (m)	Avg. tree height (m)	Mortality rate (%)	No. of rows	Other tree species
CR1	7	368	948	2.6	2.8	0	1	None
CR2	10	1600	4280	2.7	2.4	0	1	None
CR3	10	60	179	2.6	2.0	0	2	Green ash
CR4	21	32	145	4.6	3.3	0	1	None
CR5	19	80	320	4.0	3.4	0	1	None
CR6	10	74	429	5.8	3.2	0	1	None
CR7	24	123	1383	7.0	3.0	0	4	Caragana, Manchurian elm, Colorado spruce
CR8	28	388	2832	7.3	3.6	29	1	None
CR9	21	200	1165	5.8	3.2	0	1	None
CR10	32	85	784	5.5	3.3	0	4	Maple

Appendix G. The script used for deconvolution of ATR-FTIR spectra of soil samples in the Fityk software package. Changes were made to this script depending upon the unique spectral features of the different soil samples.

```
=-> define GaussianPositive(sqrt_height=sqrt(height), center, hwhm) = Gaussian(sqrt_height^2, center, hwhm)
```

```
=-> A = a and not (400 < x and x < 900)
```

```
=-> A = a and not (1800 < x and x < 4000)
```

```
=-> F += GaussianPositive(height=~0.002, center=915, hwhm=~20)
```

```
=-> F += GaussianPositive(height=~0.003, center=980, hwhm=~30)
```

```
=-> F += GaussianPositive(height=~0.01, center=~1030, hwhm=~40)
```

```
173 =-> F += GaussianPositive(height=~0.005, center=~1110, hwhm=~30)
```

```
=-> F += GaussianPositive(height=~0.005, center=1160, hwhm=~30)
```

```
=-> F += GaussianPositive(height=~0.0004, center=1260, hwhm=~30)
```

```
=-> F += GaussianPositive(height=~0.0039, center=1390, hwhm=~30)
```

```
=-> F += GaussianPositive(height=~0.0098, center=1440, hwhm=~33)
```

```
=-> F += GaussianPositive(height=~0.0098, center=1510, hwhm=~45)
```

```
=-> F += GaussianPositive(height=~0.0037, center=~1560, hwhm=~23)
```

```
=-> F += GaussianPositive(height=~0.0065, center=~1630, hwhm=~38)
```


=> F += GaussianPositive(height=~0.0065, center=~1720, hwhm=~38)

=> \$_hwhm = ~30

=> @0.F[*].hwhm = \$_hwhm

=> fit

=> \$_2 = ~{\$_2}

=> \$_5 = ~{\$_5}

=> \$_14 = ~{\$_14}

=> \$_17 = ~{\$_17}

174 => \$_20 = ~{\$_20}

=> \$_23 = ~{\$_23}

=> \$_26 = ~{\$_26}

=> fit

Appendix H. The script used for deconvolution of C K-edge XANES spectra of soil samples in the Fityk software package.

Minor changes were made to the script depending upon the unique spectral features of the different soil samples.

```
=-> define GaussianPositive(sqrt_height=sqrt(height), center, hwhm) = Gaussian(sqrt_height^2, center, hwhm)
=> define Atan(a1=0.3, center=290, a3=1.5, a4=0.5) = a1 * atan((x -center) * a3) + a4
=> define GaussianPositive2(sqrt_height=sqrt(height), center, width=hwhm) = Gaussian(sqrt_height^2, center, width)
=> guess Atan(center=290)
=> F += GaussianPositive(height=~0.301, center=~284.1, hwhm=~0.4) #Unsaturated
=> F += GaussianPositive(height=~0.501, center=~285.1, hwhm=~0.4) #aromatic
175 => F += GaussianPositive(height=~0.375, center=~286.4, hwhm=~0.4) #Ketone
=> F +=GaussianPositive(height=~0.45, center=~287.3, hwhm=~0.4) #aliphatic
=> F += GaussianPositive(height=~0.513, center=~288.5, hwhm=~0.4) #carboxylic
=> F += GaussianPositive(height=~0.488, center=~289.5, hwhm=~0.4) #carbohydrate
=> F += GaussianPositive(height=~0.48, center=~290.3, hwhm=~0.4) #carbonate
=> F += GaussianPositive2(height=~0.5, center=~292, hwhm=~1)
=> F += GaussianPositive2(height=~0.5, center=~296, hwhm=~2)
=> $_hwhm = ~0.4
```

--> @0.F[*].hwhm = \$_hwhm

--> fit

Appendix I. Mean peak positions of the deconvoluted C K-edge XANES bands for shelterbelts and agricultural fields

Shelterbelt		Field	
Mean (eV)	Std. deviation	Mean (eV)	Std. deviation
284.08	0.06	284.13	0.11
285.09	0.03	285.08	0.04
286.25	0.08	286.24	0.10
287.28	0.08	287.34	0.06
288.39	0.03	288.40	0.05
289.46	0.08	289.40	0.15
290.73	0.24	290.51	0.26

Appendix J. Mean peak positions of the deconvoluted ATR-FTIR absorbance bands for shelterbelts and agricultural fields within the wavenumber range of 1800-900 cm^{-1}

Shelterbelt		Field	
Mean (cm^{-1})	Std. deviation	Mean (cm^{-1})	Std. deviation
917.15	3.97	917.16	4.45
985.99	6.05	986.35	7.20
1036.85	3.98	1036.47	5.60
1103.26	6.49	1103.30	7.08
1162.61	6.97	1162.16	7.47
1253.36	26.64	1247.28	22.89
1369.73	14.71	1370.00	15.53
1434.47	8.43	1434.21	9.01
1509.47	15.04	1509.11	16.71
1582.92	13.37	1584.60	14.14
1643.32	7.36	1644.23	7.98
1702.20	9.64	1703.54	11.36